Article

Cell Metabolism

Semaglutide ameliorates osteoarthritis progression through a weight loss-independent metabolic restoration mechanism

Graphical abstract

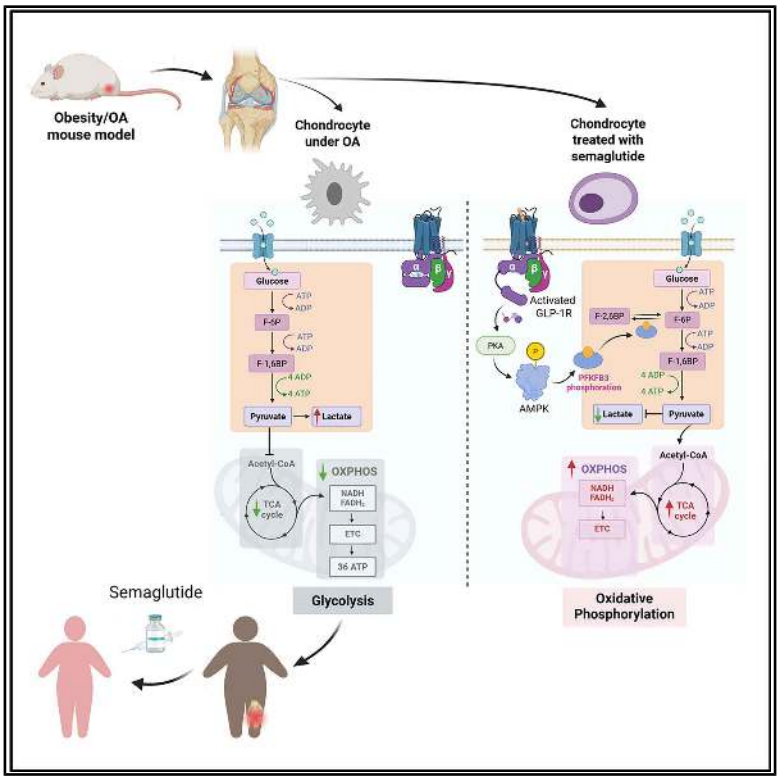

Highlights

- Semaglutide alleviates OA in a weight loss-independent manner
- Semaglutide shifts chondrocyte metabolism from glycolysis to oxidative phosphorylation
- Semaglutide exerts its chondroprotective effect via the "GLP-1R-AMPK-PFKFB3" axis
- Semaglutide could serve as an effective drug to treat metabolic OA

Authors

Hongyu Qin, Jiamin Yu, Huan Yu, ..., John R. Speakman, Di Chen, Liping Tong

Correspondence

zhanghuantian@jnu.edu.cn (H.-T.Z.), j.speakman@abdn.ac.uk (J.R.S.), di.chen@siat.ac.cn (D.C.), lp.tong@siat.ac.cn (L.T.)

In brief

Qin et al. demonstrated the chondroprotective effects of semaglutide in obesity-related osteoarthritis. Mechanistically, these effects are independent of body weight loss and involve metabolic reprogramming of chondrocyte via the GLP-1R-AMPK-PFKFB3 signaling axis.

Qin et al., 2026, Cell Metabolism *38*, 1–16
March 3, 2026 © 2026 Elsevier Inc. All rights are reserved, including those for text and data mining, AI training, and similar technologies.
https://doi.org/10.1016/j.cmet.2026.01.008

CellPress

Please cite this article in press as: Qin et al., Semaglutide ameliorates osteoarthritis progression through a weight loss-independent metabolic restoration mechanism, Cell Metabolism (2026), https://doi.org/10.1016/j.cmet.2026.01.008

Cell Metabolism

CellPress

Article

Semaglutide ameliorates osteoarthritis progression through a weight loss-independent metabolic restoration mechanism

Hongyu Qin,[1,2,3,13] Jiamin Yu,[1,2,4,13] Huan Yu,[1,13] Chuqiao Zhou,[1] Dongfeng Yuan,[1,4] Ziling Wang,[1,2] Zhenglin Zhu,[5] Guizheng Wei,[1,2] Peiyan Ou,[1] Zhibin Li,[6] Hua Jiang,[3] Jie Shen,[7] Guozhi Xiao,[8] Xiaochun Bai,[9] Huaiyu Wang,[1] Huan-Tian Zhang,[10,*] John R. Speakman,[11,12,*] Di Chen,[1,2,14,*] and Liping Tong[1,15,*]

[1]Center for AI-Driven Medical Research, Shenzhen Institutes of Advanced Technology, Chinese Academy of Sciences, Shenzhen 518055, China

[2]Department of Pharmacology, Faculty of Pharmaceutical Sciences, Shenzhen University of Advanced Technology, Shenzhen 518107, China

[3]Division of Spine Surgery, The First Affiliated Hospital of Guangxi Medical University, Nanning 530021, China

[4]University of Chinese Academy of Sciences, Chinese Academy of Sciences, Beijing 100049, China

[5]Department of Orthopaedic Surgery, The First Affiliated Hospital of Chongqing Medical University, Chongqing 400016, China

[6]Intensive Care Unit, Shenzhen Institute of Translational Medicine, The First Affiliated Hospital of Shenzhen University, Shenzhen Second People's Hospital, Shenzhen, Guangdong 518035, P.R. China

[7]Department of Orthopaedic Surgery and Cell Biology & Physiology, Washington University School of Medicine, St. Louis, MO 63110, USA

[8]School of Medicine, Southern University of Science and Technology, Shenzhen 518055, China

[9]State Key Laboratory of Organ Failure Research, Department of Cell Biology, School of Basic Medical Sciences, Southern Medical University, Guangzhou 510515, China

[10]Department of Bone and Joint Surgery, the First Affiliated Hospital of Jinan University, Key Laboratory of Regenerative Medicine of Ministry of Education, Jinan University, Guangzhou, Guangdong 510630, China

[11]Center for Energy Metabolism and Reproduction, Shenzhen Institutes of Advanced Technology, Chinese Academy of Sciences, Shenzhen 518055, China

[12]School of Biological Sciences, University of Aberdeen, Aberdeen, Scotland

[13]These authors contributed equally

[14]Senior author

[15]Lead contact

*Correspondence: zhanghuantian@jnu.edu.cn (H.-T.Z.), j.speakman@abdn.ac.uk (J.R.S.), di.chen@siat.ac.cn (D.C.), lp.tong@siat.ac.cn (L.T.)

https://doi.org/10.1016/j.cmet.2026.01.008

SUMMARY

Metabolic disorders have been recognized as a major contributor to the occurrence and progression of osteoarthritis (OA). Identifying novel therapeutic agents to ameliorate the progression of OA with metabolic disorder is crucial. In this study, we demonstrate that semaglutide (SG), a glucagon-like peptide-1 receptor (GLP-1R) agonist, exhibits strong chondroprotective effects in an OA mouse model with obesity, as evidenced by reduced pathological changes, including cartilage degeneration, osteophyte formation, synovial lesion, and pain sensitivity. A randomized pilot clinical study (ChiCTR2200066291) further supports these findings. By designing a precise diet-controlled setting to rule out the effect of appetite suppression and weight loss induced by SG, we demonstrate a weight loss-independent mechanism. Through regulating the "GLP-1R-AMPK-PFKFB3" axis, the SG reprograms chondrocyte metabolism profile from glycolysis to oxidative phosphorylation under inflammatory conditions, resulting in cartilage restoration.

INTRODUCTION

According to the World Health Organization, approximately 7% of the global population lives with osteoarthritis (OA),[1] with the prevalence rising to 73% among the elderly (≥55 years).[2] OA is widely recognized as a degenerative joint disease marked by the progressive breakdown of joint cartilage, leading to subchondral bone damage, persistent pain, and disability. Historically, OA has been considered as an inevitable part of aging, with a complex polyetiological causality.[3] OA management has primarily focused on palliative care, which has hindered the advancement of effective therapeutic interventions. Consequently, OA involves a high disability rate and imposes a substantial burden on both affected individuals and society.

Despite age generally being regarded as the primary risk factor for OA, growing epidemiological and clinical evidence now underscores metabolic dysfunction as a significant contributor, particularly among younger adults aged 30–44.[4] The relationship between metabolic syndrome (comprising obesity, diabetes, dyslipidemia, and hypertension) and OA has led to the proposal

All rights are reserved, including those for text and data mining, AI training, and similar technologies.

Please cite this article in press as: Qin et al., Semaglutide ameliorates osteoarthritis progression through a weight loss-independent metabolic restoration mechanism, Cell Metabolism (2026), https://doi.org/10.1016/j.cmet.2026.01.008

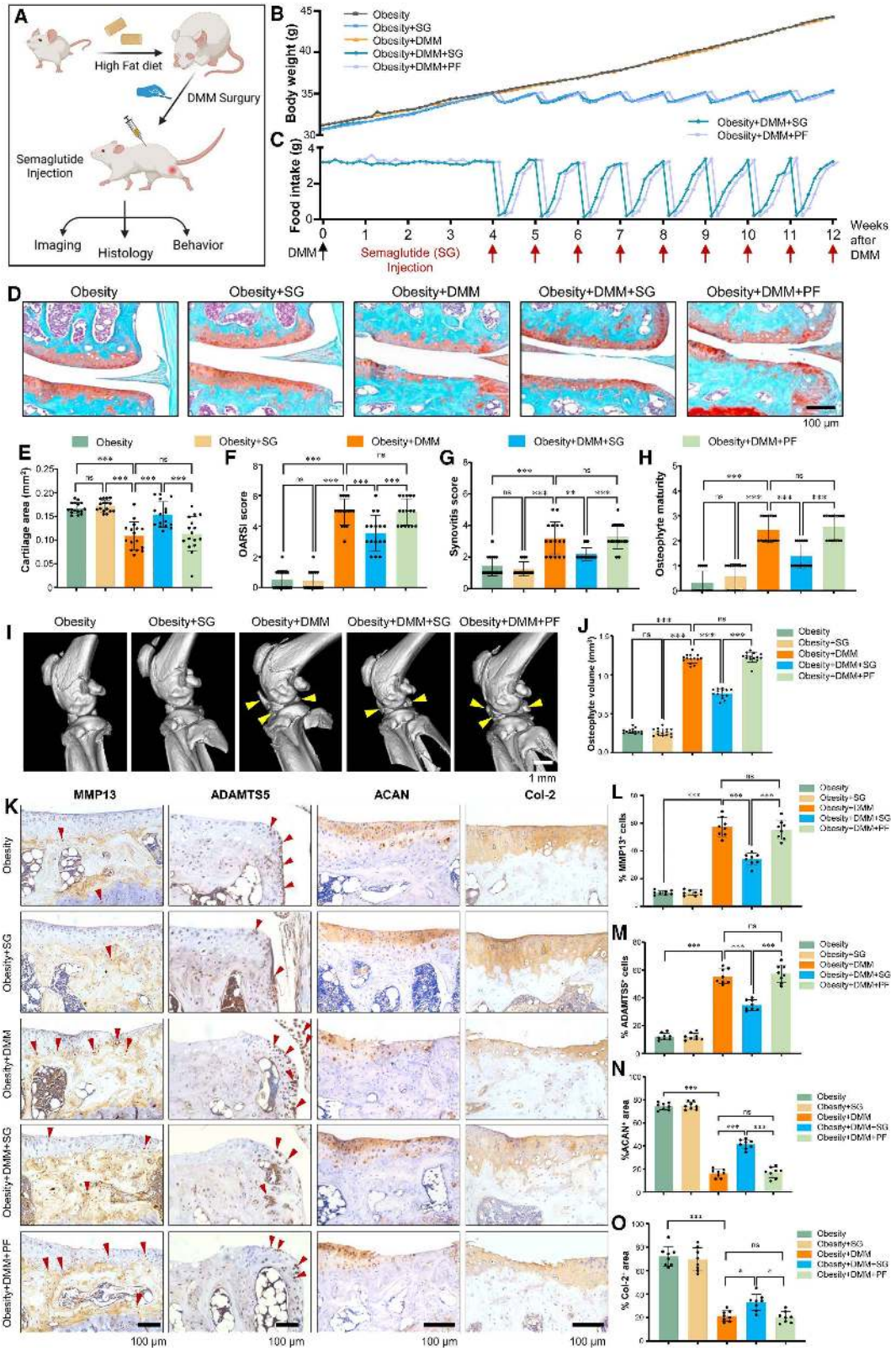

(legend on next page)

Please cite this article in press as: Qin et al., Semaglutide ameliorates osteoarthritis progression through a weight loss-independent metabolic restoration mechanism, Cell Metabolism (2026), https://doi.org/10.1016/j.cmet.2026.01.008

of a distinct subtype termed "metabolic OA."[5,6] Several hypotheses about OA mechanisms have been proposed to explain the metabolic contribution to the cartilage damage, including reduced nutrient and oxygen supply, the accumulation of lipid and advanced glycation end products (AGEs) within joint tissues, and increased mechanical load on the joints.[7] These factors together highlight multifaceted pathways involved in metabolic dysfunctions, which exacerbate OA progression.

Distilling the core feature of metabolic OA, obesity and insulin resistance emerge as essential contributors to OA.[7] Notably, obesity is frequently accompanied by hypertrophy and pathological expansion of adipocytes, along with impaired insulin signaling, which leads to insulin resistance and broader metabolic dysfunction.[8] Therefore, we hypothesize that reversing insulin resistance and targeting pathways regulating glucose metabolism may offer a novel approach for OA treatment.

Glucagon-like peptide-1 receptor (GLP-1R), known for its role in regulating glucose homeostasis and body weight, has become an attractive target for managing metabolic disorders and obesity. GLP-1R agonists, such as semaglutide (SG), liraglutide, and dulaglutide, have emerged over the past 2 decades, mimicking the action of endogenous hormone GLP-1 to aid in weight loss and obesity control through multifaceted mechanisms. This includes appetite suppression, delayed gastric emptying, enhanced insulin sensitivity, reduced glucagon secretion, and potentially improved mitochondrial function.[9,10] Increasing evidence reveals that the profound effects of GLP-1R agonists involve regulation of glucose transporter expression and activity,[11,12] activation of AMPK signaling,[13–15] and modulation of cellular glycometabolic pathways.[16–18] Furthermore, GLP-1R agonists confer additional benefits on cardiovascular diseases, such as reducing the risk of death, stroke, and myocardial infarction[19]; cutting the risk of severe kidney complications and mortality in type 2 diabetes and chronic kidney disease[20]; slowing the progression of neurodegenerative disease[21]; combating cravings[22]; and alleviating OA symptoms.[23,24] The underlying molecular mechanisms of the effects of GLP-1R agonists on OA remain to be fully elucidated.

Given the inextricable links between metabolic dysfunction and metabolic OA, alongside the exceptional effects of SG on metabolic regulation, we systematically evaluated the chondroprotective effects of SG on metabolic OA. Briefly, we utilized destabilization of medial meniscus (DMM) surgery to establish OA mouse models with obesity and administered SG weekly. A pair-feeding (PF) group was included as a control for inter-group differences in food intake due to SG-induced appetite suppression and weight loss. Key OA indicators, including cartilage degeneration, osteophyte formation, severity of synovial lesion, and pain sensitivity, were assessed. Our findings demonstrated that SG possesses a strong chondroprotective effect independent of weight loss. Mechanistic studies were conducted in *in vitro* experiments and in *Glp-1r* and *Prkaa1* gene (encoding AMPK) knockout (KO) mouse models. The results indicated that SG orchestrates an intracellular energy balance between glycolysis and oxidative phosphorylation (OXPHOS) through activation of AMPK-PFKFB3 signaling, supplying ample ATP to support chondrocyte repair. Encouraged by these outcomes, we conducted a proof-of-concept pilot clinical study in individuals with obesity and knee OA. SG treatment led to significant reductions in both cartilage degradation and joint function, compared with control.

In conclusion, this work not only highlights the potential off-target effect of SG as an effective drug to treat metabolic OA but also reveals a weight loss-independent repair mechanism that targets metabolic pathways and mediators essential to cartilage repair under OA conditions. This may lead to new strategies to develop disease-modifying therapies for OA.

RESULTS

SG decelerates OA progression in mice with obesity

To evaluate the effect of SG on the progression of OA in obese mice, we first successfully established an obesity model via a high-fat diet feeding. Once the mice reached a body weight at least 20% higher than that of the regular diet control mice, the DMM surgery was performed to generate the OA mice with obesity, designated as the obesity + DMM group. SG was then administered via subcutaneous injection beginning 4 weeks after DMM surgery. Micro-computed tomography (CT) imaging, histological evaluation, and pain behavior studies were employed to assess the progression of OA and the efficacy of drug treatments (Figure 1A).

Immunohistochemical (IHC) staining confirmed the expression of GLP-1R in cartilage collected from non-obese mice and obese mice with or without OA. These results clearly showed that the expression of GLP-1R was decreased under OA condition (Figure S1). Blood chemistry analysis showed that total cholesterol (CHO) level was significantly elevated in the obesity and obesity + DMM groups, which was notably reduced by SG treatment (Figure S2A); however, other parameters, including triglycerides (TGs), hemoglobin (GHb), low-density lipoprotein (LDL), and high-density lipoprotein (HDL), remained unchanged (Figures S2B–S2E).

Recognizing the importance of body weight control in obesity-related OA, we set up a PF control group (obesity + DMM + PF) to rule out the potential confounding effects of SG-induced weight loss. In detail, mice were weight-matched to SG-treated animals

Figure 1. SG inhibits cartilage degradation in obesity/OA mice

(A) Schematic diagram of experimental plan.

(B and C) Daily monitoring of body weight (B) and food intake (C) changes in obesity/OA mice after weekly SG injection and PF control (n = 8).

(D–H) Histological and histomorphometric analysis of cartilage showed chondroprotective effects of SG (n = 16). Scale bar, 100 μm.

(I and J) Micro-CT image (I) and histomorphometric analyses (J) of joint tissue in obesity/OA mice (n = 14). Scale bar, 1 mm.

(K–O) IHC analyses and quantification of catabolic marker proteins (MMP13 and ADAMTS5) and anabolic marker proteins (ACAN and Col-2) indicated the protective effect of SG on cartilage matrix under OA (n = 8). Scale bar, 100 μm.

Data are expressed as means ± SD. *p < 0.05, **p < 0.01, ***p < 0.001. One-way ANOVA, followed by Tukey's post hoc test, was used for multiple group comparisons.

Please cite this article in press as: Qin et al., Semaglutide ameliorates osteoarthritis progression through a weight loss-independent metabolic restoration mechanism, Cell Metabolism (2026), https://doi.org/10.1016/j.cmet.2026.01.008

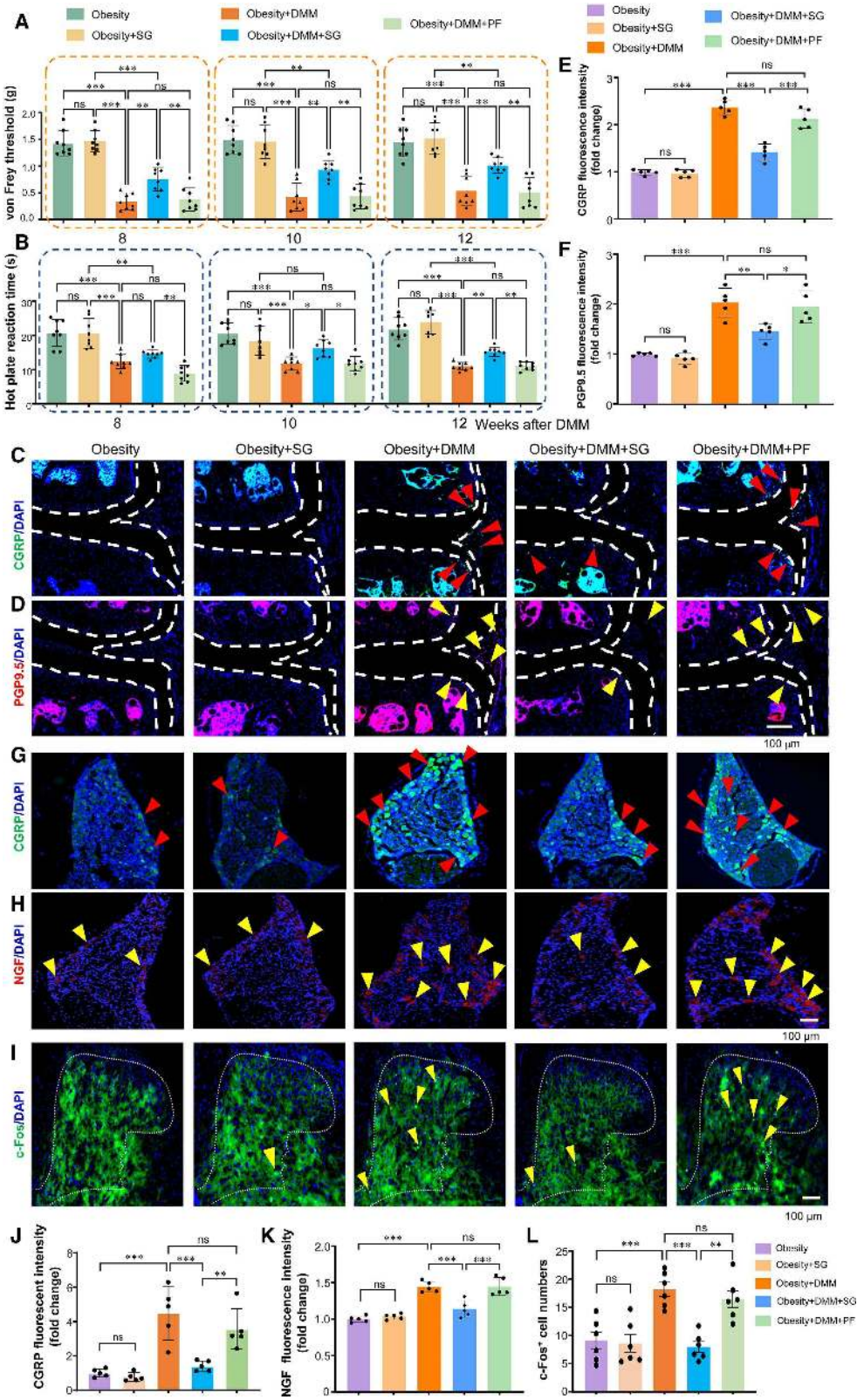

(legend on next page)

Please cite this article in press as: Qin et al., Semaglutide ameliorates osteoarthritis progression through a weight loss-independent metabolic restoration mechanism, Cell Metabolism (2026), https://doi.org/10.1016/j.cmet.2026.01.008

and housed individually, with daily monitoring of food intake and body weight. The PF group started the experiment 1 day behind the SG treatment group to ensure comparable food intake between the two groups (Figures 1B and 1C). As expected, SG showed substantial, transient appetite suppression and weight reduction within the first 3 days, followed by recovery to baseline after 7 days of SG treatment, consistent with the pharmacokinetic profile of SG in the humans, with a t_{max} of 24 h and a half-life ($t_{1/2}$) of 155 h. Interestingly, PF produced a comparable weight control effect, and no significant differences in body weight were observed between SG-treated and PF mice throughout the study.

Then, we conducted histologic, histomorphometric, and micro-CT analyses to evaluate the therapeutic effect of SG at the end of the treatment period (12 weeks post-DMM surgery). Obesity + DMM mice showed severe OA-like changes, including synovitis, cartilage degradation, and osteophyte formation. We observed a significant increase in OARSI score, synovitis score, and osteophyte maturity, alongside a reduction in cartilage area. However, SG treatment protected cartilage against degradation (OA progression), which was evidenced by a significantly reduced OARSI score, synovitis score, osteophyte maturity, and osteophyte volume and increased cartilage area in the obesity + DMM mice (Figures 1D–1J). Meanwhile, analyses of cortical, trabecular, and subchondral bone suggested that SG prevented ectopic bone formation during OA development (Figures S3A–S3M). Changes in expression of catabolic and anabolic marker proteins were analyzed in obesity + DMM mice with or without SG treatment. Results revealed a significant increase in MMP13-positive and ADAMTS5-positive (representative catabolic markers) cells in obesity + DMM mice, while SG treatment markedly reduced their expression (Figures 1K–1M). In contrast, the levels of the two anabolic markers, aggrecan (ACAN) and type II collagen (Col-2), decreased in obesity + DMM mice, but they were significantly restored by the SG treatment (Figures 1K, 1N, and 1O). Despite exhibiting a similar weight loss, the PF mice showed no significant cartilage protection. These findings clearly suggest that SG mitigates obesity-related OA progression through mechanisms independent of its weight-lowering effect.

SG relieves OA pain

Pain is the primary reason for OA patients seeking medical care, making its alleviation a crucial measure for treatment efficacy. To assess the impact of SG treatment on pain-related behaviors in obesity/OA mice, we conducted longitudinal analyses using the von Frey test (to evaluate mechanical allodynia) and the hot plate test (to evaluate thermal allodynia) from 6 to 12 weeks post-DMM surgery. We found that pain sensitivities were significantly increased in obesity + DMM mice 8, 10, and 12 weeks after DMM surgery, as reflected by lower von Frey threshold and shorter hot plate reaction times. SG treatment substantially improved both von Frey threshold scores (Figure 2A) and hot plate reaction time (Figure 2B), indicating that SG has the potential to effectively relieve OA-associated pain in obese mice. To further investigate pain-related behavior, we analyzed changes in spontaneous activity in obesity/OA mice. Metrics such as average travel speed, climbing time, climbing counts, and locomotion counts were significantly reduced in obesity + DMM mice but showed notable improvement following SG treatment (Figures S4A–S4D). However, other parameters of spontaneous activity, such as locomotion time, immobility time, and immobility counts (Figures S4E–S4G) remained unchanged across all groups.

To confirm the pain-relief effects of SG at the molecular level, we examined expression of pain-related neurochemical markers in articular cavity, dorsal root ganglia (DRGs), and spinal cord. Classical neural markers like calcitonin gene-related peptide (CGRP), protein gene product 9.5 (PGP9.5), nerve growth factor (NGF), and c-Fos were upregulated in obesity + DMM mice but significantly downregulated following SG treatment (Figures 2C–2L). These findings highlight SG's potential to alleviate OA-associated pain and restore activity levels in mice with obesity, offering promising therapeutic implications.

SG exerts its chondroprotective effects via GLP-1R-PKA-AMPK-PFKFB3 axis

A key remaining question is how SG treats OA, independent of weight loss. To comprehensively explore mechanisms of SG in knee OA, we performed proteomic profiling on articular cartilage tissues from obesity/OA mice subjected to either PF or SG treatment. Our analysis identified 8,275 differentially expressed proteins (DEPs), including 128 upregulated proteins (Figure 3A). By filtering the $p < 0.05$ and fold-change (FC) value < 0.65 or >1.7, we narrowed this down to 76 key proteins. Among them, PFKFB2, a critical regulator of glycolysis, emerged as the most upregulated protein, exhibiting a 4.3-fold increase following SG treatment (Figure S5A). As expected, the most significantly altered pathways in articular cartilage involved "extracellular molecules," "collagen-containing extracellular matrix (ECM)," and "ECM" (Figure S5B). KEGG analysis further revealed "metabolism" and "organismal systems" as the most significantly affected pathways (Figure S5C). These data suggest that SG exerts its protective effects on knee OA via metabolism-related mechanisms.

Figure 2. SG inhibits the pain in obesity/OA mice

(A and B) von Frey test (analysis of mechanical allodynia) and hot plate test (analysis of thermal allodynia) revealed that SG treatment can relieve OA-related pain at 8, 10, and 12 weeks after DMM surgery ($n = 8$).

(C and D) IF staining of CGRP (C) and PGP9.5 (D) in knee joint ($n = 5$).

(E and F) Quantification of $CGRP^+$ and $PGP9.5^+$ intensities, indicating that SG treatment significantly downregulated both protein expression in joint.

(G and H) IF staining of CGRP (G) and NGF (H) in DRG ($n = 5$).

(I) IF staining of c-Fos in spinal cord ($n = 6$).

(J and K) Quantification of $CGRP^+$ and NGF^+ intensities, and the results confirmed the pain inhibition effect of SG.

(L) Quantification of c-Fos^+ cells, and the results confirmed the pain inhibition effect of SG. Scale bar, 100 μm.

Data are expressed as means ± SD. $^*p < 0.05$, $^{**}p < 0.01$, $^{***}p < 0.001$. One-way ANOVA, followed by the Tukey's post hoc test, was used for multiple group comparisons.

Please cite this article in press as: Qin et al., Semaglutide ameliorates osteoarthritis progression through a weight loss-independent metabolic restoration mechanism, Cell Metabolism (2026), https://doi.org/10.1016/j.cmet.2026.01.008

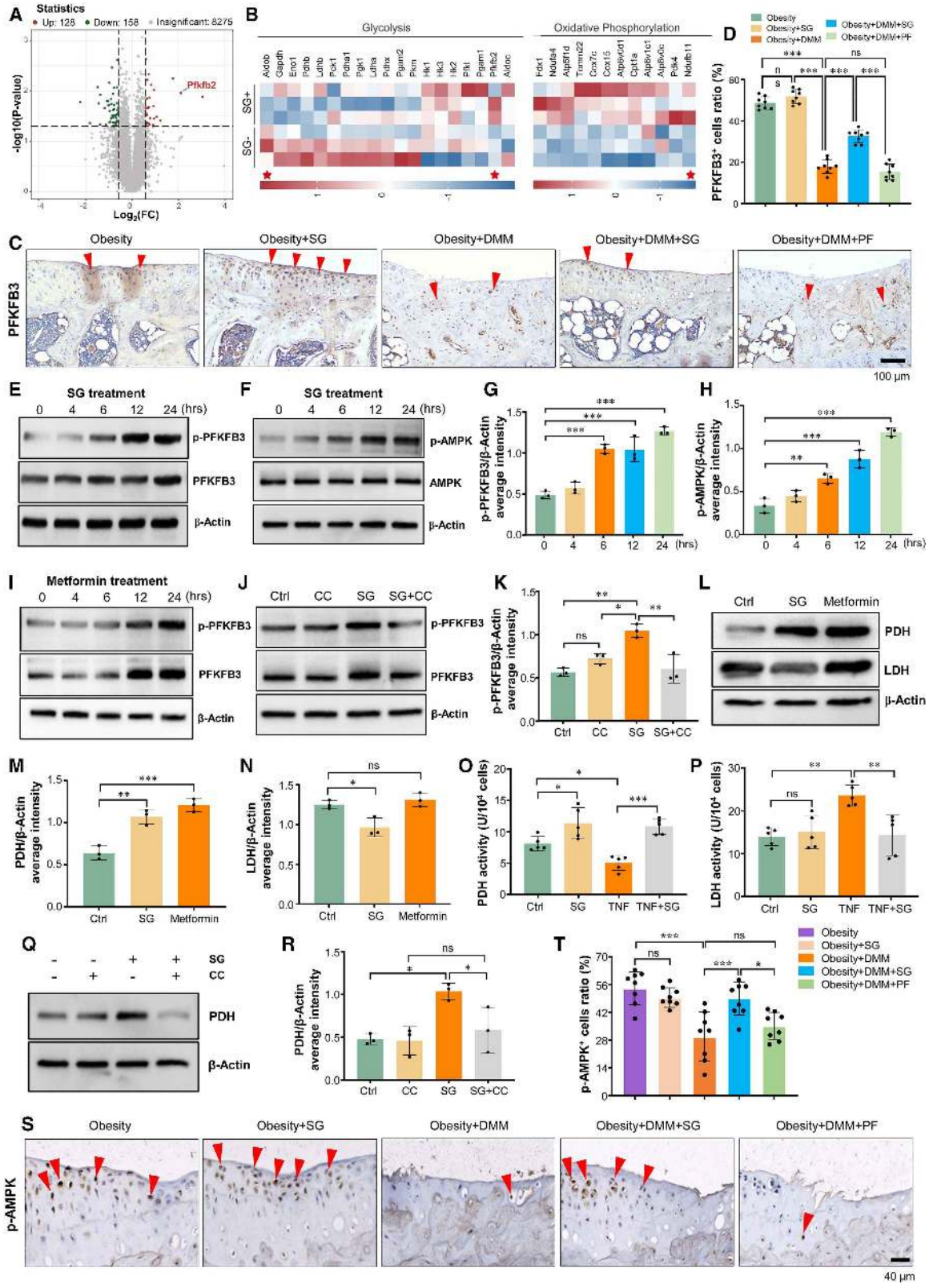

Figure 3. SG exerts its chondroprotective effects via GLP-1R-PKA-AMPK-PFKFB3 axis

(A) Volcano plot showing DEPs in mice cartilage with/without SG treatment (n = 3).

(B) Heatmap displaying the expression of glycolysis- and OXPHOS-related proteins. Red asterisk indicates $p < 0.05$.

(legend continued on next page)

Please cite this article in press as: Qin et al., Semaglutide ameliorates osteoarthritis progression through a weight loss-independent metabolic restoration mechanism, Cell Metabolism (2026), https://doi.org/10.1016/j.cmet.2026.01.008

Next, we conducted gene set enrichment analysis (GSEA) to investigate the role of SG in OA inhibition. Consistent with our findings, the "adipogenesis" and "fatty acid metabolism" were significantly suppressed (Figures S5D and S5E). Several adipogenesis-related proteins were decreased, including leptin (Lep), APOE, FABP1, and FABP4 (Figure S5H). Among these, Lep is thought to play a crucial role in maintaining energy homeostasis and regulating body weight, with its downregulation aligning with recent studies.[25] Additionally, APOE plays an important role in lipid homeostasis,[26] further reinforcing the metabolic influence of SG. Moreover, SG treatment inhibited collagen degradation, leading to reduced expression of MMP13, MMP14, MMP2, and SPP1 (Figure S5H), all of which contribute to cartilage breakdown. Interestingly, we observed that glycolysis was suppressed but overall cartilage ATP production was increased, which was evidenced by the upregulation of ATP-dependent activity (Figures S5F and S5G). Several key proteins involved in glycolysis and OXPHOS, including Aldob, Pgam1, Pkm, HK1, HK2, HK3, Ldha, Ldhb, Ndufb11, Atp6v1c1, and Pfkfb2, exhibited significant changes in their expression after SG treatment (Figure 3B). Of note, PFKFB2, a key member of the PFKFB family, was markedly upregulated, further supporting its central role in SG-mediated metabolic reprogramming in OA.

The PFKFB family has four isoenzymes (PFKFB1–PFKFB4) with distinct properties and acts as a bifunctional enzyme exerting kinase and phosphatase activities in glycolysis regulation by modulating fructose-2,6-bisphosphate (F-2,6-BP) levels.[27] By producing F-2,6-BP, PFKFB enzymes promote glycolysis, while by degrading it, they block glycolysis. Hence, we analyzed the expression of PFKFB family members by IHC assay, and we found that expression of PFKFB1–4 was significantly reduced in articular cartilage tissue of obesity + DMM mice but was markedly upregulated following SG treatment (Figures 3C, 3D, and S5K–S5N). *In vitro* studies further confirmed that SG upregulated protein levels of PFKFB family members in primary chondrocytes (Figures S5I and S5J). These findings suggest that SG may exert chondroprotective effects through enhancing PFKFB expression.

Among PFKFB1–4, all have similar kinase and phosphatase activities, except for PFKFB3 that possesses over 710-fold higher kinase activity than bisphosphatase activity. This unique property makes PFKFB3 the rate-limiting enzyme in glycolytic metabolism.[28] Given its pivotal role, we subsequently focused on PFKFB3 to explore how SG regulates its expression and associated signaling pathways. Since AMPK is a master regulator of cellular metabolism, we hypothesized that SG might activate the AMPK-PFKFB3 axis. Indeed, SG treatment induced AMPK and PFKFB3 phosphorylation in a time-dependent manner (Figures 3E–3H). Similarly, the AMPK activator metformin also upregulated PFKFB3 phosphorylation over time (Figure 3I). To confirm AMPK dependency, we employed the AMPK inhibitor compound C (CC) and found that SG-induced PFKFB3 phosphorylation was drastically blocked in the presence of CC (Figures 3J and 3K). These results indicate that SG-induced phosphorylation of PFKFB3 is AMPK-dependent.

Next, we examined how SG influences metabolic pathways by assessing protein expression and activity of pyruvate dehydrogenase (PDH) and lactate dehydrogenase (LDH), which are representative enzymes in the tricarboxylic acid (TCA) cycle and glycolysis, respectively. SG significantly upregulated PDH expression and activity in primary chondrocytes (Figures 3L, 3M, and 3O), whereas LDH activity was decreased under inflammatory conditions (Figures 3L, 3N, and 3P). To determine whether SG-induced PDH expression depends on AMPK, we applied CC, which completely inhibited SG-induced PDH upregulation (Figures 3Q and 3R), confirming that SG regulates PDH expression through an AMPK-dependent mechanism.

To validate these findings *in vivo*, we assessed phosphorylated AMPK (p-AMPK) levels in obesity/OA mice following SG treatment. OA progression led to a dramatic decrease in the p-AMPK level, but SG treatment restored it to near normal level. This effect was absent in the PF control group (Figures 3S and 3T).

The Gαs/cyclic adenosine monophosphate (cAMP) signaling pathway is the classical downstream cascade of GLP-1R activation. Upon being activated by GLP-1R agonists, the GLP-1R stimulates adenylyl cyclase (AC) by Gαs, leading to conversion of ATP into cAMP. The elevated intracellular cAMP then activates the protein kinase A (PKA) pathway, which subsequently phosphorylates downstream targets to propagate the signal.[29]

To explore whether PKA is involved in SG-induced AMPK activation, we used a PKA inhibitor (H-89) to determine its effect on SG-mediated AMPK phosphorylation. As expected, SG alone induced robust phosphorylation of AMPK. The PKA inhibitor alone had no effect, but co-treatment with SG significantly reduced AMPK phosphorylation (Figures S5O and S5P), suggesting a potential regulatory link between PKA activation and AMPK signaling in the regulatory mechanism of SG.

SG reprograms metabolic pathways in primary chondrocytes

Metabolism plays a crucial role in maintaining cartilage and synovial joint function. With OA progression, chondrocytes undergo a metabolic shift from a resting state to an active state

(C and D) Expression and quantification of PFKFB3, analyzed by IHC in obesity/OA mice with or without SG treatment (n = 8). Scale bar, 100 μm.
(E–H) Western blot analysis showed that SG treatment upregulated the phosphorylation of PFKFB3 (E and G) and AMPK (F and H) in a time-dependent manner in primary chondrocytes (n = 3).
(I) Metformin, the AMPK activator, upregulated PFKFB3 phosphorylation over time in primary chondrocytes (n = 3).
(J and K) CC, the AMPK inhibitor, inhibited the SG-induced PFKFB3 phosphorylation in primary chondrocytes (n = 3).
(L–N) SG significantly upregulated PDH expression (L and M), with no obvious change in LDH expression (L and N, n = 3).
(O and P) Determination of PDH and LDH activities in primary chondrocytes under different conditions (n = 5).
(Q and R) CC inhibited the SG-induced PDH expression in primary chondrocytes (n = 3).
(S and T) IHC staining showed that p-AMPK-positive cell numbers were dramatically decreased in cartilage after DMM surgery. SG treatment restored the p-AMPK expression level; by contrast, PF had no significant effect (n = 8). Scale bar, 40 μm.
Data are expressed as means ± SD. $^{*}p < 0.05$, $^{**}p < 0.01$, $^{***}p < 0.001$. One-way ANOVA, followed by Tukey's post hoc test, was used for multiple group comparisons.

Please cite this article in press as: Qin et al., Semaglutide ameliorates osteoarthritis progression through a weight loss-independent metabolic restoration mechanism, Cell Metabolism (2026), https://doi.org/10.1016/j.cmet.2026.01.008

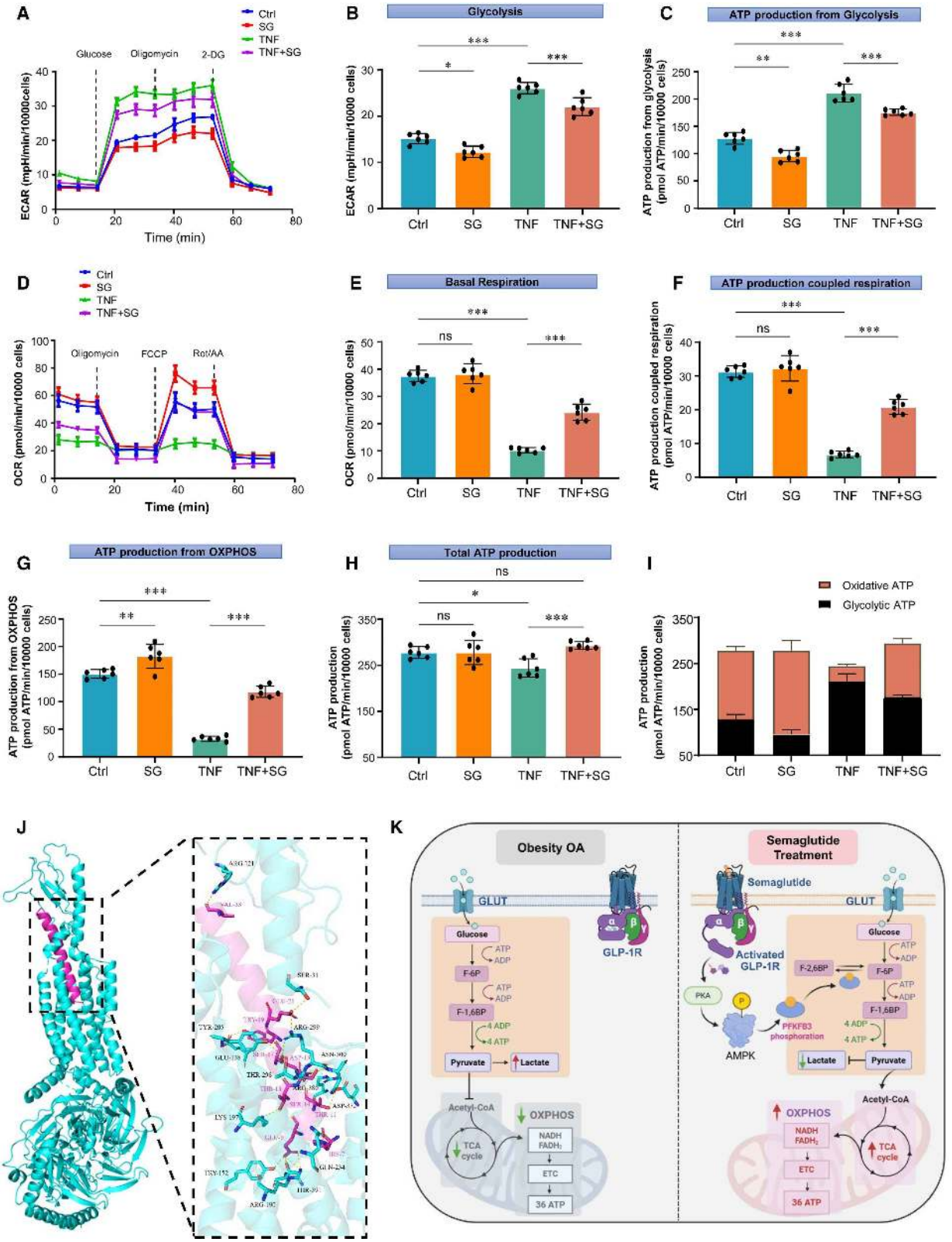

Figure 4. SG regulates mitochondrial respiration and glycolysis

(A and B) Seahorse XFe96 energetic analysis with Glycolysis Stress Test Kit (n = 6). Extracellular acidification rate (ECAR) was a key indicator used to assess the activity of glycolysis.

(legend continued on next page)

Please cite this article in press as: Qin et al., Semaglutide ameliorates osteoarthritis progression through a weight loss-independent metabolic restoration mechanism, Cell Metabolism (2026), https://doi.org/10.1016/j.cmet.2026.01.008

CellPress

to meet increased energy demands for ECM biosynthesis, cell proliferation, and survival. The balance between glycolysis and OXPHOS, two major metabolic pathways, is thought to be critical in OA development and symptom relief.[30]

Using the Seahorse assay, we detected OXPHOS and glycolysis of chondrocytes under different treatment conditions to elucidate the impact of SG on mitochondrial respiration and glycolytic activity. We demonstrated that glycolytic level of chondrocytes was significantly elevated in an inflammatory environment, but SG treatment could slightly reduce it (Figures 4A and 4B). Correspondingly, ATP production from glycolysis declined following SG treatment, although it remained above normal levels (Figure 4C). On the other hand, SG significantly enhanced both basal respiration and OXPHOS-derived ATP production under inflammatory conditions (Figures 4D–4G). Then, total ATP production from both pathways was quantified, and SG treatment restored the ATP levels comparable to those of normal chondrocytes (Figure 4H).

To determine whether SG influences metabolic pathway preference, we calculated the relative contributions of glycolysis and OXPHOS to total ATP production.[31] In normal chondrocytes, OXPHOS accounted for 53.93% of ATP generation, which increased to 65.65% after SG treatment. Under OA-like inflammatory conditions, however, glycolysis dominated energy production (86.52%), consistent with findings in OA individuals.[32] Encouragingly, SG treatment reversed this imbalance, restoring a nearly equal contribution from both pathways (Figure 4I). Molecular dynamics simulations confirmed the binding efficiency of SG to GLP-1R and identified its key interaction sites (Figure 4J). These findings indicate that SG treatment shifts energy production from glycolysis (under OA conditions) to OXPHOS, potentially alleviating OA progression and symptoms (Figure 4K).

Glp-1r KO abolishes the protective effect of SG on cartilage

To directly evaluate the role of GLP-1R in mediating the chondroprotective effects of SG, we generated a *Glp-1r* KO mouse model. The exon2-exon3 of *Glp-1r-201* transcript was modified by CRISPR-Cas9 technology. After DMM surgery and 12 weeks of SG treatment, we employed a comprehensive set of analyses, including micro-CT imaging, followed by histological and histomorphometric analyses, to assess cartilage integrity, synovitis, and osteophyte formation. IHC analysis were employed to evaluate the expression of cartilage anabolic and catabolic markers. Particularly, immunofluorescence (IF) staining and quantification of pain-related neurochemical markers (CGRP and NGF in both the knee joint and DRG) were presented.

Our findings revealed that deletion of *Glp-1r* gene completely abolished the protective effects of SG on cartilage structure and function. In *Glp-1r* KO mice, SG treatment failed to reduce OARSI scores (Figures 5A and 5B), synovitis score (Figure 5C), cartilage degradation (Figures 5A, 5D, and 5G–5K), and osteophyte formation (Figures 5E, 5F, and S6A–S6C) and pain relief (Figures 5L–5S). These results strongly support that GLP-1R is essential for SG to exert the chondroprotective actions in OA.

Prkaa1 KO diminishes the protective effect of SG on cartilage

To further validate the involvement of AMPK signaling pathway in SG-mediated chondroprotection, we generated and analyzed AMPK conditional KO (cKO) mice. Specifically, we targeted the *Prkaa1* gene, which encodes the catalytic α1 subunit of AMPK protein. Similarly, using CRISPR-Cas9 gene-editing technology, we generated the *Prkaa1*-floxed mice and mated them with *Col2-CreER* transgenic mice. Tamoxifen was injected at a dose of 0.075 mg/g body weight 2 weeks prior to DMM surgery to achieve chondrocyte-specific deletion of *Prkaa1*.

After 12 weeks of SG administration, we systematically evaluated both cartilage integrity and pain-related outcomes as previously described. Our results clearly demonstrated that the chondroprotective effects of SG were significantly diminished in *Prkaa1* cKO mice, as evidenced by higher OARSI scores (Figures 6A and 6B) and synovitis score (Figure 6C), reduced cartilage area (Figures 6A and 6D), increased osteophyte formation (Figures 6E, 6F, and S6D–S6F), and increased extracellular degradation (Figures 6G–6K) after SG injection. Importantly, the pain-relief effects of SG were also nearly abolished in the *Prkaa1* cKO mice (Figures 6L–6S), indicating that the AMPK signaling is essential not only for cartilage protection but also for pain modulation. These findings strongly support a mechanistic role for AMPK in mediating the therapeutic effects of SG in OA. Taken together, the results from the *Glp-1r* KO and *Prkaa1* cKO mouse models establish a clear mechanistic framework for the chondroprotective actions of SG. Integrated with our *in vitro* signaling data, these findings strongly support a sequential regulatory cascade in which SG activates GLP-1R, triggers PKA signaling, and subsequently stimulates AMPK. The activated AMPK in turn promotes PFKFB3-driven glycolytic flux and enhances mitochondrial OXPHOS, thereby supplying sufficient ATP for ECM synthesis and preserving cartilage integrity.

SG improves cartilage repair in individuals with obesity/OA

To investigate whether SG protects against cartilage degradation in individuals with obesity/OA, we performed a randomized pilot clinical study by recruiting individuals aged 50–75 with OA and obesity (Figure 7A). Between January 2023 and January 2025, a total of 20 participants (7 male and 13 female) were

(C) ATP production from glycolysis was measured ($n = 6$).
(D–F) Oxygen consumption rate (OCR) and ATP production-coupled respiration measured by Cell Mito Stress Test Kit ($n = 6$).
(G–I) ATP production from OXPHOS and total ATP production were measured ($n = 6$).
(J) Molecular dynamics was used to identify the binding sites and stability of SG and GLP-1R.
(K) The schematic representation of the mechanism by which SG alleviates OA progression.
Data are expressed as means ± SD. $^{*}p < 0.05$, $^{**}p < 0.01$, $^{***}p < 0.001$. One-way ANOVA, followed by Tukey's post hoc test, was used for multiple group comparisons.

Please cite this article in press as: Qin et al., Semaglutide ameliorates osteoarthritis progression through a weight loss-independent metabolic restoration mechanism, Cell Metabolism (2026), https://doi.org/10.1016/j.cmet.2026.01.008

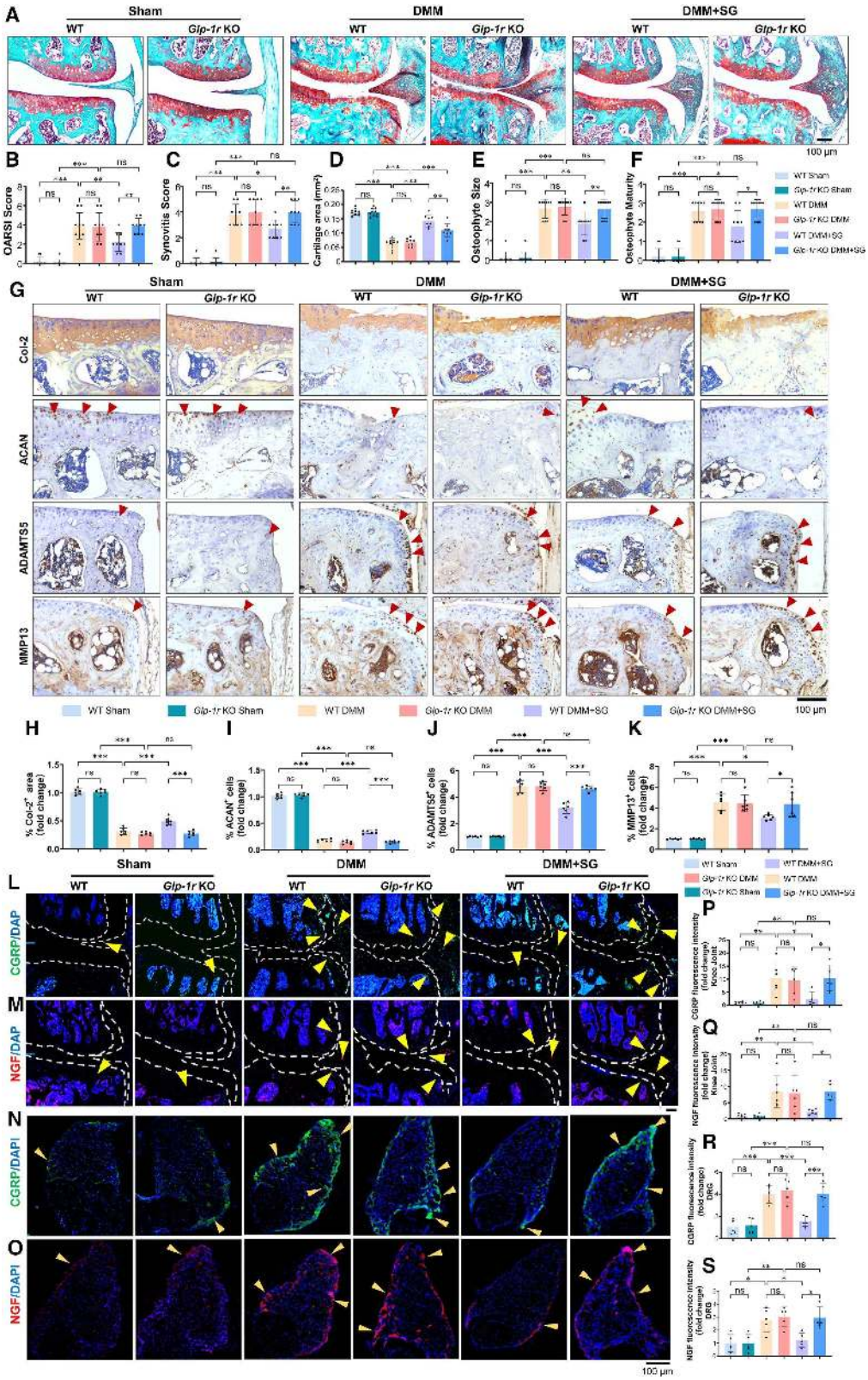

Figure 5. *Glp-1r* KO abolishes the protective effects of SG on cartilage

(A) Histological analysis (safranin-O-fast green staining) of the joint of wild-type (WT) and *Glp-1r* KO mice with or without SG treatment (n = 8–10). Scale bar, 100 μm. Six groups of mice were included: sham/WT, sham/*Glp-1r* KO, DMM/WT, DMM/*Glp-1r* KO, DMM + SG/WT, and DMM + SG/*Glp-1r* KO.

(legend continued on next page)

Please cite this article in press as: Qin et al., Semaglutide ameliorates osteoarthritis progression through a weight loss-independent metabolic restoration mechanism, Cell Metabolism (2026), https://doi.org/10.1016/j.cmet.2026.01.008

CellPress

enrolled and randomly assigned in a ratio of 1:1 to receive either sodium hyaluronate (HA) alone or HA combined with SG(HA + SG). Most participants completed the 24-week treatment period, with completion rate of 60% in the HA group and 80% in the HA + SG group (Figure S7A). No treatment-related adverse events or harms were observed during the study period. The primary endpoints included changes in body mass index (BMI) and WOMAC score (including pain, stiffness, physical function, and the total scores). Because several participants discontinued treatment within the first 4 weeks, a full analysis set (FAS) analysis was performed, confirming that inclusion or exclusion of these early dropouts did not affect the results. Consequently, data from these participants were excluded from subsequent analyses.

At week 24, the HA + SG group showed a significant reduction in BMI, with a mean change of −7.96% ± 3.18% from baseline (95% confidence interval [CI], −11.79 to −5.11; $p < 0.001$), compared with a 0.49% ± 2.28% change in the HA group (Figure 7B). In terms of pain relief, WOMAC pain score showed no significant differences between the two groups (Figure S7B). Both the weight loss and pain-relief effects were not as strong as reported in the literature,[33,34] likely due to the lower SG dose used in this study. Regarding joint stiffness, no significant improvement was observed in the HA + SG group compared with the HA group (Figure S7C). This outcome could be attributed to the well-established efficacy of HA in improving joint lubrication and joint mobility. However, over a period of 24 weeks, individuals in the HA + SG group showed a greater improvement in WOMAC physical function score than that in the HA group (mean change, −32.75 points vs. −16.2 points, 95% CI, −25.61 to −7.56; $p < 0.005$) (Figure 7C). As a result, the WOMAC total score showed a significant reduction in HA + SG group (Figure S7D), indicating substantial improvements in knee joint function. All these results demonstrated that after 24 weeks of treatment, HA + SG therapy led to significant improvements in knee joint function in individuals with obesity/OA.

Further, we analyzed changes in cartilage thickness utilizing 3D Slicer software on images of magnetic resonance imaging (MRI). The reliability of this method has been previously validated.[35] The cartilage thickness was defined as the shortest vertical distance from the cartilage-subchondral bone interface to the cartilage-soft tissue interface. MRI analysis revealed no significant changes in cartilage thickness in individuals who received HA treatment alone. Conversely, individuals with the HA + SG treatment had their cartilage layer thickened, with enhanced clarity at the cartilage-subchondral bone interface, suggesting repaired cartilage structure (Figure 7D). Quantitative analysis of cartilage thickness further demonstrated that compared with HA treatment alone, HA + SG treatment effectively protects against cartilage loss caused by obesity/OA (Figure 7E). In detail, the cartilage thickness increased about 17% in the HA + SG group, whereas HA alone led to less than a 1% increase, confirming the therapeutic efficacy of SG in combination with HA in humans (Figure 7F).

DISCUSSION

Metabolic disorders have been recognized as major contributors for OA occurrence and progression.[3] Conditions such as obesity, diabetes, and dyslipidemia, along with low-grade systemic inflammation, have been known to inflict detrimental effects on multiple tissues of the joint—including synovium, cartilage, and bone—leading to complete joint failure in OA.[36] Unfortunately, no effective pharmacological intervention has been established to decelerate OA progression. In recent years, GLP-1R agonists, including SG and liraglutide, have gained attention not only for their established roles in type 2 diabetes and obesity management but also for their potential therapeutic effects on hip and knee OA.[24,34] Clinical and preclinical studies have demonstrated that SG can alleviate OA symptoms, but the detailed molecular mechanisms remain incompletely understood.

Weight reduction is often considered the primary basis for the chondroprotective effects of SG due to the reduced joint loading. Another perspective highlights its anti-inflammatory properties, suggesting that SG may protect cartilage by inhibiting chondrocytes apoptosis.[37] A further hypothesis proposes an indirect effect through insulin-mediated effect.[38] Given that insulin receptors (IRs) are expressed in chondrocytes (Figures S8A and S8C) and that the glucose-lowering function of SG largely depends on the action of insulin, we also explored whether insulin-mediated pathways partially contribute to the chondroprotection of SG. Our findings suggest that SG may act via two complementary mechanisms: a direct GLP-1R mediated pathway and an indirect insulin-associated route (Figure S8).

Importantly, our study identified a weight loss-independent and GLP-1R-mediated mechanism by which SG alleviates OA. By setting a precise diet-controlled group, we demonstrated that SG exerts its anti-OA effects primarily through activation of the GLP-1R-AMPK-PFKFB3 axis (Figure 4K), which reprograms chondrocyte energy metabolism under inflammatory stress. This shift promotes a transition from glycolysis toward more efficient OXPHOS, thereby conferring multifaceted chondroprotective benefits.

As the primary energy source and an important precursor for the synthesis of biological macromolecules, glucose metabolism must maintain a proper balance between providing biosynthetic precursors and generating energy. Four key processes including glycolysis, the TCA cycle, OXPHOS, and Warburg effect[39,40] link these demands. In healthy cartilage, the avascular environment restricts oxygen availability, making glycolysis the predominant energy pathway.[41,42] However, during OA initiation and

(B–F) Histomorphometric analyses of knee joints from various groups of mice ($n = 8–10$).
(G) Expression of Col-2, ACAN, ADAMTS5, and MMP13 was analyzed by IHC ($n = 8–10$). Scale bar, 100 μm.
(H–K) Quantification of Col-2-, ACAN-, ADAMTS5-, and MMP13-positive cells/area in different mice ($n = 8–10$).
(L–O) Expression of CGRP and NGF in knee joint ($n = 6$) and in DRGs ($n = 5$) was measured by IF staining. Scale bar, 100 μm.
(P–S) Quantification of CGRP-positive and NGF-positive cells in knee joint ($n = 6$) and DRG ($n = 5$) based on IF images.
Data are expressed as means ± SD. $^{*}p < 0.05$, $^{**}p < 0.01$, $^{***}p < 0.001$. One-way ANOVA, followed by Tukey's post hoc test, was used for multiple group comparisons.

Please cite this article in press as: Qin et al., Semaglutide ameliorates osteoarthritis progression through a weight loss-independent metabolic restoration mechanism, Cell Metabolism (2026), https://doi.org/10.1016/j.cmet.2026.01.008

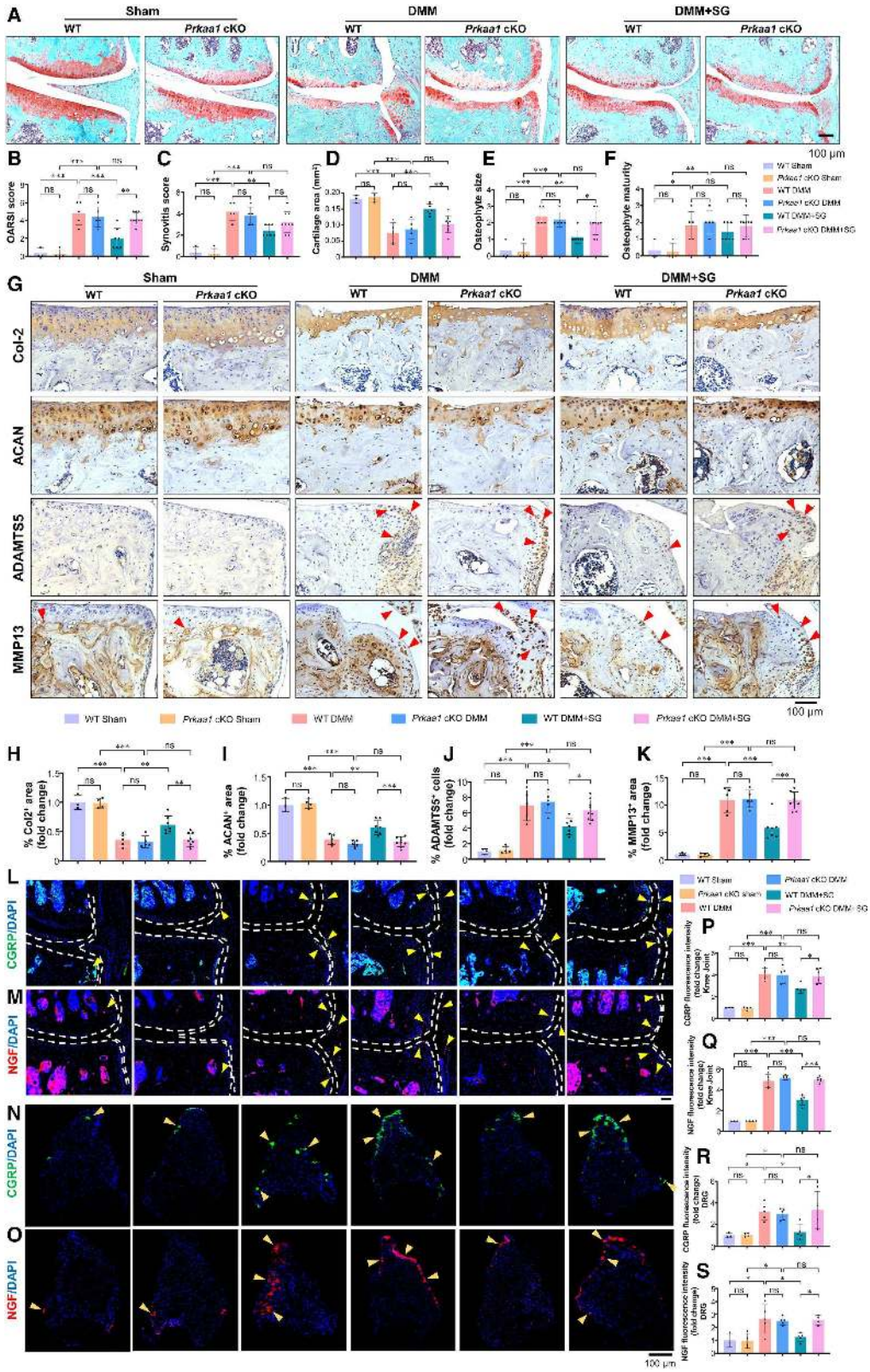

Figure 6. *Prkaa1* KO diminishes the protective effect of SG on cartilage

(A) Histological analysis of WT and *Prkaa1* cKO mice with or without SG treatment (n = 3–9). Scale bar, 100 μm. Six groups of mice were included: sham/WT, sham/*Prkaa1* cKO, DMM/WT, DMM/*Prkaa1* cKO, DMM + SG/WT, and DMM + SG/*Prkaa1* cKO.

(legend continued on next page)

Please cite this article in press as: Qin et al., Semaglutide ameliorates osteoarthritis progression through a weight loss-independent metabolic restoration mechanism, Cell Metabolism (2026), https://doi.org/10.1016/j.cmet.2026.01.008

progression, chondrocytes face increased metabolic demands for protein synthesis and cell proliferation, benefiting the cell survival and tissue repair. As a rapid energy source, glycolysis remains dominant during this transition. Our results also confirmed this phenomenon. However, glycolysis is an inefficient ATP-producing process, yielding only two ATP molecules per glucose molecule and leading to excessive lactate accumulation. In contrast, TCA cycle and OXPHOS generate up to 36 ATP molecules per glucose molecule while producing only CO_2 and H_2O as byproducts.[43] This difference highlights the importance of metabolic flexibility in maintaining chondrocyte function and survival.

To balance the dual demands for biosynthetic precursors and ATP, cells often integrate multiple metabolic pathways. Signaling networks, such as AMPK and mTOR, orchestrate these transitions by monitoring cellular energy status[44,45] and adjusting metabolic flux accordingly. AMPK, a cellular energy sensor, is phosphorylated and activated when the AMP/ATP ratio rises, leading to phosphorylation of multiple downstream targets, including PFKFB3, which was demonstrated in our work. PFKFB3 plays a central role in regulating glycolytic flux and linking it to mitochondrial metabolism. However, under OA conditions, AMPK signaling is frequently downregulated, contributing to intracellular ATP depletion. As a result, chondrocytes undergo apoptosis or cell-cycle arrest, failing to repair damaged cartilage. Therefore, AMPK is regarded as one of the key targets for OA treatment. Metformin, an AMPK activator, has been proven in both preclinical and clinical studies to exert therapeutic effects on OA.[46,47] Our study showed that SG restores AMPK phosphorylation in OA cartilage, upregulating PFKFB3 expression and activity. This dual activation stimulates both glycolysis and TCA cycle-OXPHOS pathway, boosting ATP production while generating critical biosynthetic precursors such as acetyl-coenzyme A (CoA) and NADPH for ECM synthesis.

From a broader perspective, energy regulation governs every stage of life, from growth and development to aging and disease. Following Schrödinger's concept of negative entropy, living systems extract and manage energy to maintain order and counteract entropy-driven decay.[48] Intricate regulation of energy metabolism, ensuring neither excessive nor insufficient ATP production, is essential for sustaining health and longevity. GLP-1R agonists, by fine-tuning energy metabolism, may exert system-wide benefits beyond glucose regulation. This metabolic precision could explain their promising effects in diverse diseases, including OA.

Limitations of the study

The GLP-1R is known to be widely expressed in multiple tissues, including joint tissues, suggesting that SG may exert local effects in the joint tissue in addition to its systemic effects reversing metabolic disorders. Therefore, further investigation is needed to clarify whether the anti-OA effects of SG are directly mediated through local GLP-1R signaling mechanism within the joints. Moreover, the pilot study was limited by the small sample size and the sub-millimeter level resolution of MRI. Therefore, the protective effects of SG on human knee joint should be interpreted with caution and require further validation by clinical trials with larger and well-powered sample size and employing higher-resolution imaging techniques.

RESOURCE AVAILABILITY

Lead contact

Further information and requests for resources should be directed to and will be fulfilled by the lead contact, Liping Tong (lp.tong@siat.ac.cn).

Materials availability

All unique reagents generated in this study are available from the lead contact upon request.

Data and code availability

- Uncropped western blots and source data are in Data S1. Other data are available from the lead contact upon request.
- This study did not generate any code.

ACKNOWLEDGMENTS

This project was supported by National Natural Science Foundation of China (NSFC) grants (82394445, 82030067, and 82172397) to D.C. and L.T., Shenzhen Medical Research Funds (B2502005) to D.C., and Shenzhen Science and Technology Research Funding (JCYJ20220818101414032) to L.T.

AUTHOR CONTRIBUTIONS

L.T. and D.C. conceived and designed the project and supervised the research. J.R.S. helped to design the project. L.T. and D.C. wrote the manuscript with input from all authors. H.Q., J.Y., H.Y., C.Z., Z.Z., Z.W., G.W., and P.O. collected and analyzed the data for the project. Z.L., H.J., G.X., J.S., X.B., and H.W. provided input for data analysis and manuscript revision. H.-T.Z. supervised the clinical studies, and D.Y. analyzed the clinical data. All authors have read and commented on the manuscript, and all the authors have access to the data.

DECLARATION OF INTERESTS

The authors declare no competing interests.

STAR★METHODS

Detailed methods are provided in the online version of this paper and include the following:

- KEY RESOURCES TABLE
- EXPERIMENTAL MODEL AND STUDY PARTICIPANT DETAILS
  - Mice

(B–F) Histomorphometric analyses of mice from various groups, including OARSI score (B), synovitis score (C), cartilage area (D), osteophyte size (E), and osteophyte maturity (F, n = 3–9).
(G) Expression of Col-2, ACAN, ADAMTS5, and MMP13 was analyzed by IHC (n = 3–9). Scale bar, 100 μm.
(H–K) Quantification of Col-2-, ACAN-, ADAMTS5-, and MMP13-positive cells/area in different mice (n = 3–9).
(L–O) Expression of CGRP and NGF in knee joint (n = 3–6) and in DRGs (n = 3–5) was measured by IF staining. Scale bar, 100 μm.
(P–S) Quantification of CGRP-positive and NGF-positive cells in knee joint (n = 3–6) and DRG (n = 3–5) based on IF images.
Data are expressed as means ± SD. $^{*}p < 0.05$, $^{**}p < 0.01$, $^{***}p < 0.001$. One-way ANOVA, followed by the Tukey's post hoc test, were used for multiple group comparisons.

Please cite this article in press as: Qin et al., Semaglutide ameliorates osteoarthritis progression through a weight loss-independent metabolic restoration mechanism, Cell Metabolism (2026), https://doi.org/10.1016/j.cmet.2026.01.008

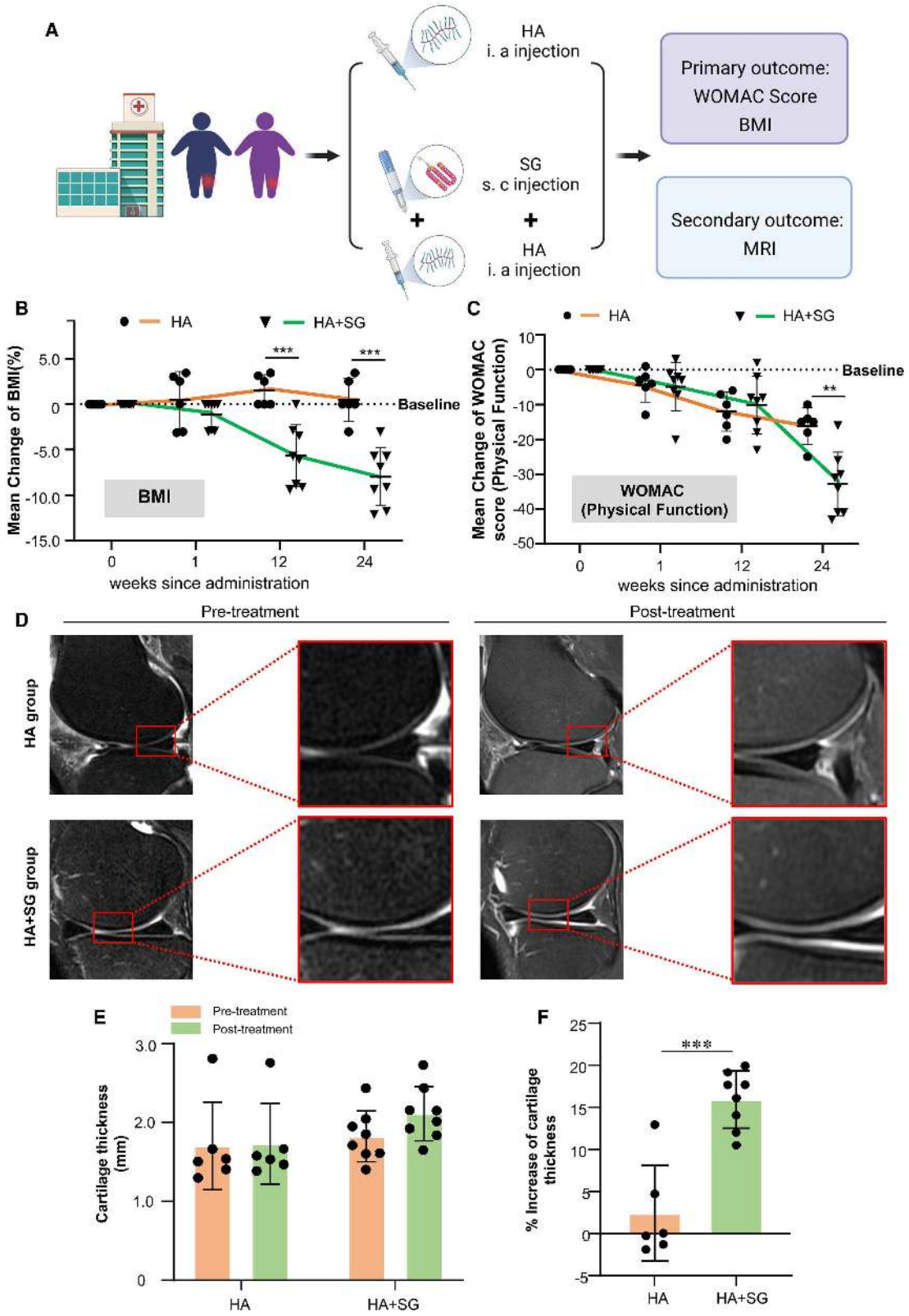

Figure 7. SG ameliorates cartilage degradation in the knee joint of individuals with obesity/OA

(A) Overall study flow of pilot clinical trial.

(B) Change of BMI and was monitored before and after HA and HA + SG administration (n = 6–8).

(legend continued on next page)

Please cite this article in press as: Qin et al., Semaglutide ameliorates osteoarthritis progression through a weight loss-independent metabolic restoration mechanism, Cell Metabolism (2026), https://doi.org/10.1016/j.cmet.2026.01.008

- Pilot clinical study
- METHOD DETAILS
  - Obesity animal model establishment
  - Osteoarthritis animal model establishment and semaglutide injection
  - Pain-related behavior tests
  - Micro-CT analysis
  - Histological analysis
  - Immunohistochemistry and immunofluorescence analyses
  - Proteomics analysis
  - Culture of primary articular chondrocytes
  - Western blot analysis
  - Lactate dehydrogenase activity assay
  - Pyruvate dehydrogenase activity assay
  - ATP production assay
  - Seahorse XF-96 energetic analysis
  - Molecular dynamics simulation
  - Generation of *Glp-1r* knockout mice and *Prkaa1-flox* mice
- QUANTIFICATION AND STATISTICAL ANALYSIS

SUPPLEMENTAL INFORMATION

Supplemental information can be found online at https://doi.org/10.1016/j.cmet.2026.01.008.

Received: February 19, 2025
Revised: August 15, 2025
Accepted: January 12, 2026

REFERENCES

1. Global Burden of Disease Collaborative Network (2020). Global Burden of Disease Study 2019 (GBD 2019) results. https://ghdx.healthdata.org/gbd-2019.
2. World Health Organization (2023). Osteoarthritis. https://www.who.int/news-room/fact-sheets/detail/osteoarthritis.
3. Tong, L.P., Yu, H., Huang, X.Y., Shen, J., Xiao, G.Z., Chen, L., Wang, H.Y., Xing, L.P., and Chen, D. (2022). Current understanding of osteoarthritis pathogenesis and relevant new approaches. Bone Res. *10*, 60. https://doi.org/10.1038/s41413-022-00226-9.
4. He, Y.X., Jiang, W.K., and Wang, W.J. (2024). Global burden of osteoarthritis in adults aged 30 to 44 years, 1990 to 2019: results from the Global Burden of Disease Study 2019. BMC Musculoskelet. Disord. *25*, 303. https://doi.org/10.1186/s12891-024-07442-w.
5. Bijlsma, J.W.J., Berenbaum, F., and Lafeber, F.P.J.G. (2011). Osteoarthritis: an update with relevance for clinical practice. Lancet *377*, 2115–2126. https://doi.org/10.1016/S0140-6736(11)60243-2.
6. Wei, G., Lu, K., Umar, M., Zhu, Z., Lu, W.W., Speakman, J.R., Chen, Y., Tong, L., and Chen, D. (2023). Risk of metabolic abnormalities in osteoarthritis: a new perspective to understand its pathological mechanisms. Bone Res. *11*, 63. https://doi.org/10.1038/s41413-023-00301-9.
7. Zhuo, Q., Yang, W., Chen, J., and Wang, Y. (2012). Metabolic syndrome meets osteoarthritis. Nat. Rev. Rheumatol. *8*, 729–737. https://doi.org/10.1038/nrrheum.2012.135.
8. Kahn, S.E., Hull, R.L., and Utzschneider, K.M. (2006). Mechanisms linking obesity to insulin resistance and type 2 diabetes. Nature *444*, 840–846. https://doi.org/10.1038/nature05482.
9. Alfaris, N., Waldrop, S., Johnson, V., Boaventura, B., Kendrick, K., and Stanford, F.C. (2024). GLP-1 single, dual, and triple receptor agonists for treating type 2 diabetes and obesity: a narrative review. EClinicalmedicine *75*, 102782. https://doi.org/10.1016/j.eclinm.2024.102782.
10. Tahrani, A.A., Bailey, C.J., Del Prato, S., and Barnett, A.H. (2011). Management of type 2 diabetes: new and future developments in treatment. Lancet *378*, 182–197. https://doi.org/10.1016/s0140-6736(11)60207-9.
11. Kim, S., Jung, J., Kim, H., Heo, R.W., Yi, C.O., Lee, J.E., Jeon, B.T., Kim, W.H., Hahm, J.R., and Roh, G.S. (2014). Exendin-4 improves nonalcoholic fatty liver disease by regulating glucose transporter 4 expression in ob/ob mice. Korean J. Physiol. Pharmacol. *18*, 333–339. https://doi.org/10.4196/kjpp.2014.18.4.333.
12. Yang, S., Zhao, X., Zhang, Y., Tang, Q., Li, Y., Du, Y., and Yu, P. (2024). Tirzepatide shows neuroprotective effects via regulating brain glucose metabolism in APP/PS1 mice. Peptides *179*, 171271. https://doi.org/10.1016/j.peptides.2024.171271.
13. Beiroa, D., Imbernon, M., Gallego, R., Senra, A., Herranz, D., Villarroya, F., Serrano, M., Fernø, J., Salvador, J., Escalada, J., et al. (2014). GLP-1 agonism stimulates brown adipose tissue thermogenesis and browning through hypothalamic AMPK. Diabetes *63*, 3346–3358. https://doi.org/10.2337/db14-0302.
14. Zhang, Y., Chen, H., Feng, Y., Liu, M., Lu, Z., Hu, B., Chen, L., Zhang, Y., Liu, J., Cai, F., et al. (2025). Activation of AMPK by GLP-1R agonists mitigates Alzheimer-related phenotypes in transgenic mice. Nat. Aging *5*, 1097–1113. https://doi.org/10.1038/s43587-025-00869-3.
15. Song, S., Guo, R.Y., Mehmood, A., Zhang, L., Yin, B.W., Yuan, C.C., Zhang, H.l., Guo, L., and Li, B. (2022). Liraglutide attenuate central nervous inflammation and demyelination through AMPK and pyroptosis-related NLRP3 pathway. CNS Neurosci. Ther. *28*, 422–434. https://doi.org/10.1111/cns.13791.
16. Koska, J., Sands, M., Burciu, C., D'Souza, K.M., Raravikar, K., Liu, J., Truran, S., Franco, D.A., Schwartz, E.A., Schwenke, D.C., et al. (2015). Exenatide protects against glucose- and lipid-induced endothelial dysfunction: evidence for direct vasodilation effect of GLP-1 receptor agonists in humans. Diabetes *64*, 2624–2635. https://doi.org/10.2337/db14-0976.
17. Wang, C.S., Li, L., Liu, S.Y., Liao, G.N., Li, L., Chen, Y.N., Cheng, J., Lu, Y., and Liu, J.P. (2018). GLP-1 receptor agonist ameliorates obesity-induced chronic kidney injury via restoring renal metabolism homeostasis. PLoS One *13*, e0193473. https://doi.org/10.1371/journal.pone.0193473.
18. Wu, L.T., Zhou, M., Li, T.Y., Dong, N., Yi, L., Zhang, Q.Y., and Mi, M.T. (2022). GLP-1 regulates exercise endurance and skeletal muscle remodeling via GLP-1R/AMPK pathway. Biochim. Biophys. Acta Mol. Cell Res. *1869*, 119300. https://doi.org/10.1016/j.bbamcr.2022.119300.
19. Lincoff, A.M., Brown-Frandsen, K., Colhoun, H.M., Deanfield, J., Emerson, S.S., Esbjerg, S., Hardt-Lindberg, S., Hovingh, G.K., Kahn, S.E., Kushner, R.F., et al. (2023). Semaglutide and cardiovascular outcomes in obesity without diabetes. N. Engl. J. Med. *389*, 2221–2232. https://doi.org/10.1056/NEJMoa2307563.
20. Perkovic, V., Tuttle, K.R., Rossing, P., Mahaffey, K.W., Mann, J.F.E., Bakris, G., Baeres, F.M.M., Idorn, T., Bosch-Traberg, H., Lausvig, N.L., et al. (2024). Effects of semaglutide on chronic kidney disease in patients with type 2 diabetes. N. Engl. J. Med. *391*, 109–121. https://doi.org/10.1056/NEJMoa2403347.
21. Meissner, W.G., Remy, P., Giordana, C., Maltête, D., Derkinderen, P., Houéto, J.-L., Anheim, M., Benatru, I., Boraud, T., Brefel-Courbon, C., et al. (2024). Trial of lixisenatide in early Parkinson's disease. N. Engl. J. Med. *390*, 1176–1185. https://doi.org/10.1056/NEJMoa2312323.

(C) Change of physical function of knee joint was evaluated by WOMAC score before and after HA and HA + SG administration (n = 6–8).
(D) Knee OA was monitored by MRI before and after treatment with HA or treatment with HA + SG (n = 6–8).
(E) Articular cartilage thickness was analyzed by 3D Slicer software based on MRI image.
(F) The percentage rate of the increased cartilage thickness in femoral condyle in the individuals with HA and HA + SG treatments was calculated (n = 6–8).
Data are expressed as means ± SD. $^{*}p < 0.05$, $^{**}p < 0.01$, $^{***}p < 0.001$. Unpaired Student's t test was used for two groups comparison.

Please cite this article in press as: Qin et al., Semaglutide ameliorates osteoarthritis progression through a weight loss-independent metabolic restoration mechanism, Cell Metabolism (2026), https://doi.org/10.1016/j.cmet.2026.01.008

22. Lenharo, M. (2024). Why do obesity drugs seem to treat so many other ailments? Nature *633*, 758–760. https://doi.org/10.1038/d41586-024-03074-1.

23. Meurot, C., Martin, C., Sudre, L., Breton, J., Bougault, C., Rattenbach, R., Bismuth, K., Jacques, C., and Berenbaum, F. (2022). Liraglutide, a glucagon-like peptide 1 receptor agonist, exerts analgesic, anti-inflammatory and anti-degradative actions in osteoarthritis. Sci. Rep. *12*, 1567. https://doi.org/10.1038/s41598-022-05323-7.

24. Zhu, H., Zhou, L., Wang, Q., Cai, Q., Yang, F., Jin, H., Chen, Y., Song, Y., and Zhang, C. (2023). Glucagon-like peptide-1 receptor agonists as a disease-modifying therapy for knee osteoarthritis mediated by weight loss: findings from the Shanghai Osteoarthritis Cohort. Ann. Rheum. Dis. *82*, 1218–1226. https://doi.org/10.1136/ard-2023-223845.

25. Maretty, L., Gill, D., Simonsen, L., Soh, K., Zagkos, L., Galanakis, M., Sibbesen, J., Iglesias, M.T., Secher, A., Valkenborg, D., et al. (2025). Proteomic changes upon treatment with semaglutide in individuals with obesity. Nat. Med. *31*, 267–277. https://doi.org/10.1038/s41591-024-03355-2.

26. Wu, C.L., Zhao, S.P., and Yu, B.L. (2015). Intracellular role of exchangeable apolipoproteins in energy homeostasis, obesity and non-alcoholic fatty liver disease. Biol. Rev. Camb. Philos. Soc. *90*, 367–376. https://doi.org/10.1111/brv.12116.

27. Bartrons, R., and Caro, J. (2007). Hypoxia, glucose metabolism and the Warburg's effect. J. Bioenerg. Biomembr. *39*, 223–229. https://doi.org/10.1007/s10863-007-9080-3.

28. De Bock, K., Georgiadou, M., Schoors, S., Kuchnio, A., Wong, B.W., Cantelmo, A.R., Quaegebeur, A., Ghesquière, B., Cauwenberghs, S., Eelen, G., et al. (2013). Role of PFKFB3-driven glycolysis in vessel sprouting. Cell *154*, 651–663. https://doi.org/10.1016/j.cell.2013.06.037.

29. Kaihara, K.A., Dickson, L.M., Ellenbroek, J.H., Orr, C.M.D., Layden, B.T., and Wicksteed, B. (2015). PKA enhances the acute insulin response leading to the restoration of glucose control. Diabetes *64*, 1688–1697. https://doi.org/10.2337/db14-1051.

30. Matsuoka, K., Bakiri, L., Bilban, M., Toegel, S., Haschemi, A., Yuan, H., Kasper, M., Windhager, R., and Wagner, E.F. (2023). Metabolic rewiring controlled by c-Fos governs cartilage integrity in osteoarthritis. Ann. Rheum. Dis. *82*, 1227–1239. https://doi.org/10.1136/ard-2023-224002.

31. Mookerjee, S.A., Gerencser, A.A., Nicholls, D.G., and Brand, M.D. (2017). Quantifying intracellular rates of glycolytic and oxidative ATP production and consumption using extracellular flux measurements. J. Biol. Chem. *292*, 7189–7207. https://doi.org/10.1074/jbc.M116.774471.

32. Wu, X., Liyanage, C., Plan, M., Stark, T., McCubbin, T., Barrero, R.A., Batra, J., Crawford, R., Xiao, Y., and Prasadam, I. (2023). Dysregulated energy metabolism impairs chondrocyte function in osteoarthritis. Osteoarthr. Cartil. *31*, 613–626. https://doi.org/10.1016/j.joca.2022.11.004.

33. Wilding, J.P.H., Batterham, R.L., Calanna, S., Davies, M., Van Gaal, L.F., Lingvay, I., McGowan, B.M., Rosenstock, J., Tran, M.T.D., Wadden, T.A., et al. (2021). Once-weekly semaglutide in adults with overweight or obesity. N. Engl. J. Med. *384*, 989–1002. https://doi.org/10.1056/NEJMoa2032183.

34. Bliddal, H., Bays, H., Czernichow, S., Uddén Hemmingsson, J., Hjelmesæth, J., Hoffmann Morville, T., Koroleva, A., Skov Neergaard, J., Vélez Sánchez, P., Wharton, S., et al. (2024). Once-weekly semaglutide in persons with obesity and knee osteoarthritis. N. Engl. J. Med. *391*, 1573–1583. https://doi.org/10.1056/NEJMoa2403664.

35. Bowers, M.E., Trinh, N., Tung, G.A., Crisco, J.J., Kimia, B.B., and Fleming, B.C. (2008). Quantitative MR imaging using "LiveWire" to measure tibiofemoral articular cartilage thickness. Osteoarthr. Cartil. *16*, 1167–1173. https://doi.org/10.1016/j.joca.2008.03.005.

36. Sampath, S.J.P., Venkatesan, V., Ghosh, S., and Kotikalapudi, N. (2023). Obesity, metabolic syndrome, and osteoarthritis-an updated review. Curr. Obes. Rep. *12*, 308–331. https://doi.org/10.1007/s13679-023-00520-5.

37. Chen, J., Xie, J.J., Shi, K.S., Gu, Y.T., Wu, C.C., Xuan, J., Ren, Y., Chen, L., Wu, Y.S., Zhang, X.L., et al. (2018). Glucagon-like peptide-1 receptor regulates endoplasmic reticulum stress-induced apoptosis and the associated inflammatory response in chondrocytes and the progression of osteoarthritis in rat. Cell Death Dis. *9*, 212. https://doi.org/10.1038/s41419-017-0217-y.

38. Claassen, H., Schicht, M., Brandt, J., Reuse, K., Schädlich, R., Goldring, M.B., Guddat, S.S., Thate, A., and Paulsen, F. (2011). C-28/I2 and T/C-28a2 chondrocytes as well as human primary articular chondrocytes express sex hormone and insulin receptors–useful cells in study of cartilage metabolism. Ann. Anat. *193*, 23–29. https://doi.org/10.1016/j.aanat.2010.09.005.

39. Bonora, M., Patergnani, S., Rimessi, A., De Marchi, E., Suski, J.M., Bononi, A., Giorgi, C., Marchi, S., Missiroli, S., Poletti, F., et al. (2012). ATP synthesis and storage. Purinergic Signal. *8*, 343–357. https://doi.org/10.1007/s11302-012-9305-8.

40. Vander Heiden, M.G., Cantley, L.C., and Thompson, C.B. (2009). Understanding the Warburg effect: the metabolic requirements of cell proliferation. Science *324*, 1029–1033. https://doi.org/10.1126/science.1160809.

41. Bora, F.W., Jr., and Miller, G. (1987). Joint physiology, cartilage metabolism, and the etiology of osteoarthritis. Hand Clin. *3*, 325–336. https://doi.org/10.1016/S0749-0712(21)00667-3.

42. Mobasheri, A., Rayman, M.P., Gualillo, O., Sellam, J., van der Kraan, P., and Fearon, U. (2017). The role of metabolism in the pathogenesis of osteoarthritis. Nat. Rev. Rheumatol. *13*, 302–311. https://doi.org/10.1038/nrrheum.2017.50.

43. Lehninger, A.L., Nelson, D.L., and Cox, M.M. (1993). Principles of Biochemistry. Second Edition (Worth Publishers).

44. Yi, D., Yu, H., Lu, K., Ruan, C.S., Ding, C.H., Tong, L.P., Zhao, X.L., and Chen, D. (2021). AMPK signaling in energy control, cartilage biology, and osteoarthritis. Front. Cell Dev. Biol. *9*, 696602. https://doi.org/10.3389/fcell.2021.696602.

45. Xu, J., Ji, J., and Yan, X.H. (2012). Cross-talk between AMPK and mTOR in regulating energy balance. Crit. Rev. Food Sci. Nutr. *52*, 373–381. https://doi.org/10.1080/10408398.2010.500245.

46. Li, J., Zhang, B., Liu, W.X., Lu, K., Pan, H., Wang, T., Oh, C.D., Yi, D., Huang, J., Zhao, L., et al. (2020). Metformin limits osteoarthritis development and progression through activation of AMPK signalling. Ann. Rheum. Dis. *79*, 635–645. https://doi.org/10.1136/annrheumdis-2019-216713.

47. Pan, F., Wang, Y., Lim, Y.Z., Urquhart, D.M., Estee, M.M., Wluka, A.E., Wolfe, R., and Cicuttini, F.M. (2025). Metformin for knee osteoarthritis in patients with overweight or obesity: a randomized clinical trial. JAMA *333*, 1804–1812. https://doi.org/10.1001/jama.2025.3471.

48. Schrödinger, E. (1944). What Is Life? (Cambridge University Press).

Please cite this article in press as: Qin et al., Semaglutide ameliorates osteoarthritis progression through a weight loss-independent metabolic restoration mechanism, Cell Metabolism (2026), https://doi.org/10.1016/j.cmet.2026.01.008

STAR★METHODS

KEY RESOURCES TABLE

REAGENT or RESOURCE	SOURCE	IDENTIFIER
Antibodies		
Rabbit anti-MMP13	Proteintech	Cat# 18165-1-AP; RRID: AB_2144858
Rabbit anti-ADAMTS5	Abcam	Cat# ab182795; RRID: AB_3674569
Rabbit anti-Aggrecan	Abcam	Cat# ab3778; RRID: AB_304071, Cat# ab313637; RRID:AB_3166183
Rabbit anti-Collagen II	Proteintech	Cat# 28459-1-AP; RRID: AB_2881147
Rabbit anti-Collagen X	Abcam	Cat# ab264571; RRID: AB_3735054
Rabbit anti-CGRP	Abcam	Cat# ab283568; RRID: AB_3105794
Rabbit anti-NGF	Abcam	Cat# ab6199; RRID: AB_2152414
Rabbit anti-PGP9.5	Abcam	Cat# ab108986; RRID: AB_10891773
Mouse anti-c-Fos	Abcam	Cat# ab208942; RRID: AB_2747772
Rabbit anti-PFKFB1	Abcam	Cat# ab155564; RRID: AB_3734921
Rabbit anti-PFKFB2	Huabio	Cat# ER1915-04; RRID: AB_3071297
Rabbit anti-PFKFB3	Proteintech	Cat# 13763-1-AP; RRID: AB_2162854
Rabbit anti-PFKFB4	Proteintech	Cat# 29902-1-AP; RRID: AB_2935486
Rabbit anti-p-PFKFB3	Abcam	Cat# ab202291; RRID: AB_3698749
Rabbit anti-AMPK	Proteintech	Cat# 10929-2-AP; RRID: AB_2169568
Rabbit anti-p-AMPK	Abcam	Cat# ab23875: RRID: AB_447741
Rabbit anti-LDHA	Proteintech	Cat# 19987-1-AP; RRID: AB_10646429
Rabbit anti-PDH	Proteintech	Cat# 18068-1-AP; RRID: AB_2162931
Mouse anti-β-Actin	Proteintech	Cat# 66009-1-Ig; RRID: AB_2687938
Mouse anti-GAPDH	Proteintech	Cat# 60004-1-Ig; RRID: AB_2107436
Rabbit anti-Insulin Receptor	Huabio	Cat# ET1705-22; RRID: AB_3070555
Rabbit anti-GLP-1 Receptor	Huabio	Cat# HA500204; RRID: AB_3071301
Mouse anti-PFKL	Proteintech	Cat# 68385-1-Ig; RRID: AB_3085103
Chemicals, peptides, and recombinant proteins		
Semaglutide	Weikeqi biotechnology	Cat# WKQ-0013363
Safranin O/Fast Green	Solarbio	Cat# G1375
Paraformaldehyde	Biosharp	Cat# BL539A
DAPI	Vector Laboratories	Cat# NC9524612
Collagenase II	Gibco	Cat# 17101015
DMEM/F-12 medium	Gibco	Cat# C11330500BT
Seahorse XF DMEM media	Agilent	Cat# 103575-100
Fetal Bovine Serum	Thermo Fisher	Cat# 10091148C
Penicillin-Streptomycin	Gibco	Cat# 15140122
Trypsin	Gibco	Cat# 25200-056
TNF-α	Peprotech	Cat# 315-01
Trizol	Invitrogen	Cat# 15586-018
Glucose	Agilent	Cat# 103577-100
Glutamine	Agilent	Cat# 103579-100
Pyruvate	Agilent	Cat# 103578-100
Automated Cell Counter	Invitrogen	Cat# AMQAX2000
Metformin	Selleck	Cat# S5958
Avexitide (GLP-1R inhibitor)	Selleck	Cat# P1203
GSK1904529A (Insulin inhibitor)	Selleck	Cat# S1093

(*Continued on next page*)

Please cite this article in press as: Qin et al., Semaglutide ameliorates osteoarthritis progression through a weight loss-independent metabolic restoration mechanism, Cell Metabolism (2026), https://doi.org/10.1016/j.cmet.2026.01.008

Continued

REAGENT or RESOURCE	SOURCE	IDENTIFIER
Compound C (AMPK inhibitor)	Selleck	Cat# S7840
PFK15 (PFKFB3 inhibitor)	Selleck	Cat# S7289
H-89 (PKA inhibitor)	Selleck	Cat# S1582
SuperSignal West Pico chemiluminescent substrate	Thermo	Cat# 34580
Sodium Hyaluronate Injection	Seikagaku	HJ20140533
Semaglutide	Novo Nordisk	SJ20210014
Critical commercial assays		
Total Cholesterol Assay Kit	Shanghai Kehua Bio-Engineering	Cat# K120
Triglycerides Assay Kit	Shanghai Kehua Bio-Engineering	Cat# K119
High-density lipoprotein Assay Kit	Shanghai Kehua Bio-Engineering	Cat# K116
Low-density lipoprotein Assay Kit	Shanghai Kehua Bio-Engineering	Cat# K117
Glycated hemoglobin ELISA Kit	Inselisa	Cat# INS-20651
VECTASTAIN Elite ABC Kit	Vector	Cat# PK-8200
ImmPACT DAB Peroxidase Substrate	Vector	Cat# SK-4105
BCA Assay Kit	Abcam	Cat# ab287853
Micro LDH Assay Kit	Abbkine	Cat# KTB1110
PDH Activity Assay Kit	Solarbio	Cat# BC0385
ATP Assay Kit	Beyotime	Cat# S0026B
Seahorse Cell Mito Stress Test Kit	Agilent	Cat# 103015-100
Seahorse Glycolysis Stress Test Kit	Agilent	Cat# 103020-100
Experimental models: Cell lines		
Mouse primary chondrocytes	Extract	N/A
Experimental models: Organisms/strains		
C57BL/6J mice	GemPharmatech	Strain Number: N000013
Glp-1r knockout mice	GemPharmatech	Customized product
Prkaa1-flox mice	GemPharmatech	Customized product
Software and algorithms		
G*power v3.1.9.7	Heinrich Heine University Düsseldorf	https://www.psychologie.hhu.de/arbeitsgruppen/allgemeine-psychologie-und-arbeitspsychologie/gpower
GraphPad Prism 10.0	GraphPad Software, LLC	https://www.graphpad.com
Image J	ImageJ.net	https://imagej.net
LABORAS 2.6 software	Metris	Netherlands
CellSens imaging software	Olympus	Japan
Avatar v1.6.7.2	PINGSENG scientific	China
Gromacs v 2021.1	Berendsen Lab	https://manual.gromacs.org
Pymol-open-source	Schrödinger	https://github.com/schrodinger/pymol-open-source
PDBFixer	OpenMM	https://github.com/openmm/pdbfixer
3D Slicer v 5.6.2	Slicer	https://www.slicer.org

EXPERIMENTAL MODEL AND STUDY PARTICIPANT DETAILS

Mice

The experiment protocol of animal studies for this project was approved by the Ethics Committee of the Shenzhen Institutes of Advanced Technology, Chinese Academy of Sciences. All experimental methods and procedures were conducted in accordance with the approved guidelines and adhered to all relevant ethical regulations for animal testing and research (SIAT-IACUC-240416-YYS-CD-A2641). All mice were housed in specific pathogen-free (SPF) conditions with five mice per cage, maintained under a

Please cite this article in press as: Qin et al., Semaglutide ameliorates osteoarthritis progression through a weight loss-independent metabolic restoration mechanism, Cell Metabolism (2026), https://doi.org/10.1016/j.cmet.2026.01.008

CellPress

12-hour light/dark cycle at a constant temperature of 22 °C. Cages, food, and water were changed weekly. We used the following genotypes of mice: C57BL/6J (GemPharmatech, Nanjing, China), *Glp-1r* knockout mice (GemPharmatech, Nanjing, China) and *Prkaa1* conditional knockout mice (GemPharmatech, Nanjing, China).

Pilot clinical study

We conducted a 24-week randomized pilot clinical study, which was approved by the ethics committee (approval number KY-2022-065 and KY-2023-209) of the First Affiliated Hospital of Jinan University, and the registration number is ChiCTR2200066291. The sample size calculation was provided in Statistical Analysis Plan (Data S2). A total of 20 persons were enrolled (Figure S7A), and all the participants signed the informed consent. Inclusion criteria included individuals aged 50-75 years with a body mass index (BMI)$\geq$28 kg/m^2, and clinically diagnosed with primary knee OA based on radiographical evidence by magnetic resonance imaging (MRI) imaging, with moderate pain present. Exclusion criteria encompassed the following: diagnosis of diabetes mellitus, rheumatoid arthritis, and other autoimmune diseases, parathyroid or renal diseases, recent use of glucocorticoid hormone, knee arthroscopy procedures, or intra-articular injections within the past 3 months, and a history of joint surgery. Following baseline assessments, participants were randomly assigned to receive either sodium hyaluronate intra-articular injection (HA group, Seikagaku Corporation, 25 mg/week for 5 weeks) or subcutaneous SG injection (HA+SG group, Novo Nordisk). Participants receiving SG treatment initiated with a dose of 0.25 mg in the first week, and increased the dose in a stepwise manner each subsequent week until reaching the target dose of 0.5 mg/week (incremental steps of 0.125 mg). The BMI and Western Ontario and McMaster Universities Osteoarthritis Index (WOMAC) score were monitored at 0-, 1-, 12- and 24- weeks. Severity of cartilage degeneration was evaluated by MRI at 0- and 24- weeks.

The MRI examination was performed on a 3.0-T MRI scanner (GE, SIGNA Premier) equipped with a phased array knee coil. The 2D MRI scanning parameters were detailed as follows: sagittal plane [TE = 40-80 ms, TR = 2500-3500 ms, slice thickness = 3.5-4.0 mm, spacing between slides = 4.0 mm], coronal plane [TE = 35-45 ms, TR = 2400-2800 ms, slice thickness = 3.5-4.0 mm, spacing between slides = 4.0 mm], and axial plane [TE = 35-45 ms, TR = 2500-3000 ms, slice thickness = 3.0-3.5 mm, spacing between slides = 4.0 mm]. All the acquired images were normalized through the Nor (3D) Modes of RIAS Medical Image Processing toolkit.[1] Then the changes in cartilage thickness were analyzed utilizing 3D Slicer software on the normalized MRI images. The reliability of method has been previously validated.[2] Manual segmentation of the articular cartilage structure was performed on the sagittal plane. The cartilage was divided into 21 subregions based on the International Cartilage Repair Association.[3] These subregions included the anterior condylar, central and posterior areas of both medial femur and lateral femur. The cartilage thickness was defined as the vertical shortest distance between the chondro-subchondral bone interface and the chondro-soft tissue surface. For each subregion, measurements were repeated three times, and mean value was used as the cartilage thickness.

METHOD DETAILS

Obesity animal model establishment

5-week-old male C57BL/6J mice were used to establish a diet-induced obesity (DIO) model. After a 5-day acclimatization period, the mice were randomly divided into a control group and a high-fat diet (HFD) group based on body weight. The control group was fed with a standard diet, while the HFD group received a diet comprising 60% of calories from fat. The HFD food was replaced every 3 days to ensure freshness. The model was considered successful when the average body weight of the HFD group was at least 20% higher than that of the control group. Key physiological and biochemical parameters, including the body weight, Lee's index [body weight (g)/nose-to-anus length (cm) x 10^3], body fat percentage [(inguinal subcutaneous fat + epididymal fat + perirenal fat + brown fat)/body weight x 100%], and serum biochemical markers (total cholesterol [TC], triglycerides [TG], high-density lipoprotein [HDL], low-density lipoprotein [LDL], and glycated hemoglobin [GHb]) were monitored.

In detail, blood samples were collected upon euthanasia of the mice, allowed to clot at room temperature for 30 minutes, and then centrifuged at 3,000 g for 10 minutes at 4 °C to separate the serum. The serum analysis was performed according to the manufacturers' instructions using the following kits: TC, TG, HDL and LDL assay Kits were purchased from Shanghai Kehua Bio-Engineering Co., Ltd., and GHb ELISA Kit (Wuhan EIAab, China).

Osteoarthritis animal model establishment and semaglutide injection

We determined the treatment effect of semaglutide (SG) on osteoarthritis (OA) and obesity/OA mice models. OA animal models were established based on destabilization of the medial meniscus (DMM) surgery as previously described.[4] In general, mice were anesthetized with 2 %–3 % isoflurane. The right knee was sterilized with 0.5% iodophor, and the hindlimb was flexed to 90° and secured. A 3-mm longitudinal skin incision was made along the medial edge of the patellar ligament, followed by blunt dissection of the subcutaneous tissue. Subsequently, the joint capsule was incised along the medial side of the patellar ligament to expose the medial meniscotibial ligament (MMTL), which was then transected using micro-scissors. Successful destabilization was confirmed intraoperatively. The wound was rinsed with sterile saline, and the joint capsule and skin were sutured. The sham group underwent the same surgical procedures, except that the MMTL was left intact. After the operation, 5 mg/kg of carprofen was injected subcutaneously every 24 hours for pain relief, and 40,000 units/kg of penicillin was injected intramuscularly to prevent infection. All the medications were administered for two consecutive days.

Please cite this article in press as: Qin et al., Semaglutide ameliorates osteoarthritis progression through a weight loss-independent metabolic restoration mechanism, Cell Metabolism (2026), https://doi.org/10.1016/j.cmet.2026.01.008

For the obesity/OA model, 80 obese mice were randomly divided into five groups: sham-operated group (Obesity), SG-injected sham-operated group (Obesity+SG), DMM surgery group (Obesity+DMM), SG-injected DMM surgery group (Obesity+DMM+SG), and pair-feeding DMM surgery group (Obesity+DMM+PF, n=16 per group). The SG-injected DMM surgery group and the pair-feeding DMM surgery group were paired by ear tag numbers, with each mouse housed individually. Compressed cotton pads were used as bedding instead of corncob to easily locate dropped food. The food-intake of Obesity+DMM+SG mice was equal to the total food intake of the previous day minus the remaining food (including food dropped on the bedding) collected the next day. The Obesity+DMM+PF mice were fed the equivalent food amount to the food-intake of Obesity+DMM+SG mice. Strict food-intake control can effectively rule out the influence of weight loss after appetite decrease induced by SG injection. All five groups continued to be fed with a high-fat diet in the aforementioned animal facility. The mice received weekly SG subcutaneous injection begun at four weeks after DMM surgery, until 12 weeks. The SG dose was calculated as before, and adjusted based on body weight measurements taken before each injection.

Pain-related behavior tests

Mechanical allodynia was assessed using a set of calibrated von Frey filaments (North Coast Medical Inc., CA, USA) in the von Frey test.[5,6] Prior to testing, mice were acclimated to a metal mesh for 1 hour to reduce stress. We applied the filaments (with force range 0.04 to 6.0 g, starting at 0.4 g) to the plantar surface of the hind paw, using an iterative method to determine the 50% withdrawal threshold. A positive response was recorded if the mouse showed any nocifensive behaviors, including rapid paw withdrawal or paw shaking, either during or immediately after the filament application.

Thermal nociception was evaluated using a hot plate apparatus (Xinruan XR1700, Shanghai, China). The hot plate temperature was set to 55 °C, and the latency to paw licking or jumping was recorded to the nearest 0.1 seconds. If no response occurred, with a maximum allowable duration of 30 seconds. Mice were returned to their cages immediately after testing for recovery.

The Laboratory Animal Behavior Observation, Registration, and Analysis System (LABORAS™, Metris, Hoofddorp, The Netherlands) was employed to evaluate long-term locomotion. Mice were placed in four separate cages with unrestricted access to food and water. The sensor platform electronically measured mechanical vibrations caused by animal movements. Detection began at 20:00 on the first night and continued until 08:00 the next morning, lasting 12 hours. Parameters analyzed included immobility, locomotion, rearing, distance, average speed, climbing, feeding. Data were acquired and calculated using LABORAS 2.6 software (Metris, The Netherlands).

Micro-CT analysis

After sacrificing the mice, the right knee joint was fixed in 4% formaldehyde overnight and rinsed with PBS before scanning. NEMO Micro-CT scanner (Pingsheng Healthcare Shanghai Inc., Shanghai, China) was used to scan samples. The voltage was set at 90 kV and the current at 70 μA, achieving a resolution of 10 μm. Images from each group were evaluated at the same threshold to allow for three-dimensional structural rendering of each sample. The region from the proximal tibial cartilage to below the growth plate was selected for three-dimensional histomorphometric analyses to determine cortical bone thickness and bone mineral density (BMD), trabecular bone volume per tissue volume (%, BV/TV), trabecular number (Tb.N.), trabecular separation (Tb.Sp.), and trabecular thickness (Tb.Th.) in subchondral bone.

Histological analysis

Following transcardiac perfusion of mice with 20 mL of ice-cold phosphate-buffered saline (PBS, pH 7.4), an additional 20 mL of 4% paraformaldehyde (PFA) was administered. Post-perfusion, the spinal cord and dorsal root ganglia (DRG) were fixed in 4% PFA overnight at 4°C, followed by dehydration through a sucrose gradient: the samples were first immersed in 15% sucrose overnight, then in 30% sucrose overnight, both steps performed at 4°C. These samples were then frozen in optimal cutting temperature (OCT) compound at −20°C. Using a cryostat microtome (Leica CM1950, Leica, Germany), transverse sections were prepared (20 μm for spinal cord and 12 μm for DRG) and promptly subjected to immunofluorescent (IF) staining. For histological staining, the knee joints were fixed in 4% PFA for 3 days, decalcified in EDTA solution for 21 days, and embedded in paraffin. Sections (4 μm thick) from the coronal plane of the knee joint were stained with Safranin O/Fast Green for morphological analysis. The severity of OA-like phenotype was assessed using OARSI scores, cartilage area, synovitis score, osteophyte size, and osteophyte maturity. The severity of OA-like phenotype was evaluated by two observers using the OARSI scoring system on three sections per joint (including the medial femoral condyle and medial tibial plateau).

Immunohistochemistry and immunofluorescence analyses

For immunohistochemistry (IHC) staining, the deparaffinized and rehydrated sections were placed in antigen retrieval solution and heated in a 99°C water bath for 5 minutes, followed by treatment with 0.5% Triton X-100 and an endogenous peroxidase blocking agent. After blocking with 10% normal goat serum for 1 hour, the sections were incubated with primary antibodies against MMP13, Aggrecan, Collagen II, Collagen X, and ADAMTS5 overnight at 4°C, followed by incubation with biotinylated goat anti-rabbit or goat anti-mouse secondary antibodies for 1 hour. Sections were then treated with the VECTASTAIN Elite ABC kit. IHC signals were visualized using the ImmPACT DAB Peroxidase Substrate.

For immunofluorescence (IF) staining, the sections were incubated with horseradish peroxidase-conjugated anti-fluorescein antibodies and mounted with VECTASHIELD mounting medium containing DAPI (Vector Laboratories, Burlingame, CA, USA). Briefly,

Please cite this article in press as: Qin et al., Semaglutide ameliorates osteoarthritis progression through a weight loss-independent metabolic restoration mechanism, Cell Metabolism (2026), https://doi.org/10.1016/j.cmet.2026.01.008

spinal cord and DRG sections were initially washed in 0.01 M PBS for 15 minutes, followed by a 1-hour incubation at room temperature with a blocking solution comprising 10% bovine serum albumin (BSA) and 0.3% Triton X-100 in 0.01 M PBS. Subsequently, the sections were incubated overnight at 4°C with primary antibodies diluted in the blocking solution. After thorough washing in 0.01 M PBS (three times for 10 minutes each), the sections were incubated with a secondary antibody for 1 hour at room temperature. Finally, they underwent three additional 10-minutes washes in 0.01 M PBS, were stained with DAPI for 10 minutes, and then mounted for examination. Histological, IHC, and IF images were captured using an Olympus IX71 microscope with CellSens imaging software. The number of IHC positive cells and ratio of IHC positive staining areas were analyzed using ImageJ software.

Proteomics analysis

Samples were lysed in 50 μL SISPROT lysis buffer *via* ultrasonication on ice for 5 minutes, and the supernatant was collected after centrifugation at 15,000 g for 10 minutes at 4°C. Protein concentrations were quantified using a BCA assay, and 10 μg of protein from each sample was subjected to pretreatment using the SISPROT kit. Peptide concentrations were measured using the Pierce Quantitative Fluorometric Peptide Assay Kit. For liquid chromatography, 200 ng of peptides were separated using a nanoElute UHPLC system (Bruker Daltonics, Germany) equipped with a reverse-phase C18 column (25 cm x 75 μm, 1.6 μm, Ion Opticks, Australia at 50°C and a flow rate of 0.3 μL/min. The elution was performed over a 60-minute gradient, with mobile phase B (0.1% formic acid in acetonitrile) increasing from 2% to 80%. The LC was coupled to a timsTOF Pro2 mass spectrometer (Bruker Daltonics, Germany) via a CaptiveSpray ion source, operating in diaPASEF mode. Raw data were processed using DIA-NN software (v1.8.1) with a library-free workflow, utilizing the Uniprot Mouse database (54,910 sequences) for spectral library generation. Match Between Runs (MBR) was applied to enhance identification, and results were filtered to a false discovery rate (FDR) <1% at both protein and precursor levels for quantification analysis.

Culture of primary articular chondrocytes

For murine chondrocyte cultures, primary mouse articular chondrocytes were isolated from articular cartilage of 5-day-old neonatal mice, as described previously.[5] To obtain primary chondrocytes, the articular cartilage from 5-day-old neonatal C57BL/6J mice was isolated using micro-scissors and forceps. After removal of attached fat and surrounding tissues, the cartilage was subjected to enzymatic digestion using 0.5% collagenase II overnight at 37 °C. The resulting cell suspension was filtered through a 70-μm cell strainer (BS-70-XBS, Biosharp), and the cells were collected by centrifugation at 1,000 rpm for 5 min. The harvested primary chondrocytes were cultured in Dulbecco's Modified Eagle Medium/Nutrient Mixture F-12 (DMEM/F-12) supplemented with 10% fetal bovine serum (FBS), 100 μg/ml streptomycin, and 100 IU/mL of penicillin at 37 °C. In order to retain the proper phenotype, chondrocytes were used for all experiments after one cell passage. The chondrocytes were treated for 24 hours with either SG (10 μM), TNF-α (20ng/mL), Compound C (an AMPK inhibitor, 1.25 μM) or PFK15 (a PFKFB3 inhibitor, 3.75 μM). Prior to SG and metformin (2 mM) treatment, chondrocytes were subjected to 1% low serum starvation for 24 hours, then changed to conventional medium with drug, and chondrocytes continued to be cultured for 4, 6,12 and 24 hours, respectively.

Western blot analysis

Protein samples were extracted from cells and separated via electrophoresis, followed by transferring to PVDF membranes (Bio-Rad, Hercules, CA, USA). The membranes were blocked with 3% skim milk and incubated with primary antibodies overnight at 4°C. After incubation with secondary antibodies for 1 hour at room temperature and washing in TBST for 30 minutes, the membranes were exposed to SuperSignal West Pico chemiluminescent substrate and visualized *via* autoradiography. Protein bands were quantitatively analyzed using ImageJ software.

Lactate dehydrogenase activity assay

The activity of lactate dehydrogenase (LDH) was assessed utilizing the Micro LDH Assay Kit post protein collection, following the manufacturer's instructions. In this process, LDH catalyzes the reduction of nicotinamide adenine dinucleotide (NAD+) to nicotinamide adenine dinucleotide hydrogenase (NADH), which subsequently reacts with WST-8 to generate a colored product for spectrophotometric quantification at a wavelength maximum (λ_{max}) of 450 nm.

Pyruvate dehydrogenase activity assay

The activity of pyruvate dehydrogenase (PDH) was assessed using the PDH Activity Assay Kit post protein collection, adhering strictly to the manufacturer's instructions. PDH catalyzes the dehydrogenation of pyruvic acid in reagent, concurrently reducing 2,6-dichlorophenolindophenol (2,6-DCPIP), resulting in a decrease in absorbance at a wavelength of 605 nm.

ATP production assay

The intracellular ATP levels were quantified using the ATP Assay Kit post protein collection, following the manufacturer's guidelines and read the relative light unit (RLU) by luminometer. ATP in the samples to be detected can participate the luciferase-mediated generation of fluorescence in the substrate. In a certain concentration range, the generation of fluorescence is proportional to the concentration of ATP, which is thereby allowing for the accurate measurement of intracellular ATP content.

Please cite this article in press as: Qin et al., Semaglutide ameliorates osteoarthritis progression through a weight loss-independent metabolic restoration mechanism, Cell Metabolism (2026), https://doi.org/10.1016/j.cmet.2026.01.008

Seahorse XF-96 energetic analysis

Primary articular chondrocytes were trypsinized, collected, quenched, and spun down, then were counted with Invitrogen Countess 3 Automated Cell Counter and plated in Seahorse XF-96 assay plates (Agilent, 103793-100) with 10,000 cells per well. After 12 hours of adherent growth at 37 °C in a 5% CO_2 incubator, the cells were treated with 20 ng/ml TNF-α and 10 μM SG for 24 hours. Media was gently removed by pipetting, and 180 μL Seahorse XF DMEM media was added to each well. Different kits were available for mitochondrial and glycolytic metabolism tests. For mitochondrial metabolism test, Seahorse Cell Mito Stress Test Kit was used in combined with XF DMEM assay media which containing 10 mM glucose, 2 mM glutamine, and 1 mM pyruvate. For glycolytic metabolism, Seahorse Glycolysis Stress Test Kit was used in cooperation with XF DMEM contains 2 mM glutamine. The assay was performed according to the instructions for Agilent Mito Stress Test and Glyco Stress Test. Extracellular acidification rate (ECAR) and oxygen consumption rate (OCR) per 10000 cells were calculated. Furthermore, total ATP production and the ratio of ATP from glycolysis and oxidative phosphorylation were calculated as reported before.[7]

Molecular dynamics simulation

Molecular dynamics (MD) simulations were conducted using the academic freeware package GROMACS 2021.1. The crystal structure of the protein and peptide was obtained from the Protein Data Bank (PDB: 7KI0).[8] The structure of the complex was preprocessed using PyMOL (Educational version) and PDBfixer, including the removal of water molecules, elimination of excess ligands, and the repair of missing atoms.[9] The protein topology parameters were generated using the AMBER99SB-ILDNP force field with the TIP3P water model, while the peptide topology was generated by the Amber force field.[10] Given that the binding site of SG is mainly located in the extracellular region of GLP-1R (encompassing the TM and ECD domain) and does not involve transmembrane processes, simulations were performed in an aqueous solution using the SPC216 water model in our study. The system was first energy-minimized using the steepest descent method. Following this, equilibration was carried out in two stages: a 100 ps NVT equilibration at 300 K and a 100 ps NPT equilibration at 1 bar, maintaining most parameters consistent with the NVT stage and using a time step of 2 fs. After equilibration, constraints were removed, and a 100 ns production MD simulation was performed with a 2 fs time step, saving energy and coordinate files at 100 ps intervals.

Generation of *Glp-1r* knockout mice and *Prkaa1-flox* mice

The *Glp-1r* gene is located on the Chr17 and the *Glp-1r* gene has 2 transcripts. According to the structure of *Glp-1r* gene, exon2-exon3 of *Glp-1r-201* transcript is recommended as the knockout (KO) region. The region contains 205 bp coding sequence. Deletion of this region will result in disruption of protein function. In this project, we have used CRISPR/Cas9 technology to modify *Glp-1r* gene. The *Glp-1r* KO mice were generated in GenPharmaTech company (Nanjing, China).

The *Prkaa1* gene encodes AMPK protein. The *Prkaa1* gene is located on the Chr15 and the *Prkaa1* gene has 2 transcripts. According to the structure of *Prkaa1* gene, exon2-exon3 of *Prkaa1-201* transcript is recommended as the KO region. The region contains 236 bp coding sequence. Deletion of this region will result in disruption of protein function. In this project we have used CRISPR/Cas9 technology to modify *Prkaa1* gene. The brief process is as follows: CRISPR/Cas9 system and Donor were microinjected into the fertilized eggs of C57BL/6JGpt mice. Fertilized eggs were transplanted to obtain positive F0 mice which were confirmed by PCR and sequencing. A stable F1 generation mouse model was obtained by mating positive F0 generation mice. The *flox* mice will be knocked out after mating with *Col2-CreER* transgenic mice, resulting in the loss of function of the *Prkaa1* gene in articular chondrocytes. The *Prkaa1-flox* mice were generated in GenPharmaTech company (Nanjing, China). Tamoxifen was injected 2 weeks before DMM surgery at the dose of 0.075 mg/g.

QUANTIFICATION AND STATISTICAL ANALYSIS

Data are presented as mean ± standard deviation (SD). Comparisons between two groups were made using unpaired Student's t-test, and multiple group comparisons were made using one-way ANOVA followed by Tukey's post hoc test. A significance level of $^{*}P < 0.05$ and $^{**}P < 0.01$, $^{***}P < 0.001$ was considered statistically significant.

Cell Metabolism, Volume *38*

Supplemental information

Semaglutide ameliorates osteoarthritis progression through a weight loss-independent metabolic restoration mechanism

Hongyu Qin, Jiamin Yu, Huan Yu, Chuqiao Zhou, Dongfeng Yuan, Ziling Wang, Zhenglin Zhu, Guizheng Wei, Peiyan Ou, Zhibin Li, Hua Jiang, Jie Shen, Guozhi Xiao, Xiaochun Bai, Huaiyu Wang, Huan-Tian Zhang, John R. Speakman, Di Chen, and Liping Tong

Supplementary Materials for

Semaglutide Ameliorates Osteoarthritis Progression through a Weight Loss Independent Metabolic Restoration Mechanism

Hongyu Qin[1,2,3,13], Jiamin Yu[1,2,4,13], Huan Yu[1,13], Chuqiao Zhou[1], Dongfeng Yuan[1,4], Ziling Wang[1,2], Zhenglin Zhu[5], Guizheng Wei[1,2], Peiyan Ou[1], Zhibin Li[6], Hua Jiang[3], Jie Shen[7], Guozhi Xiao[8], Xiaochun Bai[9], Huaiyu Wang[1], Huan-Tian Zhang[10*], John R. Speakman[11,12*], Di Chen[1,2,14*], Liping Tong[1,15*]

[13] These authors contributed equally
[14] Senior author
[15] Lead Contact

* Correspondence: zhanghuantian@jnu.edu.cn (H.Z.), j.speakman@abdn.ac.uk (J.S.), di.chen@siat.ac.cn (D.C.), lp.tong@siat.ac.cn (L.T.)

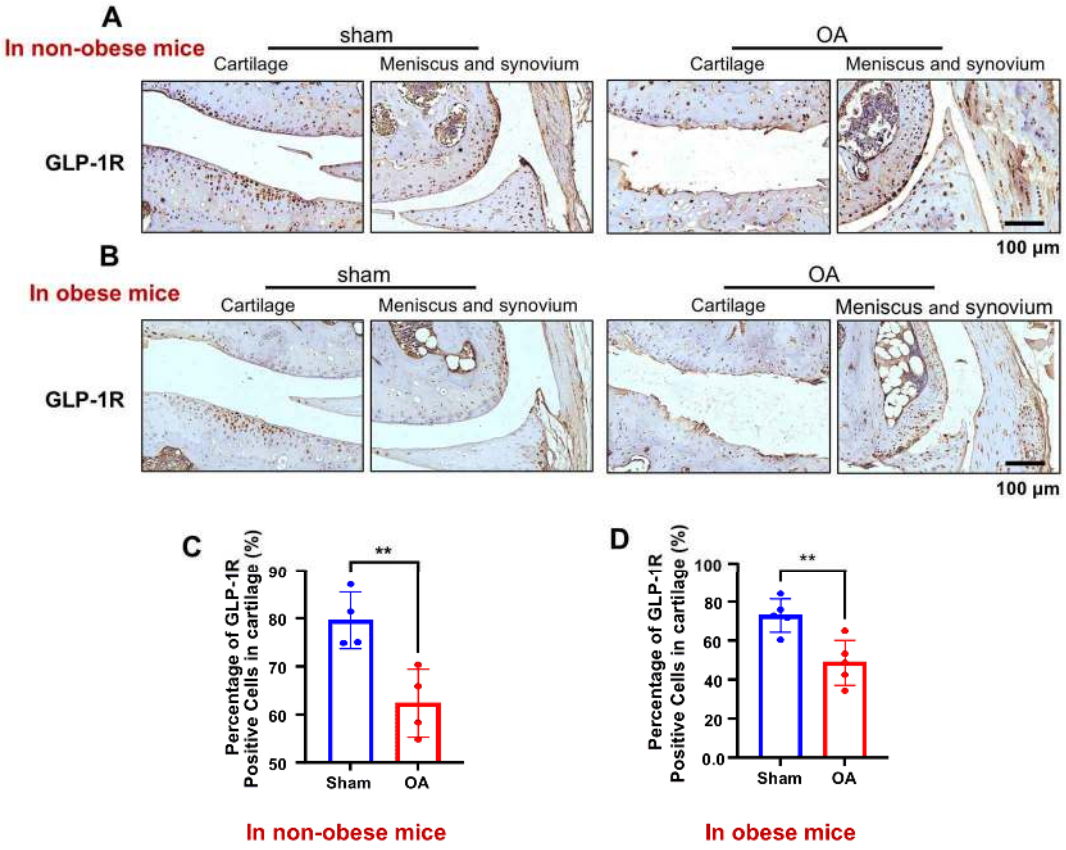

Figure S1. Distribution and expression of GLP-1 receptor (GLP-1R) in cartilage, related to Figure 1. (A) Distribution of GLP-1R in the cartilage of non-obese mice with or without OA (*n* = 4). Scale bar, 100 μm. (B) Distribution of GLP-1R in the cartilage of obese mice with or without OA (*n* = 4). Scale bar, 100 μm. (C-D) Quantification of GLP-1R positive cells based on immunohistochemical staining (*n* = 3-4). Data are expressed as means ± SD. **P* < 0.05 and ** *P* < 0.01, *** *P* < 0.001. Unpaired Student's *t*-test was used for two groups comparisons.

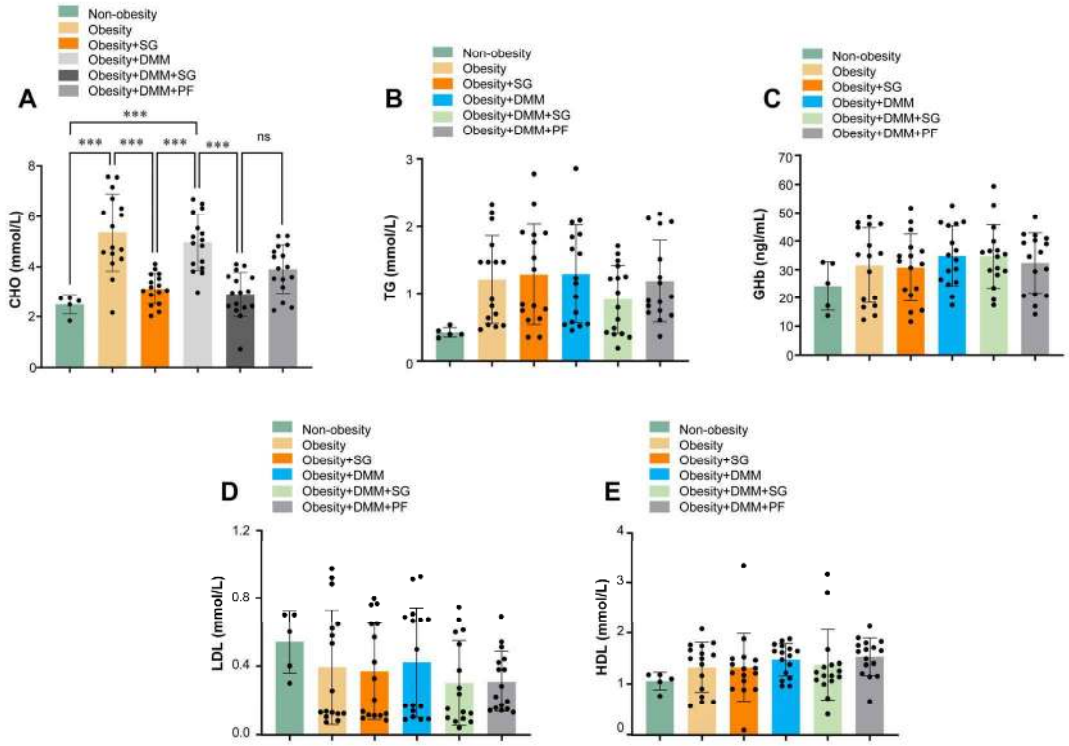

Figure S2. Semaglutide (SG) reduces total cholesterol levels in obesity mice, related to Figure 1. (A-E) Serum total cholesterol (CHO) levels, triglyceride (TG) levels, glycated hemoglobin (GHb) levels, low-density lipoprotein (LDL) levels and high-density lipoprotein (HDL) levels were measured in six groups of mice (n = 5-16). Data are expressed as means ± SD. * P < 0.05, ** P < 0.01, *** P < 0.001. One-way ANOVA, followed by the Tukey's post hoc test, was used for multiple group comparisons.

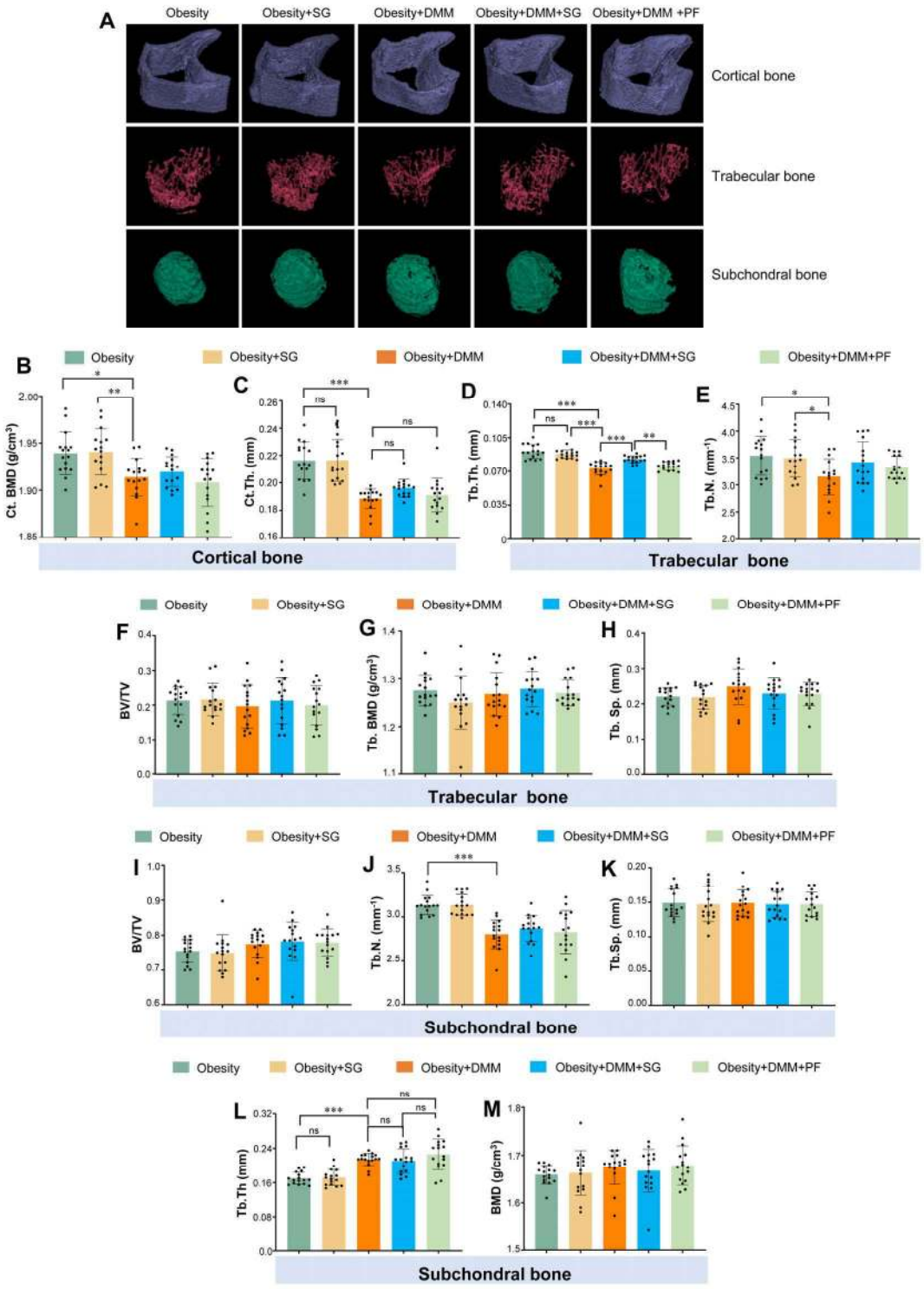

Figure S3. Histomorphometric analysis of cortical bone, trabecular bone and subchondral bone in obesity/DMM mice treated with semaglutide (SG), related to Figure 1. (A) Micro-CT image analysis of cortical bone, trabecular bone and subchondral bone (*n* = 16). (B and C) Histomorphometric analysis of cortical bone mineral density (Ct.BMD) and cortical bone thickness (Ct.Th.) in obesity/DMM mice treated with or without SG (*n* = 16). (D-H) Histomorphometric analysis of trabecular bone in obesity/DMM mice treated with or without SG (*n* = 16). The analyzed trabecular bone parameters include

trabecular thickness (Tb.Th.), trabecular number (Tb.N.), trabecular bone volume (BV/TV), trabecular bone mineral density (Tb.BMD) and trabecular separation (Tb.Sp.) (I-M) Histomorphometric analysis of subchondral bone in obesity/DMM mice treated with or without SG (n = 16). The analyzed parameters include BV/TV, Tb.N., Tb.Sp., Tb.Th. and BMD. Data are expressed as means ± SD. * $P < 0.05$, ** $P < 0.01$, *** $P < 0.001$. One-way ANOVA, followed by the Tukey's post hoc test, was used for multiple group comparisons.

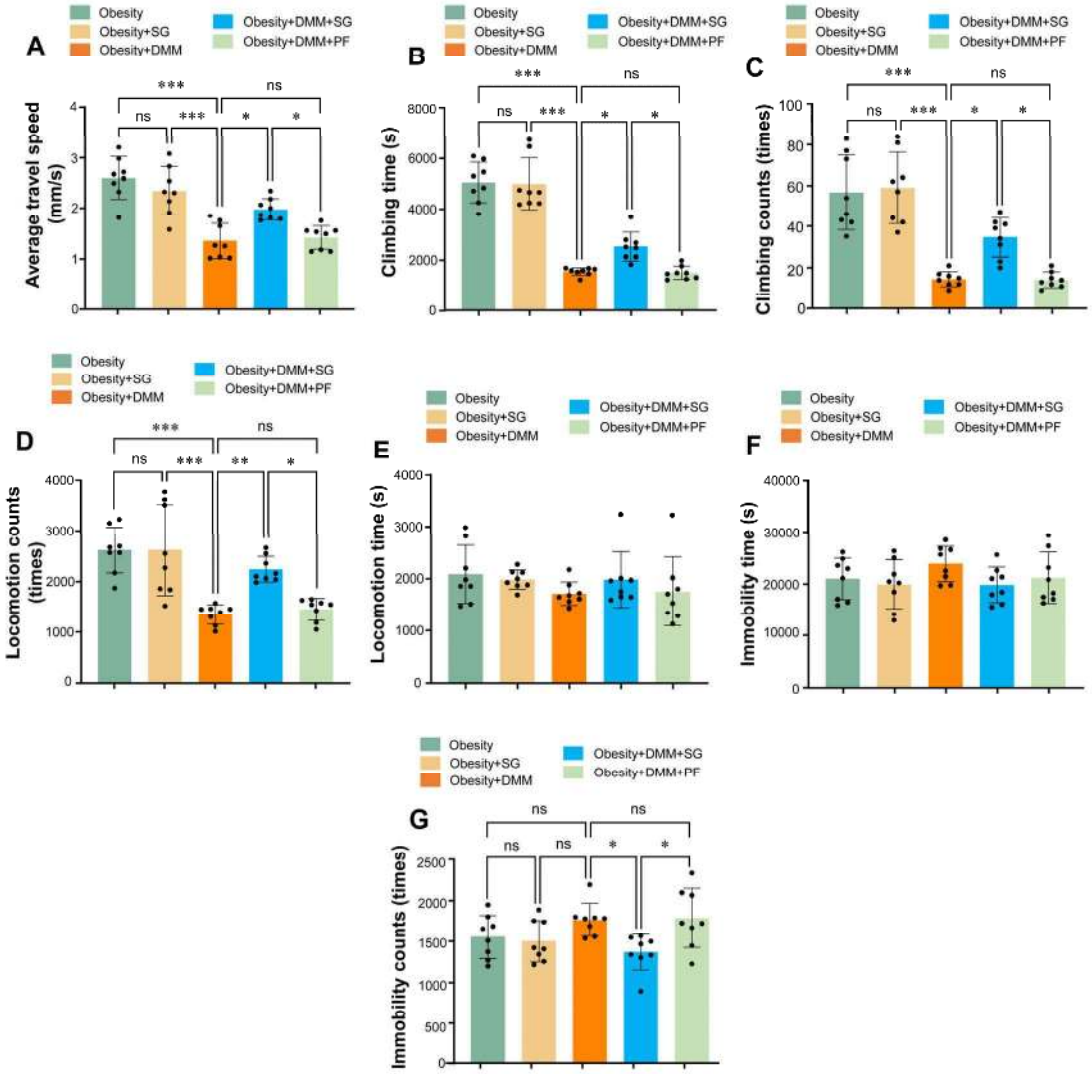

Figure S4. Semaglutide (SG) inhibits the pain in obesity/OA mice, related to Figure 2. (A-G) Pain-related behavior changes were also analyzed by Metris LABORAS system. The parameters of pain-related spontaneous activities that we have tested include average travel speed (A), climbing time (B), climbing counts (C), locomotion counts (D), locomotion time (E), immobility time (F), and immobility counts (G, n = 8). Data are expressed as means ± SD. * P < 0.05, ** P < 0.01, *** P < 0.001. One-way ANOVA, followed by the Tukey's post hoc test, was used for multiple group comparisons.

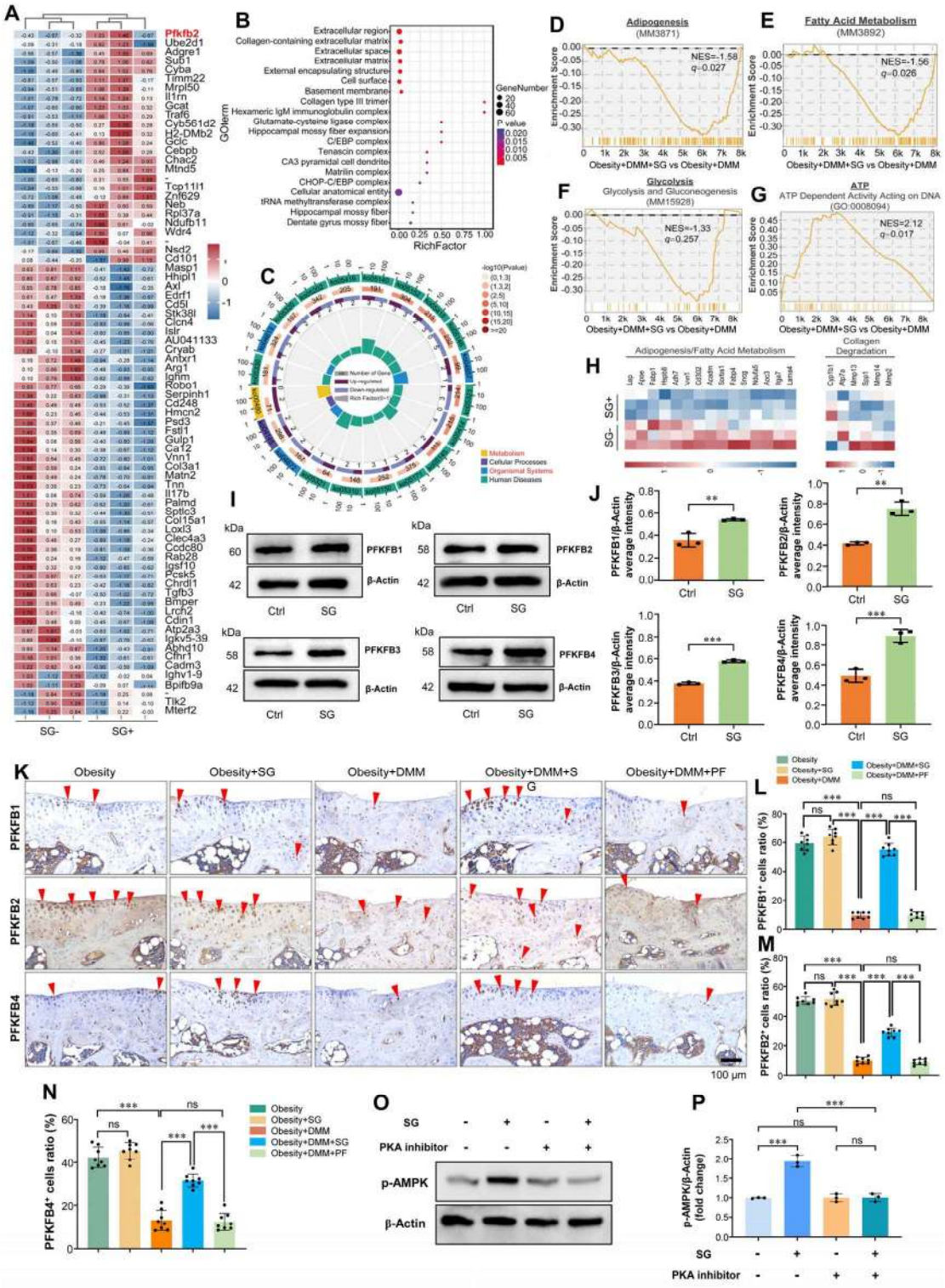

Figure S5. Semaglutide (SG) exerts its chondroprotective effects via GLP-1R-PKA-AMPK-PFKFB3 axis, related to Figure 3. (A) Heatmap presented representative differentially expressed proteins (DEPs) of cartilage in obesity/OA mouse with or without SG treatment (n = 3). (B) Gene Ontology (GO) annotations of DEPs in mice cartilage treated with SG. (C) Circle Kyoto Encyclopedia of Genes and Genomes (KEGG) enrichment plot of significantly enriched pathways. Statically significant DEPs are enriched. (D-G) Gene set enrichment analysis (GSEA) signature plots for Adipogenesis (D), Fatty

acid metabolism (E), Glycolysis (F) and ATP (G). (H) Heatmap displayed the expression of adipogenesis and fatty acid metabolism/collagen degradation related proteins. (I and J) Expression of PFKFB 1, 2, 3 and 4 were analyzed by Western blot analysis in primary articular chondrocytes with or without SG treatment (n = 3). (K) Expression of PFKFB 1, 2 and 4 were analyzed by immunohistochemical (IHC) analysis in obesity/OA mice with or without SG treatment (n = 8). Scale bar, 100 μm. (L-N) Quantification of PFKFB 1, 2 and 4 positive chondrocytes (n = 8). (O and P) Western blot analysis showed that PKA inhibitor (H-89) inhibited the SG-induced AMPK phosphorylation in primary chondrocytes (n = 3). Data are expressed as means ± SD. * P < 0.05, ** P < 0.01, *** P < 0.001. One-way ANOVA, followed by the Tukey's post hoc test, was used for multiple group comparisons.

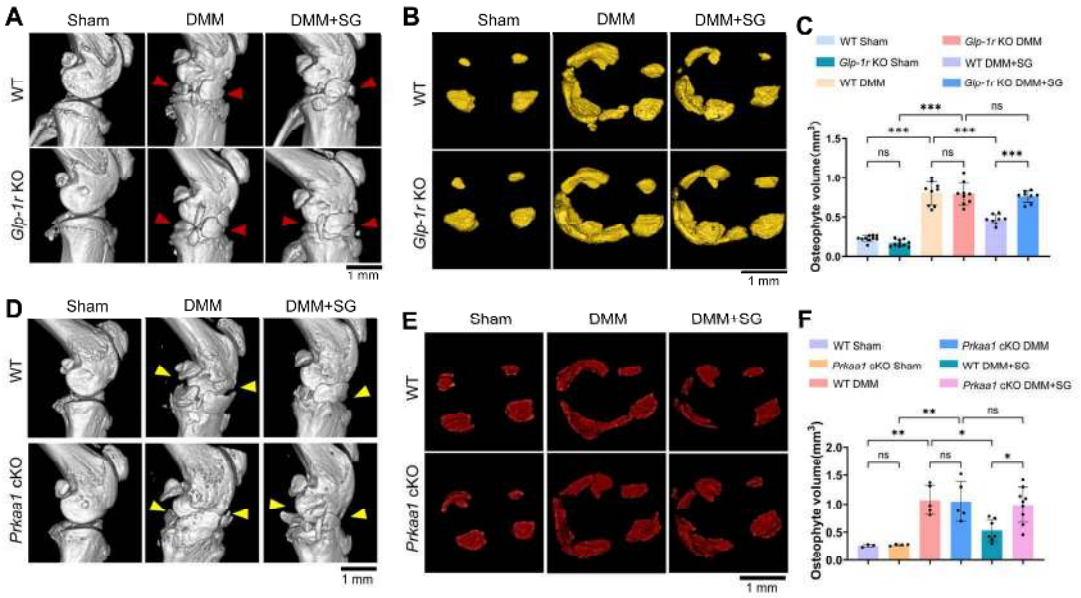

Figure S6. Deletion of *Glp-1r* and *Prkaa1* eliminate the effect of semaglutide (SG) on inhibiting of the osteophyte formation, related to Figure 5 and Figure 6. (A) Micro-CT image analysis of knee joints from wild type (WT) and *Glp-1r* knockout (KO) mice with or without SG treatment (n = 8-10). Scale bar, 1 mm. (B) Analysis of osteophyte structure in different mice (n = 8-10). Scale bar, 1 mm. (C) Quantification analysis of osteophyte volume in different mice (n = 8-10). (D) Micro-CT image analysis of knee joints from WT and *Prkaa1* conditional KO (cKO) mice with or without SG treatment (n = 3-9). Scale bar, 1 mm. (E) Analysis of osteophyte structure in different strains of mice (n = 3-9). Scale bar, 1 mm. (F) Quantification analysis of osteophyte volume in different mice (n = 3-9). Data are expressed as means ± SD. * P < 0.05, ** P < 0.01, *** P < 0.001. One-way ANOVA, followed by the Tukey's post hoc test, was used for multiple group comparisons.

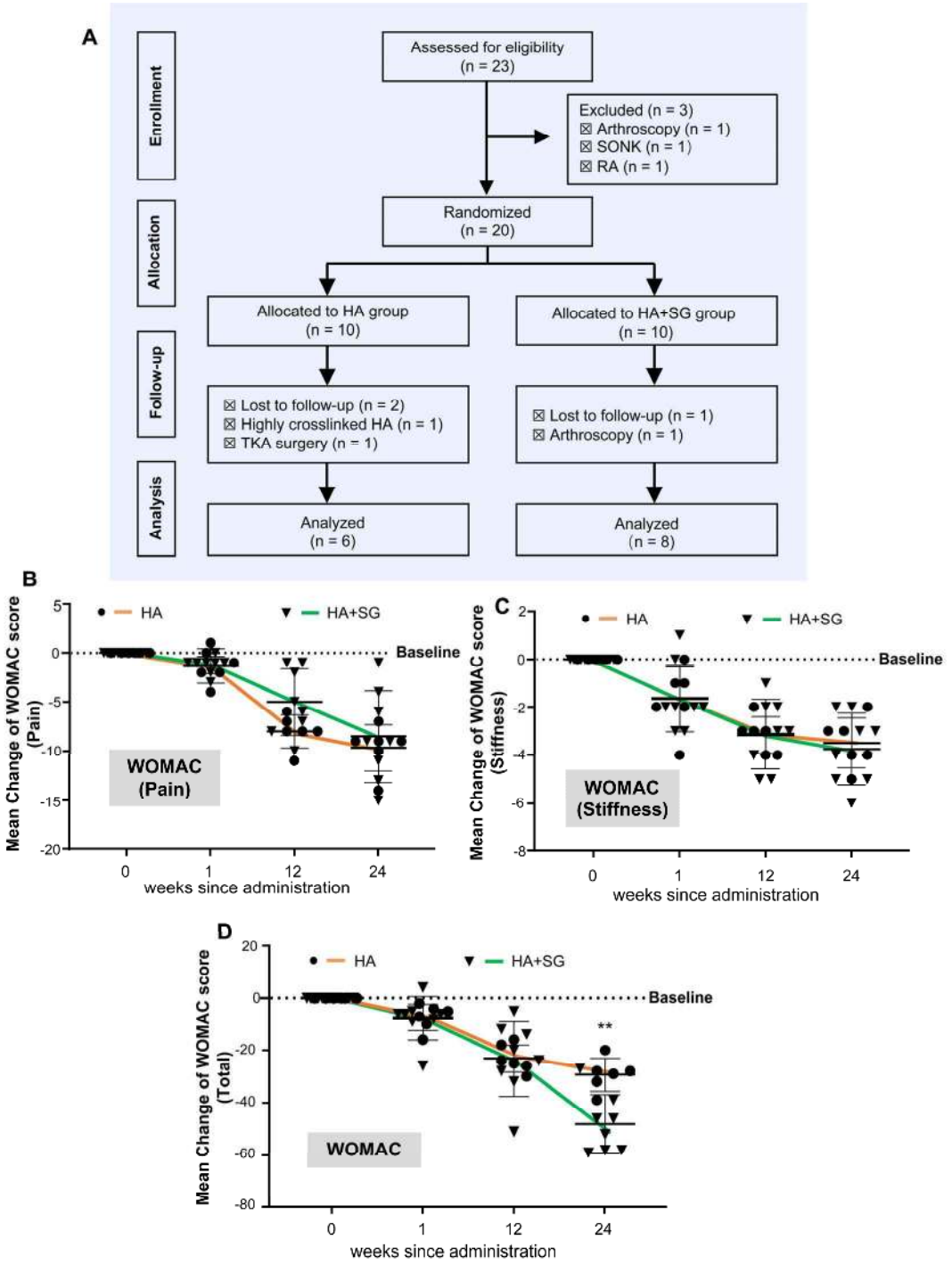

Figure S7. Efficacy scores of Semaglutide (SG) for knee joint treatment in individuals with obesity/OA, related to Figure 7. (A) The CONSORT flow diagram illustrated the screening, selection and management of study participants. (B) The pain was evaluated as WOMAC pain score, which was recorded at 0-, 1-, 12- and 24-weeks after HA or HA+SG administration (n = 6-8). (C) The daily joint stiffness was assessed by stiffness score, which was recorded at 0-, 1-, 12- and 24-weeks after HA or HA+SG administration (n = 6-8). (D) WOMAC total score is the sum of scores of pain, stiffness and physical function (n = 6-8). Data are expressed as means ± SD. * P < 0.05, ** P < 0.01, *** P < 0.001. Unpaired Student's t-test were used for two groups comparison.

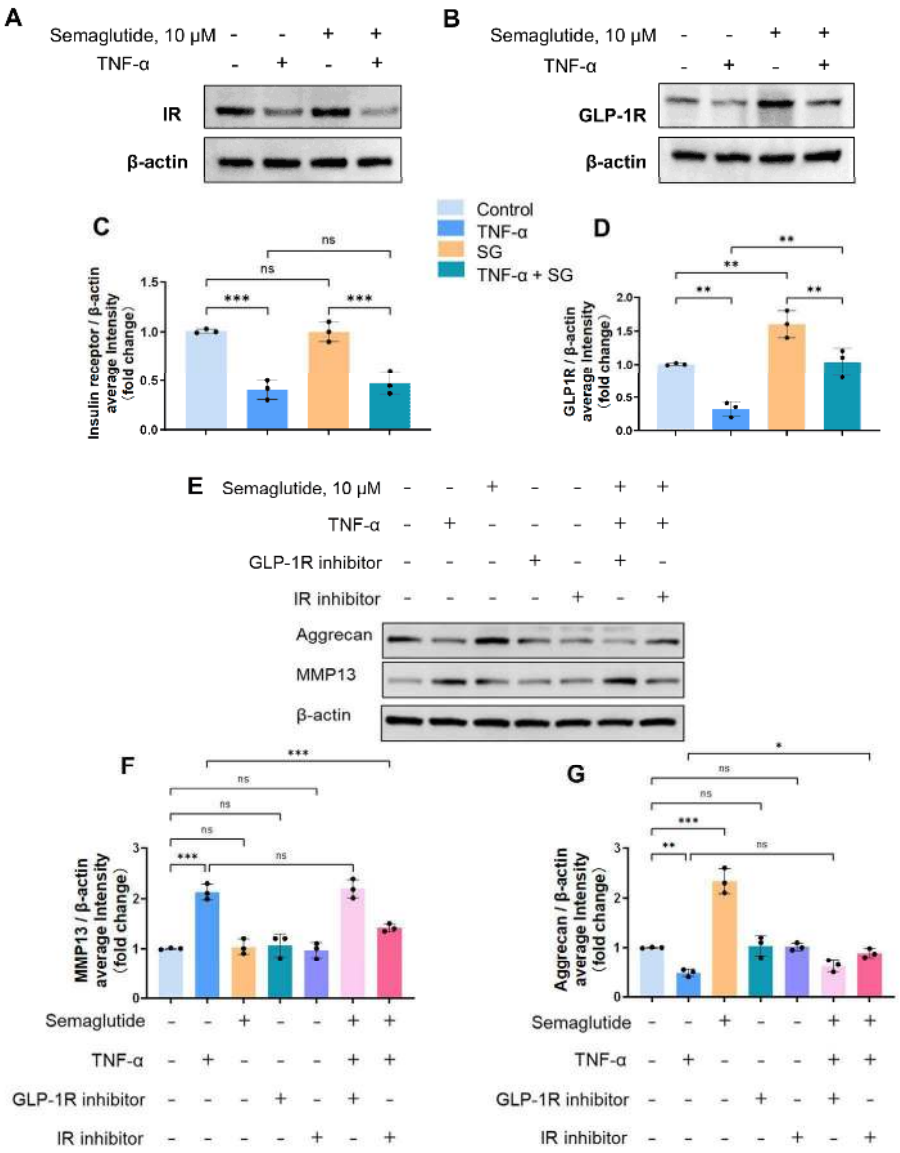

Figure S8. Involvements of GLP-1 receptor (GLP-1R) and insulin receptor (IR) in the chondroprotective effects of Semaglutide (SG), related to Discussion. (A and B) Western blot analysis of GLP-1R and IR expression in chondrocytes under different treatment conditions (n = 3). (C and D) Quantitative analysis of the expression levels of GLP-1R and IR based on Western blotting. (E) Western blot analysis of MMP13 and Aggrecan expression to assess the involvement of GLP-1R and IR in the chondroprotective effects of SG (n = 3). (F and G) Quantitative analysis of the expression levels of MMP13 and Aggrecan based on Western blotting. Data are expressed as means ± SD. * P < 0.05, ** P < 0.01, *** P < 0.001. One-way ANOVA, followed by the Tukey's post hoc test, was used for multiple group comparisons.

REFERENCES FOR STAR METHODS

1. Li, M.Y., Li, X.Y., Guo, Y., Miao, Z., Liu, X.M., Guo, S.X., and Zhang, H.M. (2020). Development and assessment of an individualized nomogram to predict colorectal cancer liver metastases. Quant. Imaging Med. Surg. 10, 397-414. 10.21037/qims.2019.12.16.
2. Bowers, M.E., Trinh, N., Tung, G.A., Crisco, J.J., Kimia, B.B., and Fleming, B.C. (2008). Quantitative MR imaging using "LiveWire" to measure tibiofemoral articular cartilage thickness. Osteoarthritis Cartilage 16, 1167-1173. 10.1016/j.joca.2008.03.005.
3. Surowiec, R.K., Lucas, E.P., Fitzcharles, E.K., Petre, B.M., Dornan, G.J., Giphart, J.E., LaPrade, R.F., and Ho, C.P. (2014). T2 values of articular cartilage in clinically relevant subregions of the asymptomatic knee. Knee Surg Sports Traumatol Arthrosc 22, 1404-1414. 10.1007/s00167-013-2779-2.
4. Glasson, S.S., Blanchet, T.J., and Morris, E.A. (2007). The surgical destabilization of the medial meniscus (DMM) model of osteoarthritis in the 129/SvEv mouse. Osteoarthr Cartilage 15, 1061-1069. https://doi.org/10.1016/j.joca.2007.03.006.
5. Li, J., Zhang, B., Liu, W.X., Lu, K., Pan, H., Wang, T., Oh, C.D., Yi, D., Huang, J., Zhao, L., et al. (2020). Metformin limits osteoarthritis development and progression through activation of AMPK signalling. Ann Rheum Dis 79, 635-645. 10.1136/annrheumdis-2019-216713.
6. Li, J., Wang, Y., Chen, D., and Liu-Bryan, R. (2022). Oral administration of berberine limits post-traumatic osteoarthritis development and associated pain via AMP-activated protein kinase (AMPK) in mice. Osteoarthritis Cartilage 30, 160-171. 10.1016/j.joca.2021.10.004.
7. Mookerjee, S.A., Gerencser, A.A., Nicholls, D.G., and Brand, M.D. (2017). Quantifying intracellular rates of glycolytic and oxidative ATP production and consumption using extracellular flux measurements. J. Biol. Chem. 292, 7189-7207. 10.1074/jbc.M116.774471.
8. Zhang, X., Belousoff, M.J., Liang, Y.-L., Danev, R., Sexton, P.M., and Wootten, D. (2021). Structure and dynamics of semaglutide-and taspoglutide-bound GLP-1R-Gs complexes. Cell reports 36.
9. Liu, H., Shen, C., Li, H., Hou, T., and Yang, Y. (2024). Discovery of potent covalent CRM1 inhibitors via a customized structure-based virtual screening pipeline and bioassays. Journal of Chemical Information and Modeling 64, 7422-7431.
10. Nerenberg, P.S., So, C., Tripathy, A., and Head-Gordon, T. (2011). Evaluation and Improvement of the Amber ff99SB Force Field with an Advanced Water Model. Biophysical Journal 100, 311a.

Data S2

Protocol and statistical analysis plan of the monocenter, comparative pilot clinical study on the efficacy and safety of semaglutide in Chinese participants with early-to-mid stage obesity-related knee osteoarthritis (V1.0, page 1-21). Statistical analysis plan (V1.0, page 22-27), CONSORT 2022 checklist (page 28-30).

Clinical Study: A Randomized, Controlled, Prospective Clinical Trial on the Efficacy and Safety of Semaglutide Injection in Patients with Early-to-Mid Stage Obesity-Related Knee Osteoarthritis

STUDY PROTOCOL

The First Affiliated Hospital of Jinan University

Version: 1.0
Date: July 2023

Content

1. BACKGROUND **4**

2. OBJECTIVE **4**

3. STUDY AND DESIGN **5**

3.1 Overall Study Design and Plan **5**

3.2 Study Population **5**

3.2.1 Diagnostic Criteria **5**

3.2.2 Inclusion Criteria **6**

3.2.3 Exclusion Criteria **6**

3.3 Number of Cases **6**

3.4 Recruitment **6**

3.4.1 Participant Recruitment **6**

3.4.2 Randomization and Blinding **7**

3.5 Interventions **7**

3.5.1 Semaglutide Administration **7**

3.5.2 Standard Care **7**

3.5.3 Compliance **7**

3.6 Study Steps and Related Examinations **8**

3.6.1 Screening Visit **8**

3.6.2 Visit Period (Total of 4 Visits) **8**

3.6.3 Specific Assessment Methods **10**

3.8 Endpoint Indicators **14**

3.8.1 Primary Endpoint Indicators **14**

3.8.2 Secondary Endpoint Indicators **14**

3.8.3 Efficacy Assessment **14**

3.8.4 Safety Assessment **14**

3.9 Criteria for Discontinuation of Clinical Studies **14**

3.10 Combined Medication and Treatment **15**

4 ADVERSE EVENT OBSERVATION **15**

4.1 Definition of Adverse Event **15**

4.2 Degree **15**

4.3 Recording and Reporting of Adverse Events **16**

4.4 Risk Prevention and Treatment **16**

5. STATISTICAL ANALYSIS **16**

5.1 Sample Content Estimation **17**

5.2 Analysis Sets and Handling of Missing Data **17**

6. RESEARCH-RELATED ETHICS **18**

6.1 Ethics Committee Review 18
6.2 Informed Consent 18
7. DATA PRIVACY AND SECURITY MONITORING PROGRAM 18
8. QUALITY CONTROL AND QUALITY ASSURANCE IN CLINICAL RESEARCH 19
8.1 Researcher Qualification and Researcher Training 19
8.2 Deviations/violations in the Research Process 19
8.3 Monitoring 19
9. EXPECTED PROGRESS AND COMPLETION DATES OF RESEARCH PROJECTS 19
10.REFERENCES 20

1. BACKGROUND

Osteoarthritis (OA) is a prevalent chronic degenerative joint disease, affecting approximately 7% of the global population with a prevalence rising to 73% among the elderly (≥55 years) [1]. Historically considered an inevitable part of aging, OA is characterized by progressive cartilage breakdown, subchondral bone damage, persistent pain, and disability [2]. Current pharmacological management, such as Acetaminophen and Non-Steroidal Anti-Inflammatory Drugs (NSAIDs), offers only palliative symptom relief without halting structural progression of knee osteoarthritis (KOA) and carries risks of long-term gastrointestinal, renal, and cardiovascular side effects. Consequently, OA imposes a substantial socioeconomic burden, underscoring an urgent need for disease-modifying therapies.

Growing evidence indicates that metabolic dysfunction is a significant contributor to OA pathogenesis, particularly among younger adults, leading to the conceptualization of a distinct "metabolic osteoarthritis" subtype [3]. Central to this subtype are obesity and insulin resistance, which drive pathological processes through mechanisms including impaired nutrient supply, accumulation of Advanced Glycation End-products (AGEs), and increased mechanical load [4, 5]. This nexus suggests that targeting metabolic pathways, especially insulin resistance and glucose metabolism may offer a novel therapeutic strategy for OA.

Glucagon-like Peptide-1 Receptor (GLP-1R) agonists, exemplified by semaglutide, are well-established for managing type 2 diabetes and obesity by improving glycemic control and promoting weight loss [6]. Beyond these primary effects, they confer pleiotropic benefits, including cardiovascular and renal protection. Mechanistically, GLP-1R agonists regulate cellular metabolism by modulating glucose transporter activity, activating AMPK signaling, and restoring energy homeostasis [7-11]. Emerging preclinical and clinical observations suggest that GLP-1R agonists may alleviate OA symptoms, hinting at a potential chondroprotective effect. However, the precise molecular mechanisms underlying this effect, particularly those independent of weight loss, remain largely unexplored. Furthermore, robust clinical evidence supporting the efficacy of GLP-1R agonists in patients with metabolic OA is still lacking.

2. OBJECTIVE

This study aims to evaluate the efficacy and safety of semaglutide in patients with early-to-moderate KOA comorbid with obesity. The objective is to assess the effects of semaglutide on pain levels, inflammatory markers, body weight, body mass index (BMI), and joint function (e.g., the Western Ontario and McMaster Universities Osteoarthritis Index/WOMAC score) through a randomized, controlled clinical trial. Assessments will be conducted at multiple timepoints before and after treatment initiation. The findings are expected to provide

evidence-based support for the conservative pharmacological management of early-to-moderate KOA in patients with obesity.

3. STUDY AND DESIGN

3.1 Overall Study Design and Plan

This study is an interventional, single-center randomized controlled pilot clinical trial. Twenty obese participants aged 50 to 75 years diagnosed with knee osteoarthritis (KOA) will be recruited from the First Affiliated Hospital of Jinan University. Following the provision of signed informed consent, participants will be randomly assigned to one of two groups: a conventional treatment group receiving sodium hyaluronate (HA) injection, or a semaglutide treatment group receiving semaglutide in addition to intraarticular HA injection. Follow-up visits will be conducted at Week 1, Week 12, and Week 24. Treatment effectiveness will be assessed by monitoring the primary outcomes such as BMI, the VAS for pain and the WOMAC score, and the secondary outcomes include inflammatory markers, and cartilage degradation as evaluated by MRI. The study aims to compare the clinical efficacy of semaglutide in obese patients with early- to mid-stage KOA.

3.2 Study Population

3.2.1 Diagnostic Criteria

(1) Diagnostic Criteria for KOA (according to the 2022 revision by the Orthopaedic Branch of the Chinese Medical Association)

① Recurrent knee pain within the past month;

② X-ray (standing or weight-bearing view) shows joint space narrowing, subchondral bone sclerosis and/or cystic changes, and osteophyte formation at the joint margins;

③ Synovial fluid (on at least two occasions) is clear and viscous, with a white blood cell count <2000 cells/ml;

④ Middle-aged or elderly patients (≥50 years);

⑤ Morning stiffness (≤30 min);

⑥ Bone crepitus during activity.

Based on a combination of clinical, laboratory, and radiographic findings, KOA can be diagnosed if the following criteria are met: ① + ②, or ① + ③ + ⑤ + ⑥, or ① + ④ + ⑤ + ⑥.

(2) Kellgren–Lawrence (K-L) Grading Criteria for Knee Osteoarthritis:

Grade 0: Normal;

Grade I: Doubtful joint space narrowing and possible osteophytic lipping;

Grade II: Definite osteophytes and possible joint space narrowing;

Grade III: Moderate osteophytes, definite joint space narrowing, some sclerosis, and possible deformity of bone ends;

Grade IV: Large osteophytes, marked joint space narrowing, severe sclerosis, and definite deformity of bone ends.

MRI can also be used for cases where X-ray findings are inconclusive.

3.2.2 Inclusion Criteria

(1) Age between 50 and 75 years ($50 \leq age \leq 75$);

(2) BMI ≥ 28 kg/m^2;

(3) Diagnosed with Osteoarthritis (OA) based on X-ray and MRI findings, with a Kellgren-Lawrence (K-L) grade between 0 and III;

(4) No restrictions based on gender or ethnicity;

(5) Voluntary signing of the informed consent form.

3.2.3 Exclusion Criteria

Individuals meeting any of the following criteria shall be excluded:

(1) Those who do not meet the diagnostic and inclusion criteria;

(2) Concurrent conditions affecting knee joint function, such as large loose bodies, tumors, tuberculosis, infection, rheumatism, rheumatoid arthritis, or gout in the knee;

(3) Significant deformity or pain in the spine, hip, ankle, or foot, or other conditions that affect normal gait;

(4) Diagnosed with diabetes, rheumatoid arthritis or autoimmune diseases, parathyroid or kidney diseases, or abnormal liver function;

(5) Use of glucocorticoids within the past three months or a history of intra-articular injections;

(6) History of infection or previous joint or arthroscopic surgery.

3.3 Number of Cases

Twenty eligible participants will be recruited from the First Affiliated Hospital of Jinan University. They will be randomly assigned to either the conventional treatment group (HA) or the semaglutide treatment group (HA+SG).

3.4 Recruitment

3.4.1 Participant Recruitment

Participants will be recruited from the Orthopedics and Sports Medicine Center of The First Affiliated Hospital of Jinan University. Recruitment posters will be displayed in the hospital's

physical examination center and outpatient areas. Potentially eligible patients will undergo an initial screening to document their medical history and confirm a diagnosis of early-to-moderate KOA. Eligible individuals will then have the study procedures explained in detail by a physician, provide written informed consent, and proceed to the baseline visit.

3.4.2 Randomization and Blinding

The participants were randomly assigned in a 1:1 ratio to either the conventional treatment group and the semaglutide treatment group. Randomization was performed using computer-generated block randomization (block size of 6), with allocation concealed *via* sequentially numbered, opaque, sealed envelopes (SNOSE). Baseline characteristics were balanced between the two groups. Due to the nature of the interventions, patients and treating clinicians were not blinded; however, outcome assessors and data analysts remained blinded to group allocation.

3.5 Interventions

3.5.1 Semaglutide Administration

Participants in the semaglutide treatment group will receive once-weekly subcutaneous injections of semaglutide. The dosage will be initiated at 0.25 mg for the first week, 0.375 mg for the second week, and titrated to a maintenance dose of 0.5 mg per week thereafter from 3rd to 24th week. If a participant experiences unacceptable side effects, a lower maintenance dose may be utilized at the investigator's discretion.

3.5.2 Standard Care

All participants, in both the conventional treatment group and the semaglutide treatment group, will receive a standard course of intraarticular HA injections as the foundational therapy. This involves an injection of 25 mg once per week for 5 consecutive weeks, administered in accordance with the 2022 clinical guidelines from the Chinese Orthopaedic Association.

3.5.3 Compliance

To ensure adherence to the protocol, semaglutide and HA will be dispensed by the study pharmacy at scheduled visits. Used semaglutide auto-injector pens and HA packaging must be returned at follow-up visits for accountability. Adherence will be calculated based on dispensed and returned supplies. Participants will also receive regular follow-up contacts to monitor tolerance and encourage visit attendance.

3.6 Study Steps and Related Examinations

3.6.1 Screening Visit

(1) Questionnaires: collecting demographic information (age, gender, occupation, etc.), lifestyle factors (alcohol consumption, smoking, dietary and exercise habits, etc.), disease history, family history, etc.

(2) Anthropometric measurements: height, weight, and BMI.

(3) Vital signs assessment: blood pressure, heart rate, respiration, and body temperature.

(4) Blood collection: blood samples will be collected for the measurement of inflammatory markers, such as erythrocyte sedimentation rate (ESR) and C-reactive protein (CRP).

(5) Scoring scales: the VAS for pain and the WOMAC will be used to evaluate treatment efficacy in participants.

(6) Knee MRI: the severity of cartilage degeneration will be assessed *via* MRI before and after interventions.

(7) Others: drug dispensing and recovery records will be collected, and the occurrence of any adverse events will be documented.

3.6.2 Visit Period (Total of 4 Visits)

3.6.2.1 Visit 1 (Week 0)

(1) Questionnaires: collecting demographic information (age, gender, occupation, etc.), lifestyle factors (alcohol consumption, smoking, dietary and exercise habits, etc.), disease history, family history, etc.

(2) Anthropometric measurements: height, weight, and BMI.

(3) Vital signs assessment: blood pressure, heart rate, respiration, and body temperature.

(4) Blood collection: blood samples will be collected for the measurement of inflammatory markers.

(5) Scoring scales: the VAS for pain and the WOMAC will be used to evaluate treatment efficacy in participants.

(6) Knee MRI: the severity of cartilage degeneration will be assessed *via* MRI.

3.6.2.2 Visit 2 (Week 1)

(1) Questionnaires: collecting demographic information (age, gender, occupation, etc.), lifestyle factors (alcohol consumption, smoking, dietary and exercise habits, etc.), disease history, family history, etc.

(2) Anthropometric measurements: height, weight, and BMI.

(3) Vital signs assessment: blood pressure, heart rate, respiration, and body temperature.

(4) Blood collection: Blood samples will be collected for the measurement of inflammatory markers.

(5) Scoring scales: the VAS for pain and the WOMAC will be used to evaluate treatment efficacy in participants.

(6) Others: Drug dispensing and recovery records will be collected, and the occurrence of any adverse events will be documented.

3.6.2.3 Visit 3 (Week 12)

(1) Questionnaires: collecting demographic information (age, gender, occupation, etc.), lifestyle factors (alcohol consumption, smoking, dietary and exercise habits, etc.), disease history, family history, etc.

(2) Anthropometric measurements: height, weight, and BMI.

(3) Vital signs assessment: blood pressure, heart rate, respiration, and body temperature.

(4) Blood collection: Blood samples will be collected for the measurement of inflammatory markers.

(5) Scoring scales: the VAS for pain and the WOMAC will be used to evaluate treatment efficacy in participants.

(6) Others: Drug dispensing and recovery records will be collected, and the occurrence of any adverse events will be documented.

3.6.2.4 Visit 4 (Week 24)

(1) Questionnaires: collecting demographic information (age, gender, occupation, etc.), lifestyle factors (alcohol consumption, smoking, dietary and exercise habits, etc.), disease history, family history, etc.

(2) Anthropometric measurements: height, weight, and BMI.

(3) Vital signs assessment: blood pressure, heart rate, respiration, and body temperature.

(4) Blood collection: Blood samples will be collected for the measurement of inflammatory markers.

(5) Scoring scales: the VAS for pain and the WOMAC will be used to evaluate treatment efficacy in participants.

(6) Knee MRI: the severity of cartilage degeneration will be assessed *via* MRI.

(7) Others: Drug dispensing and recovery records will be collected, and the occurrence of any adverse events will be documented

3.6.3 Specific Assessment Methods

3.6.3.1 VAS for Pain Assessment

Pain intensity will be assessed using a 10-cm horizontal Visual Analog Scale (VAS). The scale is anchored by two verbal descriptors: "No pain" (0 cm) on the left and "Worst imaginable pain" (10 cm) on the right. Participants will be instructed to mark a point on the line that best represents their current level of knee pain. The distance from the left endpoint ("No pain") to the participant's mark will be measured in millimeters, providing a pain score ranging from 0 to 10. Higher scores indicate greater pain intensity. VAS assessments will be conducted at all follow-up visits (Baseline, Week 1, Week 12, and Week 24).

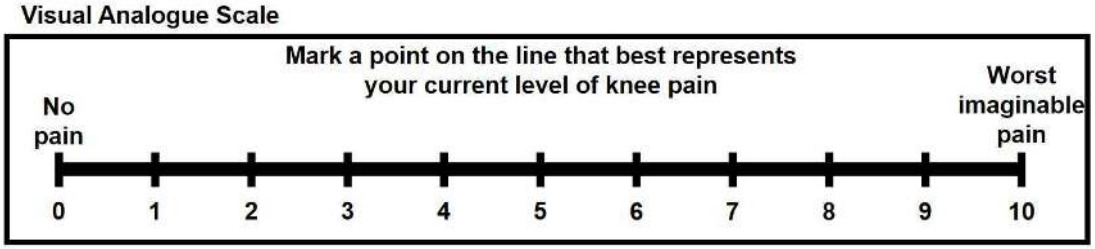

3.6.3.2 Assessment of Inflammatory Markers

Fasting venous blood samples will be collected at Baseline, Week 1, Week 12, and Week 24. Serum will be separated by centrifugation and stored at -80°C until analysis. High-sensitivity C-reactive protein (hs-CRP) levels will be measured using standardized immunoturbidimetric assays on an automated clinical chemistry analyzer. Other inflammatory markers may be analyzed as per the study protocol and laboratory capabilities. Results will be recorded in appropriate units (e.g., mg/L for CRP).

3.6.3.3 Quantitative Assessment of Cartilage Degeneration *via* Magnetic Resonance Imaging (MRI)

High-resolution MRI of the index knee will be performed at Baseline and Week 24 using a 3.0-Tesla MRI scanner with a dedicated knee coil. A standardized protocol will be employed, including sequences optimized for cartilage visualization (e.g., 3D-DESS, T2 mapping, or similar sequences as per institutional standard operating procedures). Quantitative analysis of cartilage morphology (e.g., thickness, volume) and composition (e.g., T2 relaxation times) will be conducted by experienced musculoskeletal radiologists blinded to treatment allocation, using validated semi-automated segmentation software (e.g., Chondrometrics GmbH, Germany or equivalent). Changes in cartilage parameters from Baseline to Week 24 will be calculated.

3.6.3.4 Western Ontario and McMaster Universities Osteoarthritis Index (WOMAC)

The Chinese version of the WOMAC, a validated, self-administered questionnaire, will be used to assess knee osteoarthritis-specific pain, stiffness, and physical function. The questionnaire comprises 24 items divided into three subscales:

Pain (5 items): Pain during walking, using stairs, in bed, sitting or lying, and standing upright.

Stiffness (2 items): Stiffness after first waking and later in the day.

Physical Function (17 items): Difficulty performing daily activities such as descending/ascending stairs, rising from sitting, standing, bending, walking, getting in/out of a car, shopping, putting on/taking off socks, rising from bed, lying in bed, getting in/out of bath, sitting, getting on/off toilet, and performing heavy and light household duties.

Each item is scored on a 5-point Likert scale (0=None, 1=Mild, 2=Moderate, 3=Severe, 4=Extreme). Subscale scores are summed (Pain: 0-20, Stiffness: 0-8, Physical Function: 0-68), and a total WOMAC score (0-96) can be calculated. Higher scores indicate worse pain, stiffnes, and functional limitation. The WOMAC will be administered at Baseline, Week 1, Week 12, and Week 24.

Dimensions Assessed	Specific Items	Traditional WOMAC
Pain	1. While walking on a flat surface.	√
	2. Ascending or descending stairs.	√
	3. At night while in bed.	√
	4. Sitting or lying.	√
	5. Standing upright.	√
Stiffness	1. On first waking in the morning.	√
	2. Later in the day.	√
Function	1. Descending stairs.	√
	2. Ascending stairs.	√
	3. Rising from sitting.	√
	4. Standing.	√
	5. Bending to floor.	√
	6. Walking on flat.	√
	7. Getting in/out of car.	√
	8. Going shopping.	√
	9. Putting on socks.	√
	10. Rising from bed.	√
	11. Taking off socks.	√
	12. Lying in bed.	√
	13. Getting in/out of bed.	√
	14. Sitting.	√
	15. Getting on/off the toilet.	√
	16. Heavy domestic duties.	√
	17. Light domestic duties.	√

3.7 Visitor's schedule

Study Flow Chart								
Study Phase	**HA Conventional Group**				**HA + semaglutide Group**			
	Screening Phase	Follow-up Phase			Screening Phase	Follow-up Phase		
Observation Time Point	week 0	week 1	week 12	week 24	week 0	week 1	week 12	week 24
Basic Information Form	√				√			
Inclusion/Exclusion Criteria	√				√			
Demographics	√				√			
Informed Consent Form	√				√			
Vital Signs	√	√	√	√	√	√	√	√
Weight and BMI Indicators	√	√	√	√	√	√	√	√
VAS Pain Score	√	√	√	√	√	√	√	√
WOMAC Score	√	√	√	√	√	√	√	√
Knee MRI	√			√	√			√
Blood Inflammatory Markers	√	√	√	√	√	√	√	√
Concomitant Medication Use	√	√	√	√	√	√	√	√
Drug Dispensing/Recovery	√	√	√	√	√	√	√	√
Adverse Event Documentation		√	√	√		√	√	√

3.8 Endpoint Indicators

3.8.1 Primary Endpoint Indicators

Change in Western Ontario and McMaster Universities Osteoarthritis Index (WOMAC) total score from baseline to Week 24.

Change BMI from baseline to Week 24.

3.8.2 Secondary Endpoint Indicators

Change in Visual Analog Scale (VAS) pain score from baseline to Week 24.

Change in cartilage degradation assessed by Magnetic Resonance Imaging (MRI).

Change in inflammatory markers

3.8.3 Efficacy Assessment

The efficacy of the intervention will be determined by comparing the changes in the primary endpoint indicators (WOMAC score and BMI) between the semaglutide combination with HA group and the conventional treatment (HA) group.

3.8.4 Safety Assessment

Safety will be evaluated through comprehensive monitoring of vital signs and the systematic recording of all adverse events (AEs) and serious adverse events (SAEs). Special emphasis will be placed on adverse events related to the study interventions, including:

(1) Injection-related events: such as injection-site pain, swelling, infection, or hemorrhage associated with intra-articular knee injection.

(2) Drug-related events: particularly gastrointestinal adverse events (e.g., nausea, vomiting, diarrhea, constipation) known to be associated with semaglutide therapy, as well as potential events related to glucose metabolism.

3.9 Criteria for Discontinuation of Clinical Studies

The trial may be discontinued based on the following criteria:

(1) Significant Safety Concerns: Immediate termination if multiple participants experience severe adverse events related to the interventions, such as severe joint infection, accelerated cartilage degradation, or serious systemic reactions.

(2) Confirmed Futility: Early termination if interim analysis definitively shows no therapeutic benefit of the combined intervention.

(3) Regulatory/Ethical Directive: Mandatory cessation if required by the supervising ethics committee or regulatory authority.

(4) Critical Recruitment/Protocol Failure: Discontinuation due to inability to enroll or retain sufficient participants, or widespread protocol deviations that compromise trial integrity.

All termination decisions will be formally documented and reported to relevant oversight bodies.

3.10 Combined Medication and Treatment

During the trial period, the use of medications or treatments that may interfere with the evaluation of the study interventions' efficacy on arthritis progression and cartilage metabolism is prohibited. This specifically includes, but is not limited to:

(1) Oral supplements targeting joint health, such as glucosamine or chondroitin sulfate.

(2) Anti-inflammatory medications, such as systemic or topical NSAIDs (except as permitted in a predefined rescue protocol).

(3) Other intra-articular interventions, such as corticosteroid injections, platelet-rich plasma (PRP), or alternative hyaluronic acid formulations.

Other antihypertensive drugs, anticoagulants and conventional hypoglycemic drugs are allowed to continue taking during the study period.

4 ADVERSE EVENT OBSERVATION

4.1 Definition of Adverse Event

Adverse Event (AE): Any untoward medical occurrence in a patient or clinical trial participant following administration of a medicinal product, which does not necessarily imply a causal relationship with the treatment. Such events may manifest as symptoms (e.g., nausea, chest pain), clinical signs (e.g., tachycardia, hepatomegaly), or abnormal diagnostic findings (e.g., abnormal diagnostic findings, electrocardiographic changes). In this trial, AEs encompass all medically relevant events occurring at any time, including those observed during the screening period.

Serious Adverse Event (SAE): Any AE that results in hospitalization or prolongation of hospitalization, disability or substantial disruption of normal functioning, life-threatening circumstances or mortality, congenital anomalies, occurring during the clinical trial.

4.2 Degree

Mild: Events are tolerable, do not interfere with study participation, require no special treatment, and have no effect on the clinical course.

Moderate: Events cause significant discomfort, necessitate therapeutic intervention, and demonstrate effects on clinical recovery.

Severe: Events pose life-threatening risks, may result in fatal or disabling outcomes, and

require urgent medical interventions.

4.3 Recording and Reporting of Adverse Events

During the clinical trial, participants may experience AEs. Upon occurrence of any AE (including SAEs), comprehensive documentation must be recorded in the Case Report Form (CRF) detailing the time of occurrence, clinical manifestations, severity grade, management protocol, duration, outcome, and causal relationship assessment. For laboratory abnormalities, participants need to undergo follow-up monitoring until the parameters return to normal or pre-intervention levels, and determine whether it is related to the intervention.

All SAEs must be reported to the Principal Investigator immediately. The investigator will notify the Ethics Committee and relevant regulatory authorities within 24 hours using the designated SAE reporting form.

4.4 Risk Prevention and Treatment

Based on known profiles of the interventions, the following AEs may be anticipated: Injection-related: Local pain, swelling, erythema, or infection at the knee injection site. Semaglutide-related: Gastrointestinal events (e.g., nausea, vomiting, diarrhea, constipation), which are usually transient and mild to moderate in severity.

Preventive measures include standardized aseptic injection technique and a semaglutide dose-escalation protocol to improve gastrointestinal tolerability. For gastrointestinal AEs, supportive measures (e.g., dietary adjustment, adequate hydration) are recommended. Persistent or severe events will be managed per clinical judgment, which may include dose reduction or discontinuation of semaglutide.

5. STATISTICAL ANALYSIS

Statistical analyses will be performed using GraphPad Prism (version 9.0) and SPSS Statistics (version 26.0). Data will be presented as mean ± standard deviation (SD) for normally distributed continuous variables, median (interquartile range) for non-normally distributed continuous variables, and frequency (percentage) for categorical variables. Please read statistical analysis plan for detailed information.

Baseline demographic and clinical characteristics will be compared between the two treatment groups (Conventional: HA alone; Intervention: HA + semaglutide) using independent samples *t*-tests for continuous variables. The primary endpoints are the changes in WOMAC score and BMI from Baseline at 24-Week. Each will be analyzed using unpaired Student's *t*-test. Secondary continuous outcomes, including changes in VAS pain score and MRI-based cartilage parameters will be analyzed similarly using unpaired Student's *t*-test.

Safety analyses will be descriptive. All adverse events (AEs) and serious adverse events (SAEs) will be listed and summarized by system organ class, severity, and relationship to the study intervention. Incidence rates will be calculated and presented.

A two-sided p-value < 0.05 will be considered statistically significant. Given the pilot nature of this study, emphasis will be placed on estimating effect sizes (e.g., mean differences between groups with 95% confidence intervals) alongside p-values to inform future research.

5.1 Sample Content Estimation

The sample size is estimated using G*power (version 3.1.9.7, Heinrich Heine University Düsseldorf, Germany). According to the results reported by Wilding et al (*The New England Journal of Medicine*, 2021; 384: 989-1002), semaglutide produced significant improvements in body weight loss, with estimated differences of -12.4 percentage points. Assuming a standard deviation (SD) of 10 points, the standardized effect sizes (Cohen's d) are calculated as follows: $d = \Delta/SD$, yielding values of 1.24.

The key parameters used in the G*power calculation are:

Parameter	Value
Test type	Two-tailed, two independent groups (t-test)
Effect Size (d)	1.24
Significance level (α err prob)	0.05
Power (1-β err prob)	0.69
Allocation ratio (N1/N2)	1

Based on these assumptions, the estimated sample size is 9 participants/group. Considering an anticipated dropout rate of 10-15%, the final target enrollment is 10 participants/group (total $n = 20$).

5.2 Analysis Sets and Handling of Missing Data

This exploratory pilot study will employ two analysis populations to assess the robustness of findings:

Per-Protocol (PP) Population: subjects who complete all follow-up visits without major protocol deviations. This population will serve as the primary analysis set for efficacy evaluation, as it most directly reflects the treatment effect in patients who adhered to the complete intervention protocol.

Full Analysis Set (FAS) / Intention-to-Treat (ITT) Population: all randomized subjects. Sensitivity analyses using the FAS will be conducted, applying the Last Observation Carried Forward (LOCF) method for imputation of missing data at the primary endpoint (24-week).

Both the PP and FAS results will be reported in accordance with CONSORT guidelines. The choice of the PP set as primary for this pilot study is based on its focus on generating preliminary estimates of efficacy under complete protocol adherence. Future definitive trials will designate the FAS (ITT) as the primary analysis population.

6. RESEARCH-RELATED ETHICS

6.1 Ethics Committee Review

Prior to study initiation, a detailed study protocol was developed and approved by the principal investigator and the research team. The protocol, together with the written informed consent form, was reviewed and approved by the institutional ethics committee before implementation.

Any protocol amendments during the study were submitted for ethics committee approval prior to execution. If new information emerged that could affect participants' willingness to continue participation, the informed consent form was revised accordingly, approved by the ethics committee, and re-signed by participants.

6.2 Informed Consent

Before enrollment, investigators provided potential participants or their legally authorized representatives with comprehensive information regarding the study objectives, procedures, potential benefits and risks, alternative treatments, and participant rights in accordance with the Declaration of Helsinki.

Written informed consent was obtained voluntarily from all participants or their legal representatives prior to any study-related procedures.

All participants were covered by trial-related insurance to compensate for potential study-related adverse events. Participants' contact information was recorded, and investigator contact details were provided to ensure timely communication throughout the study.

7. DATA PRIVACY AND SECURITY MONITORING PROGRAM

This study was conducted in compliance with Good Clinical Practice (GCP) guidelines and applicable regulations. Measures were implemented to ensure the confidentiality, integrity, and security of all participant data.

Personal information was accessible only to authorized study personnel and ethics committee members and was used exclusively for research purposes unless additional written consent was obtained.

All data were stored in secure, access-restricted electronic databases. Data transmission was

encrypted, and personally identifiable information was removed prior to analysis. Upon study completion, datasets were de-identified before statistical analysis.

To ensure protocol rigor, investigators, treating clinicians, and outcome assessors were assigned to independent roles. The study protocol remained unchanged after initiation. Trained study management personnel supervised the trial to ensure protocol adherence and consistency in data collection.

8. QUALITY CONTROL AND QUALITY ASSURANCE IN CLINICAL RESEARCH

8.1 Researcher Qualification and Researcher Training

The principal investigator was responsible for overall quality control. All study personnel possessed appropriate professional qualifications and clinical research experience.

Prior to study initiation, standardized training was conducted covering the study protocol, GCP requirements, informed consent procedures, CRF completion, data management SOPs, adverse event reporting, and data protection.

8.2 Deviations/violations in the Research Process

All protocol deviations were documented in source records and deviation logs, including the date, cause, description, potential impact, and corrective actions.

The principal investigator evaluated the significance of each deviation and its potential impact on participant safety and data integrity. Major deviations were promptly reported to the ethics committee and the sponsor.

8.3 Monitoring

Study monitoring was performed by institutional quality assurance personnel or independent monitors designated by the sponsor. Monitoring activities included verification of informed consent procedures, data accuracy and completeness, adverse event reporting, protocol compliance, investigational product management, and documentation integrity.

9. EXPECTED PROGRESS AND COMPLETION DATES OF RESEARCH PROJECTS

June 2022 - December 2022: Finalization of the updated study protocol, ethics approval, clinical trial registration, and investigator training.

January 2023 - December 2024: Participant recruitment, screening, follow-up visits, data entry, CRF review, and adverse event assessment.

January 2025 - February 2025: Final data verification, statistical and bioinformatics analyses, manuscript preparation and submission, and study completion.

10.REFERENCES

1. Network, G.B.o.D.C. (2020). Global Burden of Disease Study 2019 (GBD 2019) results.

2. Tong, L.P., Yu, H., Huang, X.Y., Shen, J., Xiao, G.Z., Chen, L., Wang, H.Y., Xing, L.P., and Chen, D. (2022). Current understanding of osteoarthritis pathogenesis and relevant new approaches. Bone Res. 10, 60. 10.1038/s41413-022-00226-9.

3. Bijlsma, J.W., Berenbaum, F., and Lafeber, F.P. (2011). Osteoarthritis: an update with relevance for clinical practice. The Lancet 377, 2115-2126. 10.1016/S0140-6736(11)60243-2.

4. Zhuo, Q., Yang, W., Chen, J., and Wang, Y. (2012). Metabolic syndrome meets osteoarthritis. Nature Reviews Rheumatology 8, 729-737. 10.1038/nrrheum.2012.135.

5. Kahn, S.E., Hull, R.L., and Utzschneider, K.M. (2006). Mechanisms linking obesity to insulin resistance and type 2 diabetes. Nature 444, 840-846. 10.1038/nature05482.

6. Tahrani, A.A., Bailey, C.J., Del Prato, S., and Barnett, A.H. (2011). Management of type 2 diabetes: new and future developments in treatment. The Lancet 378, 182-197. 10.1016/s0140-6736(11)60207-9.

7. Kim, S., Jung, J., Kim, H., Heo, R.W., Yi, C.O., Lee, J.E., Jeon, B.T., Kim, W.H., Hahm, J.R., and Roh, G.S. (2014). Exendin-4 Improves Nonalcoholic Fatty Liver Disease by Regulating Glucose Transporter 4 Expression in ob/ob Mice. Korean Journal of Physiology & Pharmacology 18, 333-339. 10.4196/kjpp.2014.18.4.333.

8. Beiroa, D., Imbernon, M., Gallego, R., Senra, A., Herranz, D., Villarroya, F., Serrano, M., Ferno, J., Salvador, J., Escalada, J., et al. (2014). GLP-1 Agonism Stimulates Brown Adipose Tissue Thermogenesis and Browning Through Hypothalamic AMPK. Diabetes 63, 3346-3358. 10.2337/db14-0302.

9. Itou, M., Kawaguchi, T., Sakata, M., Taniguchi, E., Sumie, S., Oriishi, T., Mitsuyama, K., Torimura, T., Tsuruta, O., and Sata, M. (2012). GLP-1R Agonist Increased Glucose Uptake and Inhibited GSK3β Phosphorylation Through the AMPK Signaling Pathways in Human Hepatocytes. Gastroenterology 142, S1024-S1024.

10. Song, S., Guo, R.Y., Mehmood, A., Zhang, L., Yin, B.W., Yuan, C.C., Zhang, H.I., Guo, L., and Li, B. (2022). Liraglutide attenuate central nervous inflammation and demyelination through AMPK and pyroptosis-related NLRP3 pathway. CNS Neurosci. Ther. 28, 422-434. 10.1111/cns.13791.

11. Wu, L.T., Zhou, M., Li, T.Y., Dong, N., Yi, L., Zhang, Q.Y., and Mi, M.T. (2022). GLP-1 regulates exercise endurance and skeletal muscle remodeling via GLP-1R/AMPK pathway.

Biochim. Biophys. Acta-Mol. Cell Res. 1869, 119300. 10.1016/j.bbamcr.2022.119300.

Clinical Study: A Randomized, Controlled, Prospective Clinical Trial on the Efficacy and Safety of Semaglutide Injection in Patients with Early-to-Mid Stage Obesity-Related Knee Osteoarthritis

STATISTICAL ANALYSIS PLAN

The First Affiliated Hospital of Jinan University

Version: 1.0
Date: July 2023

Content

1. SYNOPSIS OF STUDY DESIGN AND PROCEDURES 24

1.1 Study Objective 24

1.2 Study Design 24

1.3 Study Outcomes 24

1.4 Analysis Populations 24

1.5 Sample Size Justification 25

2. STATISTICAL ANALYSIS METHODS 25

2.1 Demographic and Baseline Characteristics 25

2.1.1 Analytical Principles 25

2.1.2 Descriptive Statistics for Baseline Data 25

2.2 Endpoint Analyses 26

2.2.1 Analysis of Primary and Secondary Endpoints 26

2.2.2 Between-Group Comparisons and Longitudinal Analysis of WOMAC Scores 26

2.3 Safety Analysis 26

2.4 Subgroup and Sensitivity Analyses 26

2.5 Handling of Missing Data 26

2.6 Statistical Software 27

1. SYNOPSIS OF STUDY DESIGN AND PROCEDURES

1.1 Study Objective

This study aims to evaluate the efficacy and safety of semaglutide in patients with early-to-moderate KOA comorbid with obesity. The objective is to assess the effects of semaglutide on body mass index (BMI), inflammatory markers, levels of joint pain, function and changes in the knee joint images (e.g., the Western Ontario and McMaster Universities Osteoarthritis Index/WOMAC score and MRI evaluation) through a randomized, controlled clinical trial. Assessments will be conducted at multiple timepoints before and after treatment initiation (0, 1, 12, and 24 weeks). The findings are expected to provide evidence-based support for the conservative pharmacological management of early-to-moderate KOA in patients with obesity.

1.2 Study Design

This prospective, randomized, controlled pilot clinical trial allocated 20 enrolled patients in a 1:1 ratio to either the hyaluronic acid (HA) conventional group or the HA combined with semaglutide (HA+SG) group. An independent statistician generated the randomization sequence using computer software with a block size of 6, and allocation was concealed using sequentially numbered, opaque, sealed envelopes (SNOSE), resulting in balanced groups of 10 patients each. While blinding of patients and clinicians was not feasible due to the nature of the interventions, outcome assessors and data analysts remained blinded throughout the study.

1.3 Study Outcomes

Primary Study Outcome

- Change in Western Ontario and McMaster Universities Osteoarthritis Index (WOMAC) score (pain, stiffness, and function).
- Change in body weight and BMI.

Secondary Study Outcomes

- Change in cartilage degradation assessed by MRI.

Safety Outcomes

- Incidence and severity of Adverse Events (AEs) and Serious Adverse Events (SAEs).

1.4 Analysis Populations

Full Analysis Set (FAS) / Intention-To-Treat (ITT) Population: all randomized subjects.

Per-Protocol (PP) Population: subjects who complete all follow-up visits without major protocol deviations.

Safety Population: all subjects who receive at least one dose of the study intervention.

For this exploratory pilot study, the Per-Protocol (PP) Population is designated as the primary analysis set for efficacy endpoints. This approach aims to provide a preliminary estimate of the treatment effect under conditions of complete protocol adherence. Concurrently, sensitivity analyses will be performed on the Full Analysis Set (FAS) to assess the robustness of findings. Results from both populations will be reported.

1.5 Sample Size Justification

The sample size is estimated using G*power (version 3.1.9.7, Heinrich Heine University Düsseldorf, Germany). According to the results reported by Wilding et al (*The New England Journal of Medicine*, 2021; 384: 989-1002), semaglutide produced significant improvements in body weight loss, with estimated differences of -12.4 percentage points. Assuming a standard deviation (SD) of 10 points, the standardized effect sizes (Cohen's *d*) are calculated as follows: d = Δ/SD, yielding values of 1.24.

The key parameters used in the G*power calculation are:

Parameter	Value
Test type	Two-tailed, two independent groups (t-test)
Effect Size (*d*)	1.24
Significance level (α err prob)	0.05
Power (1-β err prob)	0.69
Allocation ratio (N1/N2)	1

Based on these assumptions, the estimated sample size is 9 participants/group. Considering an anticipated dropout rate of 10-15%, the final target enrollment is 10 participants/group (total *n* = 20).

2. STATISTICAL ANALYSIS METHODS

2.1 Demographic and Baseline Characteristics

2.1.1 Analytical Principles

The primary efficacy analyses will be conducted on the Per-Protocol (PP) Population. Supportive analyses will be performed on the Full Analysis Set (FAS).

2.1.2 Descriptive Statistics for Baseline Data

Baseline demographic and clinical characteristics will be compared between the two

treatment groups (Conventional: HA alone; Intervention: HA + semaglutide) using independent samples *t*-tests.

2.2 Endpoint Analyses

2.2.1 Analysis of Primary and Secondary Endpoints

For the primary endpoints (change in WOMAC score and BMl) and secondary continuous endpoints such as MRI imaging. The post-treatment value will serve as the dependent variable, with treatment group as the main independent variable and the baseline value included as a covariant. For repeated measures across multiple time points, a mixed-effects model will be employed.

2.2.2 Between-Group Comparisons and Longitudinal Analysis of WOMAC Scores

In addition to the ANCOVA approach described in Section 2.2.1, between-group comparisons of WOMAC score changes from baseline will be performed at specific time points (Week 12 and Week 24). Depending on normality and variance assumptions, independent samples *t*-tests will be applied. Furthermore, a mixed-effects model will be used to analyze longitudinal WOMAC data, with time, treatment group, and their interaction included as fixed effects, and subject-specific random intercepts to account for repeated measures. This model will evaluate whether the semaglutide combination exerts a differential effect on WOMAC scores over time compared to the conventional group.

2.3 Safety Analysis

All AEs and SAEs will be listed and summarized by system organ class, severity, and relationship to study intervention.

Incidence rates will be calculated and presented descriptively.

2.4 Subgroup and Sensitivity Analyses

Pre-specified subgroup analyses based on the Per-Protocol Set will be conducted to assess the robustness of the primary findings. This will include repeating the between-group comparisons and longitudinal analyses described in Section 2.2.2 for the PP population.

2.5 Handling of Missing Data

For the primary efficacy analysis based on the PP population, a complete-case analysis will be applied. For the pre-specified sensitivity analysis on the FAS, missing data at the endpoint will be imputed using the Last Observation Carried Forward (LOCF) method to assess the robustness

of the conclusions.

2.6 Statistical Software

Analyses will be performed using GraphPad Prism (version 9.0 or higher) and SPSS Statistics (version 26.0 or higher). Full Analysis Set analysis will be performed by the R project with a mixed-effects model.

All tests will be two-sided, with a p-value < 0.05 considered statistically significant. Given the exploratory nature of this pilot study, no adjustment for multiple comparisons will be performed. Interpretation of results will emphasize effect sizes (such as mean between-group differences with 95% confidence intervals) rather than reliance solely on p-values.

CONSORT Harms 2022 integrated into CONSORT 2010 items checklist of information to include when reporting a randomised trial

Section/Topic	Item No	Checklist item	Reported on page No
Title and abstract			
	1a	Identification as a randomised trial in the title	N/A
	1b	Structured summary of trial design, methods, results of outcomes of benefits and harms, and conclusions (for specific guidance see CONSORT for abstracts)	Manuscript page 2
Introduction			
Background and objectives	2a	Scientific background and explanation of rationale	Manuscript 2-3
	2b	Specific objectives or hypotheses for outcomes benefits and harms	Manuscript 3
Methods			
Trial design	3a	Description of trial design (such as parallel, factorial) including allocation ratio	Manuscript 23-24; Study protocol-2023V1.0
	3b	Important changes to methods after trial commencement (such as eligibility criteria), with reasons	N/A
Participants	4a	Eligibility criteria for participants	Manuscript 24, Figure S7A and Study protocol-2023V1.0
	4b	Settings and locations where the data were collected	Manuscript 23-24
Interventions	5	The interventions for each group with sufficient details to allow replication, including how and when they were actually administered	Manuscript 23-24; Study protocol-2023V1.0
Outcomes	6a	Completely defined pre-specified primary and secondary outcome measures for both benefits and harms, including how and when they were assessed	Manuscript 10, Figure 7A, Study protocol-2023V1.0
	6b	Any changes to trial outcomes after the trial commenced, with reasons	N/A
	6c	Describe if and how non-prespecified outcomes of benefits and harms were identified, including any selection criteria, if applicable	N/A

Section/Topic	Item No	Checklist item	Reported on page No
Sample size	7a	How sample size was determined	Manuscript 23-24, Study protocol-2023V1.0, Statistical Analysis Plan
	7b	When applicable, explanation of any interim analyses and stopping guidelines	N/A
Randomisation:			
Sequence generation	8a	Method used to generate the random allocation sequence	Study protocol-2023V1.0
	8b	Type of randomisation; details of any restriction (such as blocking and block size)	Study protocol-2023V1.0
Allocation concealment mechanism	9	Mechanism used to implement the random allocation sequence (such as sequentially numbered containers), describing any steps taken to conceal the sequence until interventions were assigned	Study protocol-2023V1.0
Implementation	10	Who generated the random allocation sequence, who enrolled participants, and who assigned participants to interventions	Study protocol-2023V1.0
Blinding	11a	If done, who was blinded after assignment to interventions (e.g., participants, care providers, those assessing outcomes of benefits and harms) and how	Study protocol-2023V1.0
	11b	If relevant, description of the similarity of interventions	N/A
Statistical methods	12a	Statistical methods used to compare groups for primary and secondary outcomes of both benefits and harms	The legend of Figure 7, SAP-2023V1.0
	12b	Methods for additional analyses, such as subgroup analyses and adjusted analyses	SAP-2023V1.0
Results			
Participant flow (a diagram is strongly recommended)	13a	For each group, the numbers of participants who were randomly assigned, received intended treatment, and were analysed for outcomes of benefits and harms	Figure S7; Study protocol-2023V1.0
	13b	For each group, losses and exclusions after randomisation, together with reasons	Figure S7
Recruitment	14a	Dates defining the periods of recruitment and follow-up for outcomes of benefits and harms	Manuscript 9, Study protocol-2023V1.0
	14b	Why the trial ended or was stopped	N/A
Baseline data	15	A table showing baseline demographic and clinical characteristics for each group	Study protocol-2023V1.0
Numbers analysed	16	For each group, number of participants (denominator) included in each analysis and whether the analysis was by original assigned groups and if any exclusions were made	Figure S7, Study protocol-2023V1.0

Section/Topic	Item No	Checklist item	Reported on page No
Outcomes and estimation	17a	For each primary and secondary outcome of benefits and harms, results for each group, and the estimated effect size and its precision (such as 95% confidence interval)	Manuscript 10, Figure 7 and Figure S7
	17a2	For outcomes omitted from the trial report (benefits and harms), provide rationale for not reporting and indicate where the data on omitted outcomes can be accessed	N/A
	17b	Presentation of both absolute and relative effect sizes is recommended, for outcomes of benefits and harms	Manuscript 10, Study protocol-2023V1.0
	17c	Report zero events if no harms were observed	N/A
Ancillary analyses	18	Results of any other analyses performed, including subgroup analyses and adjusted analyses, distinguishing pre-specified from exploratory	N/A
Harms	19	All important harms or unintended effects in each group (for specific guidance see CONSORT for harms)	N/A
Discussion			
Limitations	20	Trial limitations, addressing sources of potential bias related to the approach to collecting or reporting data on harms, imprecision, and, if relevant, multiplicity or selection of analyses	Manuscript 12-13
Generalisability	21	Generalisability (external validity, applicability) of the trial findings	Manuscript 11
Interpretation	22	Interpretation consistent with results, balancing benefits and harms, and considering other relevant evidence	Manuscript 12-13
Other information			
Registration	23	Registration number and name of trial registry	Manuscript 2, 23
Protocol	24	Where the full trial protocol and other relevant documents can be accessed, including additional data on harms	Study protocol-2023V1.0; SAP-2023V1.0
Funding	25	Sources of funding and other support (such as supply of drugs), role of funders	Manuscript 13

Note: Adapted from Schulz (2010) to integrate items of CONSORT Harms 2022 (Junqueira 2022) [https://creativecommons.org/licenses/by/2.0/]. CONSORT items 1b, 2b, 6a, 11a, 12a, 13a, 14a, 16a, 17a, 17b, 18, 20 and 24 of were modified to incorporate elements relevant to the reporting of harms. Two new items were added (item 6c and 17a2). Please see the CONSORT Harms 2022 statement for additional details (Junqueira 2022).

We strongly recommend reading the CONSORT 2010 statement (Schulz 2010) in conjunction with the CONSORT Harms 2022 statement (Junqueira 2022) for important clarifications on all the items. If relevant, we also recommend reading CONSORT extensions for cluster randomised trials, non-inferiority and equivalence trials, non-pharmacological treatments, adaptive designs, pilot and feasibility studies, multi arm trials, cross-over and pragmatic trials. Additional extensions are forthcoming: for those and for up-to-date references relevant to this checklist, see EQUATOR Network.

Figure 1B

	Obesity		Obesity+Semaglutide	
	mean	standard deviation	mean	standard deviation
Day1	31.175	0.851102	30.6125	0.710005
Day2	31.325	0.881405	30.75	0.639196
Day3	31.4375	0.899913	30.875	0.658461
Day4	31.55	0.926013	31.05	0.641427
Day5	31.7	0.911043	31.1375	0.61861
Day6	31.875	0.929718	31.2625	0.602228
Day7	32	0.946044	31.35	0.570714
Day8	32.0875	0.938666	31.5125	0.651235
Day9	32.21875	0.877474	31.7	0.684523
Day10	32.7625	0.6	31.7625	0.722965
Day11	32.56125	0.692142	31.8875	0.758641
Day12	32.6875	0.597385	32.0125	0.703943
Day13	32.8275	0.550835	32.2	0.715142
Day14	32.98	0.483916	32.4375	0.477905
Day15	33.05	0.41833	32.525	0.455914
Day16	33.12625	0.455602	32.7125	0.494072
Day17	33.3025	0.431328	32.875	0.483292
Day18	33.495	0.36149	33.0875	0.546253
Day19	33.73125	0.341813	33.275	0.587367
Day20	33.9375	0.387097	33.4625	0.49839
Day21	34.15875	0.445994	33.6625	0.492624
Day22	34.3325	0.487231	33.9	0.444008
Day23	34.445	0.459538	34.0125	0.383359
Day24	34.52125	0.449901	34.2	0.410575
Day25	34.66625	0.455493	34.4	0.392792
Day26	34.7725	0.465611	34.5875	0.401559
Day27	34.93625	0.407674	34.7375	0.385218
Day28	35.05625	0.414908	34.825	0.399106
Day29	35.11625	0.416051	35.0375	0.515302
Day30	35.24125	0.434926	34.125	0.528475
Day31	35.36625	0.354575	33.9625	0.585388
Day32	35.53875	0.309453	34.1875	0.438952
Day33	35.68625	0.292102	34.425	0.517549
Day34	35.80125	0.279304	34.7	0.478091
Day35	35.94125	0.314103	34.9375	0.474906
Day36	36.08	0.35819	35.1	0.437526
Day37	36.2	0.357071	34.25	0.34641
Day38	36.30625	0.348602	34.0125	0.352288
Day39	36.39	0.32665	34.225	0.413176
Day40	36.53625	0.338302	34.5125	0.442194
Day41	36.6575	0.37302	34.775	0.486239
Day42	36.74625	0.370774	34.9625	0.523552
Day43	36.8375	0.373957	35.1375	0.465794
Day44	36.98125	0.385631	34.1	0.29277
Day45	37.08625	0.397899	33.9125	0.422366
Day46	37.26375	0.408899	34.0375	0.531675
Day47	37.48375	0.427608	34.375	0.46828
Day48	37.5875	0.388708	34.6875	0.540998
Day49	37.72875	0.384104	34.925	0.47132
Day50	37.8375	0.356853	35.0875	0.502671
Day51	38.0125	0.401365	34.2125	0.476408

Day52	38.175	0.426468	34.025	0.523041
Day53	38.35	0.403113	34.2375	0.611643
Day54	38.575	0.352668	34.4875	0.610474
Day55	38.7875	0.347985	34.675	0.554849
Day56	38.975	0.359687	34.8375	0.531675
Day57	39.2125	0.351559	35.075	0.49208
Day58	39.3625	0.387097	33.9375	0.580486
Day59	39.575	0.429389	34.0375	0.480885
Day60	39.7625	0.499844	34.2375	0.465794
Day61	39.95	0.484768	34.5	0.509902
Day62	40.0875	0.498592	34.7125	0.527629
Day63	40.25	0.512348	34.925	0.497853
Day64	40.4125	0.530183	35.15	0.498569
Day65	40.59625	0.40081	34.2875	0.668554
Day66	40.77125	0.394697	34.0375	0.592663
Day67	40.96625	0.40277	34.175	0.489168
Day68	41.16875	0.400732	34.45	0.501427
Day69	41.36625	0.47405	34.725	0.554849
Day70	41.5	0.5	34.9	0.523723
Day71	41.65	0.48734	35.0875	0.546253
Day72	41.8625	0.517053	34.1875	0.608129
Day73	42.05	0.507445	34.05	0.578174
Day74	42.2	0.543139	34.3125	0.548862
Day75	42.425	0.609816	34.575	0.494975
Day76	42.675	0.651441	34.7625	0.468851
Day77	42.85	0.69282	34.9625	0.489716
Day78	43.025	0.756224	35.1375	0.515302
Day79	43.225	0.751249	34.05	0.630193
Day80	43.475	0.780625	34.175	0.474342
Day81	43.675	0.749583	34.4875	0.451782
Day82	43.85	0.722842	34.7125	0.470372
Day83	44.0375	0.734741	34.95	0.507093
Day84	44.1375	0.701672	35.1	0.489898
Day85	44.275	0.679614	35.2375	0.477905

Figure1E	Cartilage area (um^2)			
	Obesity	Obesity+Semagutide	Obesity+DMM	esity+DMM+Semagut
	178542	187554	145884	165224
	165278	154558	115442	132909
	160441	176662	78541	154774
	152214	161445	123554	162242
	175442	177445	78542	125445
	162448	166552	76995	135775
	185447	189554	125447	159224
	164221	165584	98542	128554
	178344	188344	175578	187167
	154802	154802	124368	132909
	158457	178457	68445	196893
	151230	161230	122180	196616
	178344	178344	84208	119184
	164802	164802	98814	139551.2
	188457	188457	132671	192354
	161230	161230	95737	130053

Figure1H	Osteophyte maturity			
	Obesity	Obesity+Semaglutide	Obesity+DMM	Obesity+DMM+Semaglu
	0	1	3	1
	0	0	3	1
	0	1	3	1
	0	0	2	1
	1	0	2	2
	0	0	2	1
	0	1	2	1
	1	0	3	2
	0	1	2	1
	0	0	3	1
	0	1	3	1
	1	1	2	2
	1	1	2	2
	0	0	2	2
	0	1	2	1
	1	1	3	2

Figure1M	%ADAMTS+ cells			
	Obesity	Obesity+Semaglutide	Obesity+DMM	Obesity+DMM+Semaglu
	16.224158	12.21584	60.2215	38.5248
	12.55488	15.2248	51.2248	32.2158
	10.2548	16.5188	52.1548	38.2214
	10.5426	10.2548	51.26898	30.2158
	15.2248	9.2248	63.2215	35.2187
	11.25483	10.2548	49.22858	32.1154
	12.3254	11.0258	61.2248	31.5548
	9.21458	12.22158	55.0258	40.2218

Body Weight (g)					
Obesity+DMM		Obesity+DMM+Semaglutide		Obesiity+DMM	
mean	standard deviation	mean	standard deviation	mean	
31.15	0.671884	30.725	0.675595	30.725	
31.3125	0.705969	30.875	0.662786	30.9	
31.4625	0.692691	31.025	0.667083	31.05	
31.625	0.688165	31.25	0.563154	31.2125	
31.7625	0.726906	31.3625	0.575543	31.4	
31.875	0.716639	31.4875	0.610474	31.45	
31.975	0.714643	31.525	0.599404	31.5375	
32.125	0.716639	31.6	0.61412	31.6	
32.225	0.726538	31.6625	0.57802	31.6625	
32.3875	0.751071	31.8625	0.54756	31.775	
32.5	0.728991	32.0125	0.488255	31.8625	
32.65	0.7329	32.2125	0.442194	32.025	
32.7875	0.699872	32.275	0.511999	32.125	
32.85	0.648074	32.375	0.449603	32.225	
32.95	0.648074	32.45	0.424264	32.325	
33.125	0.634147	32.575	0.430116	32.4625	
33.3125	0.670687	32.8	0.489898	32.8125	
33.4625	0.539676	32.975	0.474342	33.0125	
33.6125	0.499821	33.2	0.427618	33.2	
33.725	0.483292	33.375	0.426782	33.4625	
33.85	0.414039	33.5625	0.480885	33.675	
33.95	0.424264	33.8	0.465986	33.9125	
34.0625	0.410357	33.95	0.420883	34.0375	
34.2375	0.427409	34.15	0.504268	34.2125	
34.3375	0.35431	34.2875	0.551459	34.425	
34.5625	0.399777	34.4375	0.550162	34.6125	
34.75	0.414039	34.625	0.580025	34.8	
34.85	0.498569	34.7875	0.605776	34.9125	
35.025	0.517549	34.925	0.606512	34.975	
35.125	0.497853	34.0875	0.701911	35.0875	
35.225	0.523041	33.8625	0.620915	33.9125	
35.375	0.541822	34.05	0.630193	33.9875	
35.5125	0.496955	34.3	0.58064	34.225	
35.675	0.465219	34.6	0.495696	34.4875	
35.8125	0.390741	34.7875	0.496955	34.7	
35.95	0.333809	35.05	0.434248	34.9	
36.075	0.361544	33.9	0.450397	35.125	
36.1875	0.401559	33.85	0.504268	34.15	
36.3625	0.329231	34.0125	0.593867	34.0125	
36.475	0.281577	34.2875	0.524915	34.225	
36.65	0.244949	34.6	0.475094	34.4125	
36.775	0.249285	34.8625	0.427409	34.6625	
36.9125	0.229518	35.1625	0.430739	34.8875	
37.0625	0.206588	34.425	0.446414	35.1625	
37.175	0.225198	34.1625	0.48679	34.1375	
37.3375	0.232609	34.175	0.436708	34.0875	
37.4625	0.26152	34.4625	0.399777	34.3	
37.6125	0.279987	34.7625	0.459619	34.525	
37.6	0.2	34.975	0.391882	34.75	
37.8375	0.381491	35.1625	0.430739	34.9375	
38.05	0.417475	34.3	0.682433	35.1625	

38.225	0.426782	34.0625	0.568048	34.1875
38.4	0.370328	34.3	0.547723	34.025
38.5625	0.381491	34.5375	0.555331	34.2125
38.7	0.354562	34.7875	0.540998	34.35
38.8625	0.333542	34.95	0.518239	34.6
39.0125	0.299702	35.175	0.426782	34.8375
39.125	0.315096	34.0375	0.531675	35.175
39.2875	0.290012	34.1	0.427618	34.0125
39.4875	0.335676	34.3125	0.425735	34
39.6875	0.339905	34.55	0.4	34.2375
39.9	0.420883	34.75	0.420883	34.5125
40.075	0.459036	34.9625	0.388909	34.725
40.225	0.520302	35.1875	0.368152	34.9375
40.41125	0.522506	33.925	0.625071	35.2375
40.60875	0.535895	33.975	0.486239	34.2875
40.87875	0.4628	34.2875	0.467325	34.2125
41.08125	0.467468	34.47375	0.4386	34.325
41.24125	0.4285	34.75	0.410575	34.525
41.4375	0.440576	35	0.403556	34.825
41.65	0.486973	35.25	0.392792	34.9375
41.8375	0.447014	34.075	0.601783	35.275
42.05	0.469042	34.1875	0.4734	34.175
42.2875	0.435685	34.5375	0.450198	34.125
42.45	0.410575	34.725	0.391882	34.2625
42.65	0.450397	34.9	0.396412	34.4
42.85	0.489898	35.1	0.4	34.725
43.05	0.520988	35.2875	0.352288	35.1875
43.2125	0.499821	34.17875	0.266535	35.325
43.3375	0.512522	34.25	0.38545	34.2125
43.5125	0.499821	34.55	0.302372	34.2375
43.6625	0.537022	34.7375	0.244584	34.3625
43.875	0.567576	34.9	0.267261	34.65
44.0625	0.606954	35.1625	0.302076	34.95
44.2375	0.597465	35.375	0.345378	35.05

Figure1F

esity+DMM+Pair feeding	Obesity	Obesity+Semaglutide
148995	1	0
125547	0	0
98541	1	0
88954	0	1
115472	0	2
74662	0	0
135572	1	1
99854	1	1
171333	0	0
154226	0	0
103110	2	0
102485	0	0
125444	0	0
85716	0	0
154242	1	1
23862	1	1

esity+DMM+Pair feeding
2
3
2
3
2
3
3
3
2
3
2
3
2
2
3
3

Figure1J	Osteophyt
Obesity	Obesity+Semagutide
0.325144	0.23547
0.28845	0.241115
0.30224	0.30214
0.25447	0.35547
0.274152	0.24775
0.26882	0.26552
0.241577	0.21774
0.354922	0.274922
0.261627	0.301627
0.249162	0.299162
0.272682	0.312682
0.287721	0.227721
0.264852	0.214852
0.240896	0.200896

esity+DMM+Pair feeding
58.1154
56.2214
54.2215
62.1824
48.2287
62.2254
67.2218
50.2187

Figure1N	%A
Obesity	Obesity+Semaglutide
70	71.2154
75.5	76.25
77.5	79.24
76.5	79.21
72	74.21
74.2	74.62
78.21	71.52
71.25	72.53

M+Pair feeding standard deviation
0.675595
0.578174
0.609449
0.631184
0.578174
0.611789
0.602228
0.61412
0.63457
0.620484
0.661033
0.660627
0.660627
0.629626
0.613538
0.632314
0.461171
0.479397
0.46291
0.440576
0.49208
0.445413
0.420671
0.448609
0.433425
0.458063
0.450397
0.448609
0.494975
0.461171
0.48532
0.591457
0.47132
0.48532
0.504268
0.465986
0.462138
0.611789
0.412094
0.413176
0.458063
0.468851
0.415546
0.430739
0.489716
0.432394
0.4
0.391882
0.392792
0.427409
0.430739

Figure 1C	Food intake (g)		
	Obesity+DMM+Semaglutide		Obesiity+DMM
	mean	standard deviation	mean
Day1	3.1875	0.180772	3.1875
Day2	3.175	0.260494	3.225
Day3	3.32625	0.167583	3.3125
Day4	3.1875	0.195941	3.2375
Day5	3.15	0.2	3.1125
Day6	3.1375	0.206588	3.175
Day7	3.2425	0.234992	3.32875
Day8	3.15	0.20702	3.35
Day9	3.0375	0.176777	3.5625
Day10	3.1375	0.192261	3.3
Day11	3.1125	0.13562	3.29375
Day12	3.1	0.169031	3.1875
Day13	3.025	0.175255	3.3375
Day14	3.125	0.158114	3.2375
Day15	3.1125	0.112599	3.1775
Day16	3.21375	0.15702	3.15
Day17	3.2375	0.091613	3.24625
Day18	3.225	0.128174	3.1125
Day19	3.15	0.092582	3.1875
Day20	3.14125	0.072985	3.25
Day21	3.15	0.239046	3.1625
Day22	3.0625	0.118773	3.3375
Day23	3.0875	0.195941	3.225
Day24	3.0375	0.159799	3.32125
Day25	3.1125	0.164208	3.175
Day26	3.2625	0.130247	3.21625
Day27	3.225	0.332738	3.275
Day28	3.2	0.119523	3.2875
Day29	3.176389	0.071378	3.2125
Day30	0.241667	0.072921	3.20625
Day31	0.4125	0.112599	0.241667
Day32	1.388889	0.182671	0.4125
Day33	2.565278	0.243246	1.388889
Day34	2.886111	0.267772	2.565278
Day35	3.325	0.116496	2.886111
Day36	3.284445	0.1721	3.325
Day37	0.179167	0.073328	3.284445
Day38	0.433195	0.11611	0.179167
Day39	1.159722	0.30231	0.433195
Day40	2.54625	0.302321	1.159722
Day41	2.72	0.268275	2.54625
Day42	3.066667	0.112687	2.72
Day43	3.15	0.119523	3.066667
Day44	0.15	0.053452	3.15
Day45	0.425	0.128174	0.15
Day46	1.22625	0.168433	0.425
Day47	2.275	0.128174	1.22625
Day48	2.8875	0.247487	2.275
Day49	3.0375	0.130247	2.8875
Day50	3.1125	0.099103	3.0375
Day51	0.2	0.075593	3.1125

0.375832	Day52	0.4625	0.091613	0.2	
0.47132	Day53	1.1	0.261861	0.4625	
0.438952	Day54	2.2375	0.213391	1.1	
0.338062	Day55	2.6375	0.232609	2.2375	
0.440779	Day56	2.975	0.070711	2.6375	
0.434042	Day57	3.225	0.138873	2.975	
0.426782	Day58	0.23	0.134377	3.225	
0.299702	Day59	0.4875	0.188509	0.23	
0.232993	Day60	1.0125	0.195941	0.4875	
0.350255	Day61	1.675	0.183225	1.0125	
0.429077	Day62	2.5	0.092582	1.675	
0.443203	Day63	2.9	0.106904	2.5	
0.447014	Day64	3.35	0.177281	2.9	
0.399777	Day65	0.2	0.075593	3.35	
0.331393	Day66	0.76	0.240713	0.2	
0.35632	Day67	1.525	0.175255	0.76	
0.353553	Day68	2.05	0.119523	1.525	
0.416619	Day69	2.45	0.220389	2.05	
0.436708	Day70	2.775	0.260494	2.45	
0.417261	Day71	3.3	0.185164	2.775	
0.423421	Day72	0.225	0.10351	3.3	
0.46828	Day73	0.45	0.20702	0.225	
0.452769	Day74	0.8375	0.370087	0.45	
0.406861	Day75	1.6	0.267261	0.8375	
0.417475	Day76	2.45	0.226779	1.6	
0.430116	Day77	2.6125	0.188509	2.45	
0.258775	Day78	3.3875	0.172689	2.6125	
0.37321	Day79	0.225	0.10351	3.3875	
0.458063	Day80	0.625	0.271241	0.225	
0.45336	Day81	1.4	0.185164	0.625	
0.468851	Day82	2.2875	0.188509	1.4	
0.396412	Day83	2.8	0.160357	2.2875	
0.453557	Day84	3.025	0.10351	2.8	
0.472077	Day85	3.225	0.148805	3.025	
				3.225	

OARSI score			Figure1G
Obesity+DMM	+DMM+Semity+DMM+Pair feeding		
4	3	5	
4	4	4	
6	5	6	
5	3	5	
5	4	4	
5	5	5	
5	2	6	
6	3	6	
3	3	4	
4	4	4	
6	2	6	
5	4	5	
5	4	4	
5	6	5	
5	2	4	
6	3	6	

e volume（mm³）

Obesity+DMM	+DMM+Semity+DMM+Pair feeding	
1.32541	0.78994	1.31447
1.25414	0.66547	1.28447
1.18895	0.80244	1.264447
1.25448	0.75554	1.214457
1.20441	0.698544	1.287754
1.2547	0.821114	1.24441
1.1189244	0.751114	1.20334
1.21126	0.808339	1.23126
1.21012	0.732178	1.24012
1.13942	0.798339	1.18942
1.10408	0.732178	1.21408
1.22632	0.828339	1.22632
1.21708	0.812178	1.21708
1.20632	0.638339	1.04632

Figure1L

Obesity
10.1
7.9
9.6
12.4
8.8
10.5
8.4
11.4

CAN+ area

Obesity+DMM	+DMM+Semity+DMM+Pair feeding	
21	45.21	17.51
19.25	41.25	18.54
18.24	39.54	11.25
11.5486	37.58	9.5128
11.44875	43.24	16.24
17.25	43.87	21.54
14.35	46.57	23.21
16.54	34.55	18.52

Figure1O

M+Pair feeding
standard deviation
0.223207
0.138873
0.210017
0.140789
0.164208
0.183225
0.178841
0.185164
0.118773
0.2
0.186006
0.064087
0.232609
0.118773
0.331307
0.075593
0.209689
0.099103
0.360307
0.169031
0.074402
0.184681
0.166905
0.207739
0.046291
0.164224
0.148805
0.210017
0.145774
0.120823
0.072921
0.112599
0.182671
0.243246
0.267772
0.116496
0.1721
0.073328
0.11611
0.30231
0.302321
0.268275
0.112687
0.119523
0.053452
0.128174
0.168433
0.128174
0.247487
0.130247
0.099103

0.075593
0.091613
0.261861
0.213391
0.232609
0.070711
0.138873
0.134377
0.188509
0.195941
0.183225
0.092582
0.106904
0.177281
0.075593
0.240713
0.175255
0.119523
0.220389
0.260494
0.185164
0.10351
0.20702
0.370087
0.267261
0.226779
0.188509
0.172689
0.10351
0.271241
0.185164
0.188509
0.160357
0.10351
0.148805

	Synovitis score				
Obesity	sity+Semaglu	besity+DMM	DMM+Sem	+DMM+Pair	feeding
2	2	4	2	4	
2	1	3	3	5	
1	1	4	2	4	
1	1	3	2	3	
1	1	2	2	3	
2	1	2	2	3	
1	1	5	2	2	
1	2	4	2	3	
1	1	5	3	3	
2	1	4	3	3	
2	1	3	2	3	
3	1	2	2	4	
1	2	3	2	4	
1	2	2	2	3	
1	1	2	2	4	
1	1	3	2	2	

%MMP13+ cells				
Obesity+Semaglutid	Obesity+DMM	DMM+Sem	DMM+Pair	feeding
11.2	59.4	39.5	58.4	
12.5	64.5	36.7	66.9	
8.5	47.6	35.4	54.1	
7.4	68.4	32.1	57.5	
9.6	52.4	36.8	48.7	
10.1	57.6	33.9	50.4	
7.4	56.1	31.5	45.6	
11.4	51.9	25.4	60.4	

%Col-2+ area				
Obesity	sity+Semaglu	Obesity+DMM	DMM+Sem	DMM+Pair feeding
62.5551	84.2518	15.5884	45.215	16.875
88.5541	62.5544	28.6652	25.69	28.684
74.2254	65.2214	18.547	34.221	20.487
76.221	57.2254	20.1147	30.577	21.575
65.2214	70.5548	21.557	34.825	19.885
70.2215	75.6624	25.1478	34.258	25.201
65.2148	80.2214	16.587	22.36	14.528
75.5518	60.1158	24.215	37.15	15.668

Figure2A-1

8W von Frey threshold (g)

Obesity	sity+Semagl	besity+DMM	DMM+Sem	+DMM+Pair feeding
1.305	1.825	0.32	0.578	0.491
1.258	1.432	0.258	0.926	0.553
1.432	1.504	0.166	0.858	0.345
1.226	1.305	0.222	0.545	0.193
1.869	1.395	0.458	1.036	0.222
1.669	1.669	0.553	0.705	0.16
1.398	1.329	0.491	0.429	0.773
1.226	1.226	0.193	0.913	0.258

Figure2A-2

Figure2B-1

8W Hot plate reaction time (s)

Obesity	sity+Semagl	besity+DMM	DMM+Sem	+DMM+Pair feeding
20.25	26.22	11.5	17.8	10.5
20.15	22.7	9.5	20.5	9.1
24.33	20.4	9.1	14.3	8.2
25.22	17.5	12	15	11.3
22.45	27.15	8.2	15.1	5.9
24.33	20.4	8.9	11.5	12.4
17.58	21.6	13.5	15.6	7.4
20.15	15.9	6	16.2	6.3

Figure2B-2

Figure2E

Knee joint CGRP fluorescent intensity (fold change)

Obesity	sity+Semagl	besity+DMM	DMM+Sem	+DMM+Pair feeding
1.047	1.051349	2.558096	1.61919	1.941529
0.9854	0.884558	2.481259	1.338081	2.108321
0.8994	0.877061	2.361319	1.171289	2.314468
1.01224	0.998876	2.295727	1.523613	1.913418
1	1.023238	2.164543	1.43928	2.37069

Figure2F

Figure2J

DRG CGRP fluorescent intensity (fold change)

Obesity	sity+Semagl	besity+DMM	DMM+Sem	+DMM+Pair feeding
1.147848	0.619687	2.24171	1.844968	5.569613
0.854595	0.540282	3.76877	1.575352	3.121882
1.324347	0.829908	4.852451	1.341399	2.470668
1.000204	1.192705	5.296403	1.16156	3.220821
0.673006	0.668966	6.355333	1.154147	3.450066

Figure2K

10W von Frey threshold (g)					
Obesity	sity+Semagl	besity+DMM	+DMM+Sem	+DMM+Pair	feeding
1.825	1.917	0.166	0.744	0.258	
1.504	1.825	0.222	1.036	0.774	
1.226	1.669	0.458	0.926	0.669	
1.398	1.226	0.193	0.858	0.169	
1.869	1.329	0.774	0.951	0.222	
1.226	1.036	0.858	0.669	0.533	
1.258	1.395	0.345	1.036	0.578	
1.669	1.249	0.32	1.226	0.258	

Figure2A-3
Obesity
1.669
1.869
1.504
1.226
1.669
1.395
1.036
1.226

10W Hot plate reaction time (s)					
Obesity	sity+Semagl	besity+DMM	+DMM+Sem	+DMM+Pair	feeding
21	26.22	11.5	17.8	12	
19.8	22.7	9.5	21.5	9.1	
23.3	20.4	10	17.6	8.2	
24.5	16.5	11.9	15	9.5	
23.4	26.8	8.2	15.1	6.2	
18.9	21.6	9.5	14.2	12.7	
20.5	21.6	13.5	15.6	7.4	
21.6	15.9	6	16.2	6	

Figure2B-3
Obesity
20.9
20.1
23.3
23.9
23.4
18.9
21.5
21.6

Knee joint PGP9.5 fluorescent intensity (fold change)					
Obesity	sity+Semagl	besity+DMM	+DMM+Sem	+DMM+Pair	feeding
0.9574	0.905263	2.077895	1.610526	2.157895	
1.02545	0.894737	1.92	1.526316	2.388421	
1	0.745263	2.157895	1.473684	1.821053	
1.01245	0.964211	2.389474	1.446316	1.713684	
0.95547	1.052632	1.618947	1.195789	1.646316	

NGF fluorescent intensity (fold change)					
Obesity	sity+Semagl	besity+DMM	+DMM+Sem	+DMM+Pair	feeding
0.95	0.985	1.369	1.015	1.369	
0.97	1.05	1.542	1.186	1.559	
1.01	1.081	1.419	1.117	1.339	
1	1.01	1.381	1.063	1.365	
1.06	1.05	1.491	1.309	1.6	

Figure2L
Obesity
10.33333
14.33333
12
7.333333
5.666667
4.666667

12W von Frey threshold (g)			
sity+Semaglu	besity+DMM	+DMM+Sem	+DMM+Pair feeding
1.917	0.345	1.173	0.345
1.825	0.32	1.036	0.258
1.669	0.222	1.226	0.858
1.226	0.458	1.036	0.578
1.329	0.774	0.926	0.858
1.173	0.926	0.926	0.669
1.305	0.858	0.951	0.226
1.669	0.345	0.774	0.222

12W Hot plate reaction time (s)			
sity+Semaglu	besity+DMM	+DMM+Sem	+DMM+Pair feeding
25.8	11.5	18.2	13.2
23	9.5	22	9.1
20.2	9.9	17.8	8.1
17	11.9	15	9.5
26.8	8.3	15.1	6.2
21.6	9.5	14	12.7
21.6	13.5	16.1	7.1
16.2	7.2	16.2	6.2

c-Fos+ cell numbers			
sity+Semaglu	besity+DMM	+DMM+Sem	+DMM+Pair feeding
5.666667	17	6.666667	12
14.66667	22	11.66667	18
11.66667	19.33333	9.333333	13.66667
8	21	6.333333	16.33333
5.333333	14.33333	8.333333	22.66667
6	15.33333	5.333333	16

Figure3A and 3B

Accession	Description	Gene	HFD-V-C1	HFD-V-C2	HFD-V-C3	HFD-S-C1	HFD-S-C2
O09111	11, mitocho	Ndufb11	0	0.256305	0.163154	2.6802872	0.9131345
P70265	tase 2 OS=M	Pfkfb2	0.6138674	0	0.7688302	2.6667369	0
Q6A085	nusculus OX	Znf629	0.1381857	0.1035446	0.1605253	0.1950316	0.3510592
Q61549	S=Mus mus	Adgre1	0.5226469	0.5205403	0.3219574	0.7767489	0.8367833
P61080	=Mus muscu	Ube2d1	0.5220966	0.445286	0.49072	0.8756671	0
A8E0Y8	S=Mus mus	Cd101	0.0833794	0.0569409	0.0691012	0	0.1374169
Q9CQ85	nit Tim22 O	Timm22	0.3913629	0.4457062	0.3632433	0.8269107	0.5351054
G3UWS1	nusculus OX	Neb	0.7330556	0.6396298	0.8642098	1.4928288	1.2320093
Q9WUE3	-Mus muscu	Cyb561d2	0.1682896	0.2343157	0.2402745	0.3188963	0.320184
Q8BVE8	OS=Mus mu	Nsd2	0.3224778	0.2371475	0.2021194	0.4409339	0.4534562
P11031	vator p15 OS	Sub1	3.8277972	4.7648064	3.8418882	6.8092114	6.8768763
Q31099	us OX=1009	H2-DMb2	0.4890682	0.6443845	0.6966026	0.8445107	0.8961574
P61514	=Mus musc	Rpl37a	1.9745198	1.7708704	2.4793727	4.0540543	3.114267
O88986	hondrial OS=	Gcat	0.1001165	0.1190502	0.1068605	0.1932412	0.156273
Q9EP82	ıbunit WDR	Wdr4	0.555567	0.7491271	0.5981803	1.15288	1.0572979
P70196	Mus muscul	Traf6	0.3517841	0.3980905	0.3273895	0.5897512	0.497294
Q8VDT9	=Mus musc	Mrpl50	0.5445119	0.6353494	0.5551741	0.965534	0.7190971
Q8BTG3	Mus muscul	Tcp11l1	0.1788643	0.2277654	0.2183822	0.2782533	0.358358
Q61462	Aus musculu	Cyba	2.5013008	3.3300144	3.0188007	4.5454372	4.4728368
P28033	S=Mus mus	Cebpb	0.5068604	0.37035	0.479745	0.6569997	0.6184555
P03921	OS=Mus mu	Mtnd5	0	0.2098528	0.2014871	0.2587528	0.3544078
Q9CQG1	nsferase 2 O	Chac2	0.2071656	0.2105819	0.2343384	0.3021961	0.3321487
P97494	t OS=Mus m	Gclc	1.3412494	1.8561754	1.9251647	2.614522	2.2760172
Q3TBV5	culus OX=1	Il1rn	0.814008	0.8710771	0.8861326	1.3635639	1.1061563
Q80XI7	culus OX=1	Bpifb9a	0.4792562	0	0.5324393	0.2322421	0
Q9JHU2	ulus OX=10	Palmd	0.7274974	0.4954932	0.5562589	0.3236167	0.3257404
P08121	s musculus	Col3a1	56.139173	41.492384	36.353701	23.512778	19.105304
F6VQ19	aining 2 (Fra	Lrch2	4.9126356	3.4313648	2.3881895	2.0607958	1.2500886
B1ATS5	us musculus	Atp2a3	1.4631775	1.787457	1.0079894	0.7063152	0.6633491
P01872	=Mus musc	Ighm	38.574343	52.164023	67.059408	24.166306	20.270004
Q8CI85	musculus O	Ca12	0.4366282	0.230341	0.2500925	0.1627861	0.0668787
Q80Z71	culus OX=1	Tnn	30.269271	17.99507	16.968698	8.3736747	6.5495603
Q61418	-Mus muscul	Clcn4	0.3001895	0.187741	0.3013473	0.0830175	0.121413
Q3U4G0	Aus musculu	Cdin1	6.1045607	3.4100187	2.356415	1.3734982	0
A0A075B5M7	-Mus muscul	Igkv5-39	2.9409241	4.608666	1.7195131	0.4714762	0.8763259

Figure3D

% PFKFB3+ cells

Obesity	sity+Semagl	besity+DMM	+DMM+Sem	+DMM+Pair feeding
45.88452	51.1245	18.214	28.214	18.2224
49.2157	53.2145	12.545	31.2154	15.2487
50.1247	49.548	17.2254	34.2215	11.24458
52.214	48.2157	15.2487	34.21578	21.2145
53.2148	47.21578	17.20145	37.2145	19.224
45.2158	55.2154	18.2158	28.3145	11.2457
47.2157	54.21558	21.548	33.21452	13.2145
46.2115	56.321547	23.11547	34.21154	12.8745

Figure3G

Figure3M

Figure3P

HFD-S-C3	FC	P-value	FDR	SG treatment/vehicle
1.5659126	8.1999836	0.0131556	0.8100623	up
3.2642468	4.2894294	0.0110028	0.8100623	up
0.2910865	2.0812072	0.0326816	0.8100623	up
1.0045395	1.9177981	0.0357073	0.8100623	up
0.9849134	1.9140428	0.0096083	0.8100623	up
0.1284727	1.9044574	0.0201517	0.8100623	up
0.8863971	1.87319	0.0474329	0.8100623	up
1.2362959	1.7708178	0.0075982	0.8100623	up
0.4660246	1.7189914	0.0345981	0.8100623	up
0.3892088	1.6850773	0.0470009	0.8100623	up
7.2488772	1.6836205	0.0136364	0.8100623	up
1.2854294	1.6535552	0.0450342	0.8100623	up
3.0622615	1.6435297	0.0210063	0.8100623	up
0.1848694	1.6390769	0.0046431	0.8100623	up
0.8441107	1.6050921	0.0216446	0.8100623	up
0.6080109	1.5734824	0.0060401	0.8100623	up
1.0343171	1.5670852	0.042345	0.8100623	up
0.3383	1.5598283	0.0141945	0.8100623	up
4.7112371	1.5513369	0.0302565	0.8100623	up
0.8179383	1.5427135	0.0284784	0.8100623	up
0.3338409	1.5348238	0.043978	0.8100623	up
0.3522031	1.5129108	0.0023528	0.8100623	up
2.8429094	1.5096757	0.0464143	0.8100623	up
1.3900032	1.5011267	0.0217501	0.8100623	up
0.2677941	0.4942556	0.0194298	0.8100623	down
0.2155876	0.486129	0.016045	0.8100623	down
20.692999	0.4725227	0.0159168	0.8100623	down
1.6091446	0.4584366	0.0467099	0.8100623	down
0.5052334	0.440259	0.0218976	0.8100623	down
16.893694	0.388662	0.0119558	0.8100623	down
0.1250033	0.386744	0.0464485	0.8100623	down
9.1805936	0.3695034	0.0176758	0.8100623	down
0.0781076	0.3579705	0.0084116	0.8100623	down
0.8844611	0.2853122	0.0435306	0.8100623	down
0.6395332	0.2144043	0.0166534	0.8100623	down

p-PFKFB3 / β-actin average intensity				
SG 0h	SG 4h	SG 6h	SG 12h	SG 24h
0.476705	0.513774	1.057792	0.93085	1.239977
0.45	0.65	1.1	0.98	1.24
0.54	0.55	0.99	1.21	1.32

Figure3H

PDH / β-Actin average intensity		
Ctrl	Semagluti	Metformin
0.729645	1.098186	1.213653
0.625556	1.144134	1.283521
0.56654	0.970868	1.1296

Figure3N	LDH/ β-Actin average int	
	Ctrl	Semagluti
	1.2	0.9
	1.31	1.1
	1.237883	0.89

LDH activity			
Ctrl	SG	TNF	TNF+SG
12.356977	13.726382	22.973686	18.564219
15.348848	11.382861	21.168533	16.714936
16.034318	19.921392	26.850514	9.4695562
14.822232	18.291575	25.386792	8.815648
11.119209	11.636838	21.468024	17.72796

Figure3R	PDH /
	Ctrl
	0.425642
	0.458226
	0.543792

p-AMPK/ β-actin average intensity				
SG 0h	SG 4h	SG 6h	SG 12h	SG 24h
0.25258	0.381873	0.589486	0.777833	1.136082
0.425	0.45	0.67	0.87	1.21
0.33	0.51	0.7	0.98	1.23

Figure3K	p-PFKFB3 / β-Actin	
	Ctrl	Compound C
	0.525305	0.760105
	0.61831	0.752318
	0.551665	0.652

ensity	
Metformin	
1.3	
1.4	
1.228738	

Figure3O	PDH activity			
	Ctrl	SG	TNF	TNF+SG
	7.5275497	9.3760665	4.3514739	11.731574
	8.4450211	10.657332	3.2644265	9.5631229
	7.1364172	8.8467357	5.6355523	9.4950521
	7.4451625	13.389714	5.8647477	12.224561
	9.910969	14.498835	6.0356555	11.204004

/ β-Actin Average intensity		
Compound C	Semaglutide	SG + CC
0.26873	1.116863	0.575973
0.530031	1.062531	0.322516
0.574606	0.930425	0.851671

Figure3T	% p-AMPK+ cells			
	Obesity	sity+Semagl	besity+DMM	DMM+Sem
	38.696538	51.595745	10.144928	43.552632
	46.391753	46.493902	32.339956	46.710526
	58.914729	49.504951	41.843972	58.962264
	62.831858	54.225352	36.935867	55.463918
	56.060606	46.561886	21.09375	54.481132
	59.88024	42.587601	17.261905	55.4
	59.8234	46.689895	45.844504	43.643512
	50.205761	57.755776	32.475397	34.223919

average intensity	
Semaglutide	SG + CC
0.965736	0.498798
1.043401	0.516075
1.121091	0.789146

+DMM+Pair feeding
27.407407
31.656805
39.8
25.348542
43.352601
39.317181
31.323877
41.877256

Figure4A

Time (minutes)	Ctrl					
1.310556	6.21291	6.545535	6.869481	6.787192	6.600354	6.89014
7.721651	6.507307	5.893514	6.358475	6.737531	6.423457	6.712969
14.178508	6.174219	5.590978	6.169141	6.76914	6.407744	6.953176
20.731533	18.930146	19.335722	19.086263	19.707037	19.65347	19.864131
27.188211	19.83574	21.060328	21.307307	21.340364	21.062741	20.467751
33.642806	20.627563	21.989954	22.161029	21.76313	22.047106	20.379273
40.184389	24.586429	26.405794	26.290443	22.65028	25.640485	22.423312
46.640286	25.908945	27.575412	27.852866	25.765058	27.272511	25.083706
53.099829	26.05927	26.856369	28.08184	26.979617	27.012057	25.996894
59.642401	8.47302	8.596781	8.921368	8.827996	8.245317	8.952823
66.09934	6.87855	6.729747	7.694138	6.488677	7.00886	6.514818
72.559925	5.830331	6.030419	6.617307	5.789996	5.806706	5.486731

Figure4B

Glycolysis			
Ctrl	SG	TNF	TNF+SG
14.45	14.01	26.68	19.77
16.4	13.37	27.85	25.22
15.99	11.14	25.26	23.23
14.99	10.95	26.18	20.81
15.64	12.09	24.27	21.59
13.43	12.18	26.14	21.79

Figure4C

Figure4D

Time (minutes)	Ctrl					
1.311077	50.620001	53.707175	63.243198	55.356789	56.430644	58.769944
7.777132	48.124708	50.888548	60.031238	51.873436	51.591618	53.850532
14.243446	47.503723	50.806352	59.916789	51.144447	47.980623	53.162308
20.790499	18.968821	19.765341	27.435096	18.572695	19.006294	21.844641
27.252292	18.609642	19.350843	29.088304	20.00964	18.769276	20.936442
33.721472	18.346361	19.656641	26.741678	19.340426	18.491427	20.411599
40.271772	51.789608	54.605978	53.150661	59.356148	44.985517	66.42365
46.740291	45.917622	46.608194	53.134014	52.060534	42.157124	55.865205
53.206254	47.391485	47.521968	56.420232	52.045391	43.484724	54.794015
59.753211	14.107099	14.200758	21.501611	13.815602	13.361636	16.5012
66.220568	12.639761	13.927092	19.082369	13.322816	11.959503	15.478018
72.690268	12.737072	13.191059	19.400997	13.001821	12.454286	14.671599

Figure4E

Basal Respiration			
Ctrl	SG	TNF	TNF+SG
34.77	43.18	9.31	21.08
37.62	39.85	11.07	20.73
40.52	37.91	11.09	28.45
38.14	36.84	10.99	25.24
35.53	39.58	10.31	25.95
38.49	32.35	8.99	23.85

Figure4F

ATP
Ctrl
29.16
31.15
33.18
31.8
29.49
32.75

Figure4H

Total ATP production			
Ctrl	SG	TNF	TNF+SG
263.1	318.3	226.5	292.3
290.4	292.8	242.1	303.2
294.4	262.2	271.9	288.2

Figure4I

Ctrl
SG
TNF

	279.1	263.1	266.2	285	TNF+SG
	276.1	289.2	231.4	287.8	
	267.6	244.1	227.6	304.8	

ECAR (mpH/min/10000cells)

SG						TN		
5.630521	6.252225	6.573551	6.004416	6.599385	6.37244	9.942393	10.052266	10.953072
5.411821	6.333689	6.291945	6.301672	6.547439	5.51173	7.824865	8.794294	9.109199
5.449668	6.652026	6.42582	5.847847	6.440873	5.412144	7.715541	8.020251	8.245417
18.265293	18.940957	18.04161	17.294571	18.572604	16.253493	31.382923	32.433869	30.709171
18.997954	19.689713	17.596352	17.002652	18.432401	17.099515	34.390706	35.873708	33.501382
19.46321	20.025411	17.568185	16.796483	18.530941	17.588444	34.028258	35.010464	33.539792
22.652972	23.358984	21.864635	19.828318	20.911315	18.752492	34.782748	34.537189	32.839523
24.347972	24.399506	21.690155	20.969351	22.145993	20.799123	35.849255	37.066191	35.011524
23.417748	24.109519	20.945584	20.884553	21.551365	20.876968	36.845897	38.290534	36.150751
8.044327	9.2539	7.563406	6.415451	7.358125	6.673807	13.129809	14.099572	11.734322
6.483556	7.779969	5.691916	5.241599	5.88091	5.766186	7.839563	8.860668	7.358981
5.215437	6.094855	4.370585	3.847128	4.42936	4.941496	6.537478	7.345735	6.12693

ATP production from Glycolysis			
Ctrl	SG	TNF	TNF+SG
123	109.2	199.8	183.7
140.7	105.1	210.5	169.4
134.8	85.2	235.4	180.6
126.3	83.4	226.9	170.3
134.4	91.9	198.8	172.6
110.4	98.8	196.8	178.1

OCR (pmol/min/10000 cells)

SG						TN		
67.57769	62.13254	59.11309	61.43156	62.63227	53.14538	25.883125	28.577122	31.78649
62.0458	57.13017	56.02276	57.09959	56.8411	49.085	24.34554	26.47822	29.98315
60.8356	55.73156	54.68136	56.05296	55.36997	48.36807	25.30747	26.7837	31.22334
26.73462	23.47896	22.3687	24.57131	21.99226	23.12288	19.49776	19.69383	23.77106
24.86626	22.59298	21.87992	24.1045	21.45086	22.0463	19.512521	20.829797	23.90342
23.93826	23.03879	22.17643	23.88419	21.44779	22.9367	19.90362	20.318196	23.80261
82.10411	83.56465	76.21702	68.28396	72.42211	73.19327	24.010527	28.52478	29.27404
70.55584	71.6366	66.28703	60.44129	62.82778	62.80062	25.966378	27.746979	29.51615
70.82076	72.15286	66.44468	60.94634	63.59973	60.77801	24.235194	26.327068	28.61383
18.44974	16.56455	16.74073	19.41251	15.90736	14.30237	16.617158	17.128015	20.65401
18.40379	17.31969	16.53224	18.89721	15.98555	15.40001	15.99824	15.71114	20.13049
17.65996	15.88097	16.76914	19.21073	15.79033	16.02106	15.55975	16.87564	19.1857

production coupled respiration		
SG	TNF	TNF+SG
36.9	5.4	18.39
32.69	6.47	18.54
32.5	7.42	23.97
32.17	8.08	21.47
33.92	6.69	22.12
25.43	6.29	20.43

Figure4G

ATP production from OXPHOS			
Ctrl	SG	TNF	TNF+SG
140	209.1	26.8	108.6
149.7	187.7	31.6	133.8
159.6	177	36.4	107.7
152.8	179.7	39.3	114.6
141.7	197.3	32.6	115.2
157.2	145.4	30.8	126.7

ATP production								
Glycolytic ATP						Oxidati		
123	140.7	134.8	126.3	134.4	110.4	140	149.7	159.6
109.2	105.1	85.2	83.4	91.9	98.8	209.1	187.7	177
199.8	210.5	235.4	226.9	198.8	196.8	26.8	31.6	36.4

183.7	169.4	180.6	170.3	172.6	178.1	108.6	133.8	107.7

NF			TNF+SG					
11.675701	9.967446	10.138028	6.816763	7.675296	6.711622	7.462265	8.796452	8.432072
9.584678	9.251286	8.40989	7.253313	6.338116	6.603722	7.823575	8.560463	7.477479
9.092234	8.089955	7.516582	6.912505	5.929102	6.105725	7.501924	8.025672	7.157721
32.452891	29.781297	30.43534	26.766705	26.612314	26.329533	28.609964	29.093389	27.427309
35.272585	32.357024	33.655749	26.677609	31.14704	29.335926	28.311787	29.615142	28.947654
33.930544	31.48942	32.807292	26.331953	31.129265	28.860454	28.130334	29.47616	28.071518
34.570645	32.107793	31.40822	32.480868	30.816579	28.817382	33.630103	33.899849	28.30231
35.907452	33.920706	32.883104	32.824625	31.457423	30.353613	32.945212	35.508385	29.11342
36.627873	34.136982	34.118376	32.819784	31.433505	29.86267	32.374867	35.371465	29.508257
12.591633	10.56174	12.767624	9.022942	11.779586	10.08454	8.939619	10.343275	9.889957
7.124006	6.226025	7.097521	5.829001	7.036864	5.810901	5.385542	6.647457	5.302505
6.24787	4.804524	5.982094	4.350657	5.857	4.516087	4.176565	5.470791	4.354901

NF			TNF+SG					
30.092458	29.384234	22.483155	34.887123	39.975332	39.117473	39.082656	40.855862	39.667093
29.91699	27.64702	21.31807	32.431566	35.965133	36.237481	36.165505	38.167086	36.209595
27.9008	27.65731	22.82818	30.780751	35.150782	35.2463	35.84359	37.644938	35.213176
20.99	21.33	16.46	11.950161	17.815763	9.291828	15.386622	15.810395	15.337357
21.14	21.89	17.43	12.535706	16.606278	11.279393	14.375729	15.520813	14.781156
19.82	20.97	16.53	12.390573	17.293679	11.202252	15.215251	15.65135	14.37994
24.40	24.48	20.19	44.59075	59.061663	62.572114	52.997898	60.322458	57.309298
24.86	27.37	21.19	42.085542	49.68936	50.584122	48.73741	48.701188	48.88381
24.46	25.26	20.11	41.572025	49.205806	50.459762	49.633985	48.597058	48.537664
17.48343	18.64495	15.32993	9.374929	13.848722	5.69667	11.039492	11.189438	11.693353
16.90759	17.351081	13.835703	10.290629	13.576173	6.780978	10.972621	11.632526	11.679278
16.140013	17.57353	12.88202	9.701332	14.418377	6.798239	10.601318	11.699352	11.366978

ive ATP		
152.8	141.7	157.2
179.7	197.3	145.4
39.3	32.6	30.8

114.6	115.2	126.7

Figure5B

OARSI score

Sham	Glp-1R Sham	DMM	Glp-1R+DMM	DMM+SG	Glp-1R+DMM+SG
0	0	4	4	2	3
0	0	3	2	1	3
1	0	6	6	2	4
0	0	4	3	2	4
0	0	6	3	3	3
0	1	3	4	3	4
0	0	3	4	2	5
1	0	4	2	4	5
0	0	2	6	1	4
0	0				

Figure5C

Figure5E

Osteophyte Size

Sham	Glp-1R Sham	DMM	Glp-1R+DMM	DMM+SG	Glp-1R+DMM+SG
0	0	3	3	2	3
0	0	2	3	1	3
0	0	2	2	2	3
0	0	3	3	2	3
0	0	2	2	2	3
0	0	3	3	3	2
0	0	3	3	2	2
0	0	3	3	2	3
0	0	3	3	1	2
0	0				

Figure5F

Figure5H

% Col-2+ area（fold change）

Sham	Glp-1R Sham	DMM	Glp-1R+DMM	DMM+SG	Glp-1R+DMM+SG
1.11	1.03335	0.25	0.24	0.48	0.31
1	1.07244	0.35	0.28	0.61	0.28
0.98	0.94	0.41	0.31	0.52	0.34
1.03	1.0111	0.31	0.27	0.49	0.24
1.05	1.01	0.31	0.3	0.42	0.21
0.95	1.05555	0.26	0.24	0.43	0.26

Figure5I

Figure5K

% MMP13+ area（fold change）

Sham	Glp-1R Sham	DMM	Glp-1R+DMM	DMM+SG	Glp-1R+DMM+SG
1.02	1.02	5.48	3.87	3.48	6.01
1	1.07	3.69	3.78	3.12	5.48
0.98	0.94	3.48	5.98	2.85	4.85
1.03	1.001	4.65	4.15	3.14	3.24
1.05	0.99	4.87	4.68	2.75	3.15
0.95	1.05	5.21	4.23	3.25	3.48

Figure5P

Figure5R

CGRP fluorescence intensity（fold change）DRG

Sham	Glp-1R Sham	DMM	Glp-1R+DMM	DMM+SG	Glp-1R+DMM+SG
0.72	0.55	4.84	5.32	0.97	4.69
0.53	0.54	4.14	5.18	1.99	3.69
1.56	1.11	3.4	3.74	2.11	3.78
1.79	1.81	2.98	2.92	1.4	2.89

Figure5S

	0.39	1.9	4.66	4.52	1.4	5.22

Synovitis Score					
Sham	Glp-1R Sham	DMM	Glp-1R+DMM	DMM+SG	Glp-1R+DMM+SG
0	0	5	4	2	3
1	1	3	3	3	3
0	0	5	5	2	4
0	0	4	3	2	4
0	0	4	3	3	3
0	0	3	5	3	4
0	0	4	5	2	5
0	0	3	3	4	5
0	0	3	5	3	5
0	0				

Figure5D	
	Sham
	176524
	168854
	175515
	162257
	185547
	195524
	157885
	165547
	178859
	172158

Osteophyte Maturity					
Sham	Glp-1R Sham	DMM	Glp-1R+DMM	DMM+SG	Glp-1R+DMM+SG
0	0	2	3	1	3
0	0	3	3	1	3
0	0	2	3	1	3
0	0	3	2	2	3
0	0	3	2	3	3
0	0	2	2	3	2
0	0	3	3	2	3
0	0	3	3	1	2
0	0	2	3	2	2
0	0				

% ACAN+ cells (fold change)					
Sham	Glp-1R Sham	DMM	Glp-1R+DMM	DMM+SG	Glp-1R+DMM+SG
1.01	1.02	0.14	0.11	0.35	0.11
1.08	1.07	0.16	0.098	0.35	0.17
0.98	0.97	0.21	0.14	0.32	0.16
1.03	1.05	0.18	0.15	0.37	0.15
1.05	1.04	0.16	0.16	0.32	0.13
0.95	1.05	0.19	0.18	0.29	0.15

Figure5J	
	Sham
	1.02
	1
	0.98
	1.03
	1.05
	0.94

CGRP fluorescence intensity（fold change）Knee Joint					
Sham	Glp-1R Sham	DMM	Glp-1R+DMM	DMM+SG	Glp-1R+DMM+SG
0.97	1.05	7.56	13.94	0.92	13.06
0.85	0.07	6.7	4.54	1.28	8.52
1.23	1.61	12.04	9.94	0.58	17.68
0.48	1.03	2.99	13.81	2.27	8.25
1.52	1.08	13.43	13.08	6.94	4.86
0.95	0.48	19.73	2.13		

Figure5Q	NGF f
	Sham
	1.47
	0.96
	1.86
	0.13
	1.03
	0.55

NGF fluorescence intensity（fold change）DRG					
Sham	Glp-1R Sham	DMM	Glp-1R+DMM	DMM+SG	Glp-1R+DMM+SG
0.25	0.59	2.85	3.42	1.57	2.57
0.77	1.92	1.43	1.86	0.57	2.58
0.65	1.46	2.44	2.69	0.93	2.42
1.94	0.24	3.75	3.75	1.12	4.21

1.38	0.72	3.48	3.41	1.98	

cartilage area (μm²)				
Glp-1R Sham	DMM	Glp-1R+DMM	DMM+SG	Glp-1R+DMM+SG
187765	39729.231	73470	152242	99856
168457	30740.769	59270.769	132254	154475
175125	67720	60798.462	157845	125547
156984	74240.769	73998.462	178542	112546
195547	68194.615	50215.385	123647	98241
153687	68870.769	70354.615	115478	72212
175428	64649.231	79922.308	132548	102145
186254	87083.077	50792.308	154425	112354
165875	73385.385	87313.846		
162485				

% ADAMTS5+ cells(fold change)				
Glp-1R Sham	DMM	Glp-1R+DMM	DMM+SG	Glp-1R+DMM+SG
1.02	4.28	4.94	3.25	4.26
1.07	4.98	4.26	3.14	4.65
0.94	4.78	5.2	2.98	4.87
1.02	4.19	4.68	2.48	4.639
1.01	5.12	4.78	3.65	4.74
1.05	5.32	5.02	3.51	4.632

fluorescence intensity（fold change）Knee Joint				
Glp-1R Sham	DMM	Glp-1R+DMM	DMM+SG	Glp-1R+DMM+SG
1.04	4.11	17.73	1.65	11.76
0.63	4.62	3.89	1.21	10.72
0.28	8.16	6.39	2.64	5.82
0.26	5.73	8.88	3.13	7.42
1.83	17.15	8.78	2.93	6.96
0.72	10.59	1.68	1.79	

Figure6B

OARSI score					
WT+Sham	aa1 cKO+Sh	WT+DMM	aa1 cKO+DM	WT+DMM+SG	aa1 cKO+DMM+SG
1	0	3	4	3	5
0	0	4	4	2	4
0	0	6	6	1	4
	1	6	5	1	5
		5	3	2	4
				1	3
				4	4
					5
					4

Figure6C

Figure6E

Osteophyte Size					
WT+Sham	aa1 cKO+Sh	WT+DMM	aa1 cKO+DM	WT+DMM+SG	aa1 cKO+DMM+SG
0	1	3	2	1	3
1	0	3	2	1	2
0	0	2	2	1	1
	0	2	2	2	1
		2	3	1	2
				1	2
				1	2
					3
					2

Figure6F

Figure6H

% Col-2+ area（fold change）					
WT+Sham	aa1 cKO+Sh	WT+DMM	aa1 cKO+DM	WT+DMM+SG	aa1 cKO+DMM+SG
1.14	0.92	0.22	0.28	0.47	0.24
0.91	1.08	0.29	0.25	0.74	0.53
0.96	0.91	0.43	0.34	0.52	0.34
	1.04	0.47	0.49	0.87	0.32
		0.36	0.27	0.5	0.47
				0.65	0.48
				0.55	0.37
					0.2
					0.27

Figure6I

Figure6K

% MMP13+ area（fold change）					
WT+Sham	aa1 cKO+Sh	WT+DMM	aa1 cKO+DM	WT+DMM+SG	aa1 cKO+DMM+SG
0.85	0.52	8.12	10.75	3.97	10.23
1.27	0.84	11.85	10.65	5.78	12.25
0.88	1.18	8.86	11.93	4.25	8.8
	1.06	12.68	8.96	5.89	13.13
		13.02	13.27	4.53	8.69
				5.98	10.33
				10.23	10.98
					12.58
					10.51

Figure6P

Figure6R

CGRP fluorescence intensity（fold change）DRG

WT+Sham	aa1 cKO+Sh	WT+DMM	aa1 cKO+DM	WT+DMM+SG	1 cKO+DMM+SG
1.24	1.18	3.62	3.36	1.33	1.56
0.91	0.9	4.25	2.29	2.46	3.74
0.85	0.83	2.66	2.42	1.07	2.49
	1.13	2.23	3.46	0.64	5.53
		3.18	3.18	0.97	

Figure6S

Synovitis Score					
WT+Sham	aa1 cKO+Sh	WT+DMM	aa1 cKO+DM	WT+DMM+SG	aa1 cKO+DMM+SG
1	0	4	3	2	4
0	1	3	3	2	3
0	0	5	4	3	5
	0	4	5	3	3
		5	4	2	4
				2	3
				3	2
					3
					2

Figure6D	
	WT+Sham
	169439.09
	192556.72
	183422.51

Osteophyte Maturity					
WT+Sham	aa1 cKO+Sh	WT+DMM	aa1 cKO+DM	WT+DMM+SG	aa1 cKO+DMM+SG
0	0	1	2	1	3
1	1	1	1	1	2
0	0	2	2	2	1
	0	2	2	2	1
		3	3	2	2
				1	2
				1	2
					2
					1

% ACAN+ cells (fold change)					
WT+Sham	aa1 cKO+Sh	WT+DMM	aa1 cKO+DM	WT+DMM+SG	aa1 cKO+DMM+SG
0.99	1.12	0.39	0.23	0.5	0.25
0.89	1.05	0.47	0.3	0.62	0.32
1.13	0.92	0.49	0.36	0.45	0.43
	1.01	0.27	0.37	0.77	0.42
		0.32	0.3	0.77	0.32
				0.61	0.45
				0.52	0.34
					0.38
					0.2

Figure6J	
	WT+Sham
	1.3
	1.08
	0.62

CGRP fluorescence intensity（fold change）Knee Joint					
WT+Sham	aa1 cKO+Sh	WT+DMM	aa1 cKO+DM	WT+DMM+SG	aa1 cKO+DMM+SG
1.01	1.08	3.68	4.95	2.58	4.26
1.03	1.03	4.25	3.12	3.45	3.24
0.97	0.98	4.68	3.24	2.68	3.15
	0.78	3.42	4.36	2.64	4.57
		4.42	4.28	2.34	4.62
					3.54

Figure6Q	NGF f
	WT+Sham
	0.99
	1
	0.98

NGF fluorescence intensity（fold change）DRG					
WT+Sham	aa1 cKO+Sh	WT+DMM	aa1 cKO+DM	WT+DMM+Sc	1 cKO+DMM+SG
0.82	1.16	4.06	2.35	1.61	2.94
1.6	1.7	2.32	2.96	1.19	2.74
0.58	0.42	2.62	2.08	1.35	2.11
	0.62	3.22	2.56	1.35	2.45
		1.08	2.56	0.72	

cartilage area (μm²)				
aa1 cKO+Sh	WT+DMM	aa1 cKO+DM	WT+DMM+SG	1 cKO+DMM+SG
171309.81	38926.45	42719.58	158724.35	148500.44
200052.23	45638.72	102467.58	171485.63	82754.06
180486.7	117429.61	124596.34	141629.85	97673.73
194673.5	92685.41	74819.52	135742.18	122528.19
	78642.93	88217.35	165237.84	112332.99
			126177.63	105533.17
			145678.2	110648.47
				88354.4
				56328.41

% ADAMTS5+ cells(fold change)				
aa1 cKO+Sh	WT+DMM	aa1 cKO+DM	WT+DMM+SG	1 cKO+DMM+SG
0.99	7.16	8.09	4.28	6.99
0.84	8.26	5.32	4.92	4.59
1.87	5.52	7.58	3.25	6.71
1.06	4.5	7.08	4.7	5.86
	9.3	8.97	5.86	7.89
			2.88	5.16
			3.68	8.51
				5.05
				5.96

luorescence intensity（fold change）Knee Joint				
aa1 cKO+Sh	WT+DMM	aa1 cKO+DM	WT+DMM+SG	1 cKO+DMM+SG
1.02	5.24	4.98	3.24	5.15
1.01	5.68	5.24	2.25	5.36
0.99	4.98	4.97	2.98	4.58
1.04	4.32	5.23	3.15	4.87
	4.16	5.47	3.54	4.96
				5.04

General information					
List	Group	Name	Age (50-75y)	Sex	OA (K-L grading)
1	HA+Semaglutide	LJH	57	F	/
2	HA+Semaglutide	XC	50	M	II
3	HA+Semaglutide	CYH	55	F	III
4	HA+Semaglutide	ZFR	54	F	II
5	HA+Semaglutide	ZXJ	57	M	/
6	HA+Semaglutide	LCH	68	F	III
7	HA+Semaglutide	LYF	51	F	III
8	HA+Semaglutide	CYH	60	F	III
9	HA+Semaglutide	LJH	64	F	III
10	HA+Semaglutide	SMZ	63	F	III
1	HA	LXG	75	M	II
2	HA	XJH	56	M	II
3	HA	ZGY	58	F	II
4	HA	CYQ	68	F	II
5	HA	ZJ	57	F	II
6	HA	YHZ	50	F	III
7	HA	CSX	58	M	/
8	HA	ZHC	74	M	III
9	HA	ZZZ	54	M	II
10	HA	LXZ	73	F	III

Figure 7E

General information			Catrilage thickness	
List	Group	Name	Pre-treatment	Post-treatment
1	HA+Semaglutide	LJH	2.046	2.439
2	HA+Semaglutide	XC	1.604	1.924
3	HA+Semaglutide	CYH	1.71	2.013
4	HA+Semaglutide	ZFR	1.853	2.152
5	HA+Semaglutide	ZXJ	1.403	1.651
6	HA+Semaglutide	LCH	2.437	2.731
7	HA+Semaglutide	LYF	1.611	1.838
8	HA+Semaglutide	CYH	1.95	2.156
1	Conventional	LXG	2.81	2.759
2	Conventional	XJH	1.663	1.665
3	Conventional	ZGY	1.539	1.534
4	Conventional	CYQ	1.506	1.578
5	Conventional	ZJ	1.405	1.387
6	Conventional	YHZ	1.299	1.468

Figure 7B

	Before	After 1 week	After 12 week	After 24 week
MRI evaluation	**BMI (>28kg/m²)**			
Checked	35	35	34	33
Checked	33	32	30	29
Checked	29	29	28	27
Checked	33	33	31	30
Checked	32	32	29	29
Checked	34	33	31	30
Checked	33	33	33	32
Checked	35	34	33	33
/	29	28		
/	33			

Checked	40	41	41	41
Checked	33	34	33	33
Checked	33	32	33	32
Checked	32	31	33	32
Checked	33	33	33	33
Checked	29	30	30	30
Checked	28			
/	28	27		
/	32	32		
/	33	33		

Figure 7F

List	Group	Name	Improvement %
1	HA+Semaglutide	LJH	19.17
2	HA+Semaglutide	XC	19.98
3	HA+Semaglutide	CYH	17.72
4	HA+Semaglutide	ZFR	16.12
5	HA+Semaglutide	ZXJ	17.73
6	HA+Semaglutide	LCH	12.06
7	HA+Semaglutide	LYF	14.11
8	HA+Semaglutide	CYH	10.53

1	Conventional	LXG	-1.84
2	Conventional	XJH	0.10
3	Conventional	ZGY	-0.28
4	Conventional	CYQ	4.76
5	Conventional	ZJ	-1.23
6	Conventional	YHZ	12.98

Figure S7B				
Before	**After 1 week**	**After 12 week**	**After 24 week**	**Before**
WOMAC-Pain				
15	13	8	4	7
16	15	6	3	7
12	12	7	3	4
15	14	9	6	5
20	17	12	5	8
13	12	11	7	5
12	11	11	11	5
15	14	14	11	6
16	15			6
20				8
15	14	7	6	7
20	18	9	6	5
17	17	9	8	5
15	16	9	8	6
14	12	7	5	6
14	10	6	4	6
20				6
13	12			7
19	18			7
20	18			8

Figure S7C			Figure	
After 1 week	**After 12 week**	**After 24 week**	**Before**	**After 1 week**
WOMAC-Stiffness				**WOMAC-Physi**
5	2	2	63	62
5	3	2	65	62
5	3	2	45	48
5	2	1	48	41
5	3	2	63	43
3	2	2	65	62
3	3	3	64	58
3	4	3	57	55
5			60	46
			60	
3	3	3	55	50
3	2	2	48	45
5	3	3	59	55
5	3	3	45	43
5	3	1	53	40
4	2	2	44	45
			63	
6			53	56
5			55	50
8			63	60

7C		Figure S7D			
After 12 week	**After 24 week**	**Before**	**After 1 week**	**ter 12 we**	**After 24 week**
cal Function		**WOMAC-Total score**			
55	33	85	80	65	39
47	31	88	82	56	36
37	29	61	65	47	34
33	22	68	60	44	29
25	20	91	65	40	33
42	24	83	77	55	24
55	23	81	72	69	23
55	26	78	72	73	32
		82	66		
		88			

42	40	77	67	52	49
38	33	73	66	49	41
43	41	81	77	55	52
38	35	66	64	50	46
33	28	73	57	43	34
38	30	64	59	46	36
		89			
		73	74		
		81	73		
		91	86		

Figure S1C	GLP-1R $^{+}$ (%)	
Non-obesity mice	**sham**	**OA**
	81.37	70.34
	74.84	65.88
	75.02	58.33
	87.12	54.86

Figure S1D	GLP-1R $^{+}$ (%)	
Obesity mi	**sham**	**OA**
	60.48	53.28
	71.88	48.81
	75.84	42.66
	84.27	65.15
	72.80	34.30

FigureS2A	CHO (mmol/L)					
Non Obesity	Obesity	sity+Semagl	besity+DMM	+DMM+Sem	+DMM+Pair	feeding
2.62	6.72	3.24	2.96	3.43	3.58	
1.83	7.55	4.11	6.33	3.01	3.93	
2.74	7.17	3.71	3.75	4.1	4.8	
2.72	6.16	3.52	6.69	3.88	3.52	
2.48	6.06	3.37	6.51	3.61	2.24	
	6.32	3.9	5.31	2.35	3.49	
	7.58	3.04	5.53	4.03	2.53	
	2.16	3.7	6.18	3.57	4.86	
	5.6	3.03	5.18	2.02	4.58	
	4.56	3.17	4.21	2.41	4.43	
	4.51	2.43	3.8	2.24	5.21	
	3.48	2.02	4.92	2.96	3.17	
	4.75	2.5	4.12	2.94	2.35	
	4.67	2.18	5.05	0.73	5.22	
	4.13	2.86	3.94	2.49	3.99	
	4.31	2.98	4.82	2.41	4.38	

FigureS2D	LDL (mmol/L)					
Non Obesity	Obesity	sity+Semagl	besity+DMM	+DMM+Sem	+DMM+Pair	feeding
0.3	0.577	0.647	0.496	0.67	0.44	
0.6	0.917	0.797	0.669	0.272	0.42	
0.4	0.882	0.76	0.664	0.375	0.38	
0.7	0.645	0.645	0.91	0.526	0.22	
0.7	0.62	0.766	0.704	0.598	0.38	
	0.531	0.568	0.686	0.237	0.69	
	0.971	0.422	0.671	0.611	0.54	
	0.134	0.328	0.924	0.745	0.51	
	0.256	0.111	0.164	0.096	0.148	
	0.12	0.12	0.087	0.092	0.141	
	0.103	0.113	0.087	0.073	0.283	
	0.08	0.11	0.137	0.075	0.17	
	0.122	0.094	0.102	0.15	0.129	
	0.129	0.083	0.166	0.039	0.193	
	0.127	0.133	0.09	0.123	0.14	
	0.071	0.202	0.169	0.13	0.154	

FigureS2B		TG (mmol/L)				
Non Obesity	Obesity	sity+Semagu	besity+DMM	+DMM+Sem	+DMM+Pair	feeding
0.53	1.47	2.34	2.8545	1.59	1.51	
0.44	2.21	2.78	1.88	1.49	0.95	
0.39	1.47	1.76	2.09	1.22	2.19	
0.39	1.72	1.87	2.06	1.25	2.04	
0.34	2.33	1.91	1.23	1.01	2.07	
	1.47	1.53	1.66	1.23	2.122	
	1.47	1.36	1.59	1.71	1.16	
	2.1154	1.9	1.84	1.41	1.24	
	0.91	0.62	0.51	0.39	0.71	
	0.46	0.35	0.45	0.42	0.81	
	0.63	0.81	0.53	0.4	0.87	
	0.53	0.6	0.54	0.35	0.67	
	0.69	0.74	0.71	0.61	0.6	
	0.81	0.35	0.95	0.19	0.74	
	0.52	0.76	0.57	0.79	0.36	
	0.5	0.83	1.15	0.48	0.89	

FigureS2E		HDL (mmol/L)				
Non Obesity	Obesity	sity+Semagu	besity+DMM	+DMM+Sem	+DMM+Pair	feeding
1.1	1.49	0.89	1.61	1.14	0.65	
0.76	1.16	0.9	1.22	1.23	1.14	
1.18	0.56	3.33	1.38	0.71	2.13	
1.18	0.74	1.22	0.96	1.25	1.4	
1.04	0.64	0.88	0.96	1.06	1.2	
	0.9	0.09	1.11	2.8	1.49	
	1.49	1.31	1.06	3.16	1.71	
	0.64	1.88	1.74	1.67	1.8	
	2.08	1.46	1.84	0.99	1.75	
	1.59	1.52	1.64	1.16	1.63	
	1.76	1.3	1.47	1.08	1.9	
	1.38	1.06	1.77	1.37	1.37	
	1.8	1.21	1.64	1.4	1.15	
	1.66	1.17	1.88	0.4	1.83	
	1.74	1.38	1.55	1.33	1.67	
	1.56	1.49	1.68	1.16	1.65	

FigureS2C	GHb (ngl/mL)					
Non Obesity	Obesity	sity+Semagu	besity+DMM	+DMM+Sem	+DMM+Pair	feeding
13.68065	13.68065	32.0117	24.70328	36.46498	20.726	
17.10263	17.10263	34.71019	30.2329	29.49643	14.088	
32.6082	46.52523	23.27348	39.29078	30.52826	30.233	
25.115	12.19361	11.52138	17.37897	23.41599	38.982	
32.2147	48.45623	30.67611	29.49643	17.37897	20.726	
	19.88364	34.77752	26.43282	35.31487	39.291	
	35.16353	36.36515	25.56616	19.32429	29.349	
	38.36618	22.84655	45.40733	36.68217	36.073	
	34.72846	51.69325	46.74214	44.79902	34.5515	
	16.63875	14.80054	52.57845	34.5515	41.97352	
	44.79902	46.74214	46.03546	29.76476	48.5094	
	46.03546	43.91599	33.48935	39.85433	21.18006	
	35.61299	20.81907	20.27691	35.96669	40.91397	
	45.85881	32.95798	35.08232	52.75554	42.32669	
	19.37144	37.73439	36.67392	59.32092	17.00469	
	29.23156	15.53762	46.56546	28.16414	40.20756	

FigureS3B

Ct. BMD (g/cm³)				
Obesity	Obesity+S	Obesity+	Obesity+D	Obesity+DMM+Pair feeding
1.921457	1.96654	1.909855	1.900244	1.91142
1.94552	1.95114	1.92054	1.90995	1.91124
1.899987	1.93554	1.92114	1.92548	1.92857
1.912544	1.94552	1.892524	1.902145	1.90214
1.92245	1.90554	1.89554	1.92154	1.921454
1.93554	1.902587	1.94522	1.9325478	1.921112
1.94555	1.93114	1.910024	1.92457	1.87551
1.94256	1.9222	1.90214	1.942547	1.92145
1.9794	1.9844	1.91889	1.89925	1.85681
1.9867	1.9777	1.91133	1.90995	1.89056
1.96144	1.94144	1.92233	1.92889	1.93876
1.94567	1.95367	1.8643	1.895	1.89448
1.92897	1.92997	1.91889	1.9376	1.93962
1.92145	1.90345	1.93273	1.91265	1.91647
1.93486	1.94386	1.90916	1.92657	1.86581
1.94256	1.95356	1.94606	1.9444	1.93495

FigureS3C

FigureS3F

BV/TV				
Obesity	Obesity+S	Obesity+	Obesity+D	Obesity+DMM+Pair feeding
0.24551	0.31224	0.32114	0.24115	0.24551
0.25114	0.25114	0.25441	0.23551	0.26554
0.23554	0.18554	0.26885	0.25887	0.21114
0.22114	0.185547	0.211244	0.26699	0.20114
0.25446	0.21001	0.225654	0.274415	0.28554
0.16884	0.20112	0.23544	0.30221	0.24556
0.20115	0.16554	0.201154	0.22445	0.26998
0.20114	0.2500011	0.255541	0.20114	0.23221
0.234922	0.306466	0.112378	0.142378	0.140102
0.231627	0.240607	0.132878	0.112878	0.111151
0.230162	0.199397	0.125378	0.132378	0.180868
0.215682	0.194023	0.118878	0.112878	0.194263
0.267721	0.18773	0.143994	0.213994	0.130102
0.154852	0.193987	0.165548	0.325548	0.109151
0.150896	0.213877	0.185475	0.189575	0.177622
0.139273	0.146734	0.168826	0.162926	0.172836

FigureS3G

FigureS3I

BV/TV Subchondral bone				
Obesity	Obesity+S	Obesity+	Obesity+D	Obesity+DMM+Pair feeding
0.745214	0.754414	0.782245	0.785545	0.7552
0.721448	0.698854	0.792224	0.824415	0.801124
0.765488	0.765214	0.801142	0.79224	0.78224
0.778545	0.721145	0.720014	0.814424	0.801124
0.7011452	0.751142	0.766524	0.758842	0.721142
0.795824	0.75524	0.745884	0.7855243	0.7100245
0.75441	0.77445	0.782242	0.76224	0.732254
0.76225	0.720014	0.735502	0.741524	0.756624
0.736995	0.746995	0.816987	0.865038	0.773366
0.709646	0.689646	0.788151	0.737809	0.760983
0.786995	0.776995	0.806987	0.842407	0.823624
0.699646	0.679646	0.798151	0.822712	0.799926
0.755048	0.785048	0.816852	0.804264	0.858896

FigureS3J

0.787241	0.897241	0.799262	0.788078	0.800783
0.776824	0.776824	0.771917	0.769556	0.790418
0.797688	0.697688	0.674439	0.622542	0.80375

FigureS3L	Tb.Th (mm) Subchondral bone				
Obesity	Obesity+S	Obesity+	Obesity+D	Obesity+DMM+Pair feeding	
0.165444	0.1685547	0.2211452	0.2455114	0.2844551	
0.154472	0.155474	0.214557	0.178542	0.1584755	
0.1778441	0.178444	0.215888	0.25447	0.247851	
0.154745	0.152245	0.21442	0.198554	0.268854	
0.170021	0.175114	0.2241558	0.214452	0.254775	
0.18554	0.19854	0.2284775	0.218655	0.201142	
0.1875224	0.189951	0.235475	0.214477	0.221445	
0.165472	0.16584	0.185547	0.187524	0.214557	
0.152183	0.162183	0.215747	0.243391	0.243692	
0.158669	0.150669	0.21267	0.173267	0.163715	
0.170829	0.171829	0.210747	0.251763	0.241101	
0.156692	0.146692	0.20267	0.186224	0.256633	
0.166251	0.176251	0.215492	0.209244	0.241374	
0.193807	0.213807	0.224143	0.210817	0.19767	
0.195672	0.190672	0.224747	0.217477	0.215941	
0.164587	0.154587	0.178034	0.168007	0.204048	

FigureS3M

Ct.Th. (mm)					
Obesity	Obesity+S	Obesity+	Obesity+D	Obesity+D	MM+Pair feeding
0.225874	0.2298524	0.1758841	0.18557	0.18251	
0.230114	0.235514	0.192342	0.199954	0.225512	
0.210034	0.201145	0.195114	0.192251	0.201144	
0.201245	0.211142	0.189554	0.20114	0.19857	
0.210025	0.24521	0.1912254	0.214452	0.18854	
0.231454	0.209445	0.187224	0.198854	0.1924778	
0.242215	0.201422	0.1978	0.1899574	0.195475	
0.202214	0.22145	0.187214	0.189954	0.1954566	
0.22337	0.2407	0.192933	0.196829	0.185454	
0.223927	0.219927	0.192342	0.197685	0.183402	
0.21377	0.20977	0.187777	0.192251	0.1960955	
0.191233	0.199267	0.170398	0.19579	0.19227	
0.212999	0.208999	0.192933	0.196694	0.181666	
0.225645	0.226645	0.19248	0.191223	0.187334	
0.213158	0.203158	0.182345	0.196704	0.177792	
0.201741	0.198741	0.187661	0.197898	0.172176	

FigureS3D	
Obesity	
0.098854	
0.10554	
0.098774	
0.089554	
0.096554	
0.089554	
0.091224	
0.08775	
0.091171	
0.085433	
0.098124	
0.082319	
0.081245	
0.089538	
0.082346	
0.080871	

Tb. BMD (g/cm^3)					
Obesity	Obesity+S	Obesity+	Obesity+D	Obesity+D	MM+Pair feeding
1.35482	1.36884	1.352248	1.342551	1.321155	
1.31254	1.26554	1.28775	1.29885	1.30224	
1.26584	1.242155	1.33524	1.28445	1.25664	
1.30225	1.20114	1.26554	1.26554	1.24558	
1.251445	1.25662	1.25447	1.29887	1.266654	
1.29554	1.32114	1.26654	1.32145	1.30224	
1.24587	1.24558	1.301142	1.34552	1.24775	
1.2648	1.23554	1.24552	1.25668	1.26554	
1.24408	1.11408	1.34963	1.26146	1.3236	
1.22332	1.25632	1.22274	1.27688	1.28179	
1.26408	1.22708	1.24513	1.27339	1.25801	
1.28632	1.20632	1.25199	1.2533	1.25517	
1.26223	1.26623	1.21963	1.29689	1.24484	
1.28126	1.30196	1.20274	1.2273	1.25969	
1.26012	1.25812	1.24285	1.2269	1.2595	
1.29942	1.24162	1.24257	1.23133	1.23745	

FigureS3H	
Obesity	
0.24115	
0.21445	
0.23554	
0.22114	
0.20114	
0.19221	
0.18772	
0.24552	
0.243079	
0.231677	
0.256779	
0.211377	
0.23427	
0.17233	
0.192131	
0.242299	

Tb.N. (mm^{-1}) Subchondral bone					
Obesity	Obesity+S	Obesity+	Obesity+D	Obesity+D	MM+Pair feeding
3.01584	3.12447	2.89557	2.988457	2.68745	
3.115777	3.311445	2.76669	2.92457	3.1445	
3.21444	3.315478	3.012445	2.6985441	2.875145	
3.127884	3.02147	3.041117	3.021475	2.788542	
3.401115	3.02144	2.88745	2.875999	2.688755	
3.175142	3.127884	2.78954	2.687554	3.024047	
3.0002447	3.07472	2.68874	2.82214	2.982247	
3.120747	3.12414	2.75842	2.8799954	2.74458	
3.02051	3.02051	2.85105	2.7282	2.51201	
3.11948	3.21948	2.73184	2.9243	3.22314	
3.21051	3.31051	2.95105	2.55648	2.62755	
3.12948	3.02948	2.93184	3.15346	2.3179	
3.30398	3.27398	2.66391	2.87072	2.68902	

FigureS3K	
Obesity	
0.1420014	
0.16241	
0.138854	
0.175514	
0.125999	
0.135542	
0.145521	
0.184422	
0.131024	
0.16934	
0.140239	
0.173398	
0.139188	

3.12717	3.1717	2.64022	2.87103	3.04289	0.121481
2.98931	2.98931	2.39347	2.90619	2.8556	0.133854
3.0741	3.0341	2.85123	3.00638	3.05137	0.171115

BMD (g/cm^3) Subchondral bone				
Obesity	Obesity+S	Obesity+	Obesity+D	Obesity+DMM+Pair feeding
1.6455514	1.6851442	1.685542	1.7022145	1.6751452
1.652014	1.632542	1.6988524	1.642251	1.6485245
1.654857	1.687745	1.675514	1.682242	1.685542
1.6652214	1.624414	1.6852004	1.69242	1.627758
1.657884	1.6788541	1.710114	1.701245	1.674582
1.6755412	1.695542	1.682247	1.654782	1.62254
1.6844575	1.701224	1.682044	1.665287	1.64588
1.642251	1.63445	1.610224	1.63245	1.701257
1.66846	1.67846	1.67212	1.72832	1.66519
1.648028	1.628028	1.70962	1.63039	1.63988
1.66846	1.66846	1.68212	1.71832	1.72228
1.68028	1.58028	1.68962	1.68885	1.67998
1.64101	1.66101	1.70008	1.69906	1.77449
1.66737	1.76737	1.67876	1.64085	1.69793
1.68494	1.69494	1.66196	1.65293	1.66004
1.60985	1.58985	1.57286	1.54306	1.73553

Tb.Th. (mm)			
Obesity+S	Obesity+	Obesity+D	Obesity+DMM+Pair feeding
0.091241	0.065547	0.078869	0.074451
0.098541	0.068845	0.0811452	0.068995
0.086543	0.054478	0.081154	0.069985
0.089975	0.078845	0.086652	0.075415
0.091124	0.069954	0.084424	0.068875
0.087745	0.075541	0.086654	0.074451
0.092445	0.071154	0.084452	0.080024
0.086654	0.081124	0.075541	0.075514
0.0890171	0.068726	0.08495	0.080388
0.085899	0.071705	0.088705	0.072901
0.082171	0.079935	0.081685	0.081049
0.083199	0.077193	0.085611	0.076185
0.081865	0.075726	0.082126	0.077964
0.089254	0.074705	0.081488	0.077694
0.084296	0.075432	0.079892	0.080835
0.083431	0.078252	0.076467	0.070578

FigureS3E	
Obesity	Obesity+S
3.84472	4.12241
4.21454	3.44785
3.99854	3.8854174
3.11452	3.22458
3.77541	3.55654
3.66584	3.447541
3.7514	4.012524
3.55417	3.55471
3.12369	3.24169
3.231312	3.11412
3.26169	3.34169
3.102	3.00412
3.50016	3.47016
3.82411	3.81411
3.69094	3.70094
3.01016	2.99016

Tb. Sp. (mm)			
Obesity+S	Obesity+	Obesity+D	Obesity+DMM+Pair feeding
0.25441	0.25441	0.15774	0.13554
0.16551	0.21445	0.25445	0.19885
0.23664	0.14558	0.31554	0.23554
0.21114	0.30224	0.14558	0.25447
0.25221	0.25668	0.22558	0.25668
0.17554	0.28554	0.26665	0.24551
0.19885	0.15335	0.24775	0.26658
0.18557	0.23665	0.21544	0.24115
0.256079	0.264784	0.223736	0.187686
0.245677	0.317197	0.240567	0.198834
0.227079	0.234821	0.168178	0.223826
0.259677	0.235423	0.244667	0.224498
0.206307	0.274784	0.194928	0.241369
0.17293	0.327197	0.26596	0.232864
0.195906	0.216216	0.253361	0.236123
0.250999	0.254074	0.235799	0.254816

Tb.Sp. (mm) Subchondral bone			
Obesity+S	Obesity+	Obesity+D	Obesity+DMM+Pair feeding
0.1455214	0.12547	0.125477	0.15744
0.154427	0.136547	0.168472	0.15472
0.136524	0.145726	0.154752	0.168852
0.1902472	0.1524472	0.1784155	0.1751442
0.119885	0.168475	0.145242	0.162543
0.135447	0.147515	0.1254756	0.1258745
0.165542	0.165247	0.1547752	0.1289554
0.1354712	0.135452	0.168542	0.142215
0.131024	0.129115	0.123152	0.154396
0.17934	0.130413	0.168694	0.146541
0.130239	0.128115	0.1394	0.139482
0.183398	0.138413	0.130888	0.174792
0.129188	0.159896	0.139101	0.130509

0.101481	0.154613	0.13749	0.130965
0.143854	0.193057	0.126617	0.134248
0.175	0.172693	0.16462	0.123673

Tb.N. (mm^{-1})		
Obesity+	Obesity+D	Obesity+DMM+Pair feeding
3.22547	3.55478	3.6245
3.55887	3.88954	3.55415
3.66547	3.99542	3.21554
3.02145	4.01254	3.62554
3.66874	3.254487	3.221463
3.21554	3.36544	3.12455
3.11458	3.11447	3.33254
3.25475	3.45218	3.11452
2.91298	3.23953	3.64865
2.68817	3.037	3.54943
3.167	4.00221	3.28004
3.19881	3.02775	3.32577
2.85298	3.63564	3.13153
2.48817	2.88644	3.22001
3.42878	3.02798	3.11568
2.98218	3.23346	3.03588

Figure S4A

Average travel speed (mm/s)

Obesity	sity+Semagl	Obesity+DMM	DMM+Sem	DMM+Pair feeding
2.671692	2.308855	1.256145	2.180883	1.137592
2.717288	2.829254	1.012144	1.861923	1.5462
2.496527	2.143291	1.8415	2.002192	1.52339
2.327163	2.324764	1.64154	2.343965	1.16995
3.204173	2.537957	1.010882	1.753754	1.7451
1.807093	1.912021	1.2456	1.782916	1.54812
2.981704	1.57101	1.031999	1.795023	1.4826
2.590473	3.081417	1.747544	2.067286	1.136779

Figure S4B

Figure S4E

Locomotion time (s)

Obesity	sity+Semagl	Obesity+DMM	DMM+Sem	DMM+Pair feeding
2988.85	1696.12	1682.87	2010.61	1344.25
2819.88	1928.01	1435.81	1594.91	2021.38
2200.98	1874.8	1726.9	1977.01	1284.9
1861.92	1885.42	1565.62	1756.14	3230.15
1476.09	2002.91	1651.19	1656.34	1531.33
1861.9	2274.24	2171.01	3244.59	1123.21
1987.38	2128.33	1615.96	1653.39	1712.04
1514.81	2117.76	1885.3	1962.09	1807.53

Figure S4D

Figure S4G

Immobility counts (times)

Obesity	sity+Semagl	Obesity+DMM	DMM+Sem	DMM+Pair feeding
1949	1407	2192	897	1727
1806	1256	1785	1465	1729
1662	1890	1557	1339	1448
1690	1743	1693	1567	2334
1372	1215	1794	1498	2096
1198	1758	1803	1332	2064
1508	1420	1536	1547	1675
1267	1342	1783	1301	1225

Climbing time (s)					
Obesity	sity+Semagl	besity+DMM	+DMM+Sem	+DMM+Pair	feeding
3810.41	4191.51	1680.98	2130.02	1516.17	
4265.29	4762.06	1654.62	2510.19	1477.13	
4847.99	4680.27	1601.45	3684.93	1238.62	
4721.45	4237.62	1545.314	2137.57	1507.18	
5312.55	4255.63	1596.91	2787.96	1324.17	
5982.44	4671.42	1692.37	2673.71	1781.95	
5470.83	6751.77	1238.84	1832.92	1275.35	
6095.72	6476.77	1479.23	2472.82	1987.32	

Figure S4C	
	Obesity
	35
	42
	43
	46
	54
	73
	77
	83

Locomotion counts (times)					
Obesity	sity+Semagl	besity+DMM	+DMM+Sem	+DMM+Pair	feeding
1876	3625	1301	2063	1048	
2167	3511	1575	1985	1576	
2563	3773	1393	2658	1654	
2670	1523	1463	2041	1546	
2692	2267	1458	2102	1632	
3230	1842	1121	2547	1426	
2561	2549	1456	2354	1548	
3153	1859	1010	2154	1182	

Figure S4F	
	Obesity
	16465.88
	22894.6
	24826.48
	15861.68
	26120.8
	17061.4
	23528.94
	21130.14

Climbing counts (times)			
sity+Semagl	besity+DMM	DMM+Sem	DMM+Pair feeding
37	12	23	9
42	14	20	12
44	15	31	15
57	16	34	14
62	17	39	13
64	9	42	11
81	12	41	18
84	21	47	21

Immobility time (s)			
sity+Semagl	besity+DMM	DMM+Sem	DMM+Pair feeding
21849.43	21419.68	22575.23	27285.45
26325.14	25622.01	16065.44	20837.6
12863.56	28453.65	15512.64	17068.23
14102.42	19685.55	25591.61	23095.13
18480.5	22472.05	17922.47	18256.73
20452.44	19793.88	21041.06	17478.12
20219.05	26765.9	18438.18	29330.98
25003.1	26567.04	21350.92	16338.53

Accession	Description	Gene	HFD-V-C1	HFD-V-C2	HFD-V-C3
O09111	ıbunit 11, mitochondrial	Ndufb11	0	0.2563049522	0.163154
P70265	ıosphatase 2 OS=Mus mı	Pfkfb2	0.6138674	0	0.7688302
Q6A085	:Mus musculus OX=100	Znf629	0.1381857	0.1035445583	0.1605253
Q61549	: E1 OS=Mus musculus (	Adgre1	0.5226469	0.5205402914	0.3219574
P61080	)1 OS=Mus musculus O	Ube2d1	0.5220966	0.4452859802	0.49072
A8E0Y8	er 2 OS=Mus musculus (	Cd101	0.0833794	0.0569408795	0.0691012
Q9CQ85	: subunit Tim22 OS=Mu	Timm22	0.3913629	0.4457062175	0.3632433
G3UWS1	:Mus musculus OX=100	Neb	0.7330556	0.6396298092	0.8642098
Q9WUE3	)2 OS=Mus musculus O	Cyb561d2	0.1682896	0.2343157176	0.2402745
Q8BVE8	NSD2 OS=Mus musculu	Nsd2	0.3224778	0.2371475439	0.2021194
P11031	coactivator p15 OS=Mus	Sub1	3.8277972	4.7648064003	3.8418882
Q31099	ıusculus OX=10090 GN	H2-DMb2	0.4890682	0.6443845394	0.6966026
P61514	43 OS=Mus musculus O	Rpl37a	1.9745198	1.7708703926	2.4793727
O88986	mitochondrial OS=Mus	Gcat	0.1001165	0.1190502001	0.1068605
Q9EP82	ytic subunit WDR4 OS=	Wdr4	0.555567	0.7491270923	0.5981803
P70196	5 OS=Mus musculus OX	Traf6	0.3517841	0.3980904672	0.3273895
Q8VDT9	.50 OS=Mus musculus C	Mrpl50	0.5445119	0.6353494377	0.5551741
Q8BTG3	1 OS=Mus musculus OX	Tcp11l1	0.1788643	0.227765428	0.2183822
Q61462	OS=Mus musculus OX=	Cyba	2.5013008	3.3300144138	3.0188007
P28033	)eta OS=Mus musculus (	Cebpb	0.5068604	0.3703500306	0.479745
P03921	ıain 5 OS=Mus musculus	Mtnd5	0	0.2098528135	0.2014871
Q9CQG1	/clotransferase 2 OS=Mu	Chac2	0.2071656	0.2105818615	0.2343384
P97494	;ubunit OS=Mus muscul	Gclc	1.3412494	1.856175379	1.9251647
Q3TBV5	s musculus OX=10090 (	Il1rn	0.814008	0.8710770889	0.8861326
Q80XI7	s musculus OX=10090 (	Bpifb9a	0.4792562	0	0.5324393
Q9JHU2	musculus OX=10090 G	Palmd	0.7274974	0.4954931938	0.5562589
P08121	S=Mus musculus OX=1(	Col3a1	56.139173	41.492383597	36.353701
F6VQ19	n containing 2 (Fragmen	Lrch2	4.9126356	3.4313648241	2.3881895
B1ATS5	)S=Mus musculus OX=1	Atp2a3	1.4631775	1.7874570311	1.0079894
P01872	nu OS=Mus musculus C	Ighm	38.574343	52.164023072	67.059408
Q8CI85	=Mus musculus OX=10(	Ca12	0.4366282	0.2303409732	0.2500925
Q80Z71	s musculus OX=10090 (	Tnn	30.269271	17.995070171	16.968698
Q61418	4 OS=Mus musculus OX	Clcn4	0.3001895	0.1877410097	0.3013473
Q3U4G0	OS=Mus musculus OX=	Cdin1	6.1045607	3.4100186799	2.356415
A0A075B5M7	9 OS=Mus musculus OX	Igkv5-39	2.9409241	4.6086659615	1.7195131

FigureS5J-1	Relative PFKFB1 level (PFKFB1/β-Actin)
CTRL	SG
0.329808	0.530963
0.425896	0.54869
0.318359	0.5374853

FigureS5J-2	Relative lev (PFKFB2/
CTRL	
0.401251	
0.42489	
0.426824	

FigureS5L	% PFKFB1+ cells				
Obesity	)besity+Semaglutid	)besity+DMI	y+DMM+Sema	+DMM+Pair	
60	71.2154	11.5487	55.2145	7.1154	
65.224	66.558	11.58	50.14782	11.2488	
55.47	69.542	8.2147	51.2458	10.2488	
66.87	59.1148	11.5486	54.21158	9.5128	
52.154	64.215	11.44875	58.2147	6.21487	
54.548	54.2115	7.21547	63.2154	11.5487	

	58.945	65.2154	8.2145	56.2157	13.2154
	61.548	61.224	6.9985	51.2157	8.21547

FigureS5N	% PFKFB4+ cells				
	Obesity	Obesity+Semaglutid	Obesity+DMM	Ly+DMM+Sema	+DMM+Pair
	45.21547	50.2154	21.2154	29.3245	8.3254
	48.5514	48.5521	18.2457	31.2154	11.2157
	49.6562	45.2215	11.2548	30.2244	9.2154
	38.2157	48.2157	14.2154	32.2154	10.2154
	41.2215	46.23115	12.314	37.2157	15.24578
	38.552	45.2157	8.324	26.8754	20.1124
	37.21548	38.21214	9.324	33.2154	14.232
	40.1224	41.2285	8.2445	31.248	9.3254

HFD-S-C1	HFD-S-C2	HFD-S-C3	FC	P-value	FDR	SG treatment/vehicle
2.6802872	0.9131345	1.565912551839	8.1999836	0.0131556	0.8100622574601	up
2.6667369	0	3.264246788352	4.2894294	0.0110028	0.8100622574601	up
0.1950316	0.3510592	0.291086501028	2.0812072	0.0326816	0.8100622574601	up
0.7767489	0.8367833	1.004539482888	1.9177981	0.0357073	0.8100622574601	up
0.8756671	0	0.984913415354	1.9140428	0.0096083	0.8100622574601	up
0	0.1374169	0.128472672249	1.9044574	0.0201517	0.8100622574601	up
0.8269107	0.5351054	0.886397149276	1.87319	0.0474329	0.8100622574601	up
1.4928288	1.2320093	1.23629592347	1.7708178	0.0075982	0.8100622574601	up
0.3188963	0.320184	0.466024631881	1.7189914	0.0345981	0.8100622574601	up
0.4409339	0.4534562	0.389208798524	1.6850773	0.0470009	0.8100622574601	up
6.8092114	6.8768763	7.248877189541	1.6836205	0.0136364	0.8100622574601	up
0.8445107	0.8961574	1.285429433795	1.6535552	0.0450342	0.8100622574601	up
4.0540543	3.114267	3.062261508305	1.6435297	0.0210063	0.8100622574601	up
0.1932412	0.156273	0.184869355194	1.6390769	0.0046431	0.8100622574601	up
1.15288	1.0572979	0.844110652106	1.6050921	0.0216446	0.8100622574601	up
0.5897512	0.497294	0.60801090891	1.5734824	0.0060401	0.8100622574601	up
0.965534	0.7190971	1.034317075563	1.5670852	0.042345	0.8100622574601	up
0.2782533	0.358358	0.338300017528	1.5598283	0.0141945	0.8100622574601	up
4.5454372	4.4728368	4.711237109589	1.5513369	0.0302565	0.8100622574601	up
0.6569997	0.6184555	0.817938273967	1.5427135	0.0284784	0.8100622574601	up
0.2587528	0.3544078	0.333840936391	1.5348238	0.043978	0.8100622574601	up
0.3021961	0.3321487	0.352203088392	1.5129108	0.0023528	0.8100622574601	up
2.614522	2.2760172	2.842909449939	1.5096757	0.0464143	0.8100622574601	up
1.3635639	1.1061563	1.390003167829	1.5011267	0.0217501	0.8100622574601	up
0.2322421	0	0.267794113627	0.4942556	0.0194298	0.8100622574601	down
0.3236167	0.3257404	0.215587648361	0.486129	0.016045	0.8100622574601	down
23.512778	19.105304	20.69299877629	0.4725227	0.0159168	0.8100622574601	down
2.0607958	1.2500886	1.609144573605	0.4584366	0.0467099	0.8100622574601	down
0.7063152	0.6633491	0.505233350003	0.440259	0.0218976	0.8100622574601	down
24.166306	20.270004	16.89369441224	0.388662	0.0119558	0.8100622574601	down
0.1627861	0.0668787	0.125003336673	0.386744	0.0464485	0.8100622574601	down
8.3736747	6.5495603	9.180593590051	0.3695034	0.0176758	0.8100622574601	down
0.0830175	0.121413	0.078107567895	0.3579705	0.0084116	0.8100622574601	down
1.3734982	0	0.8844610751	0.2853122	0.0435306	0.8100622574601	down
0.4714762	0.8763259	0.639533219592	0.2144043	0.0166534	0.8100622574601	down

PFKFB2 vel /β-Actin) SG
0.701251
0.72489
0.826824

FigureS5J-3	Relative PFKFB3 level (PFKFB3/β-Actin)	
	CTRL	SG
	0.389644	0.589644
	0.3748959	0.5748959
	0.36789	0.56789

FigureS5J-4

feeding	FigureS5M	% PFKFB2+ cells				
	Obesity	sity+Semagl	Obesity+DM	sity+DMM+Semagl	esity+DMM+Pair feedi
	49.5147	50.1547	10.2154	25.1224	7.2154
	51.2145	55.2187	12.2145	30.2214	11.2154
	52.3244	56.2157	8.2154	34.2145	8.2145
	55.5472	58.1247	13.215	25.1248	9.21554
	48.52158	48.2157	11.2458	29.2215	6.2158
	50.1124	46.5528	8.2457	28.547	10.2154

	47.5484	48.52144	7.0244	30.2154	11.3254
	49.22148	50.1248	9.5147	31.0244	8.2154

feeding

FigureS5P	p-AMPK / β-Actin Average intensity (fold change)			
	Ctrl	Semaglutide	PKA inhibi	iaglutide +PKA inhibitor
	1.021254	1.8774	1.011224	1.03254
	1	12.1244	0.98524	0.98745
	0.99554	1.9124	1.03154	1.0215

Relative PFKFB4 level (PFKFB4/β-Actin)	
CTRL	SG
0.444943	0.818565
0.46695	0.92385
0.564753	0.937488

ng

Figure S6C	Osteophyte volume（mm^3）					
	Sham	Glp-1R Sham	DMM	Glp-1R+DMM	DMM+SG	Glp-1R+DMM+SG
	0.22114	0.15874	0.85459	1.06678	0.541147	0.77224
	0.25314	0.22541	0.993509	0.788565	0.553719	0.839226
	0.21224	0.21457	0.84697	0.759248	0.4485558	0.763755
	0.19884	0.13654	0.641527	0.694779	0.469023	0.657287
	0.254447	0.12115	0.887247	0.793504	0.4735555	0.7817
	0.257878	0.14785	0.949245	0.666218	0.3559082	0.770215
	0.22115	0.19854	0.631895	0.600009	0.476831	0.63424
	0.22115	0.16865	0.822728	0.941107	0.408228	0.821523
	0.21448	0.11755	0.590431	0.798144		
	0.13321	0.11145				

Figure S6F

Osteophyte volume（mm^3）

WT+Sham	aa1 cKO+Sh	WT+DMM	aa1 cKO+DM	WT+DMM+SG	aa1 cKO+DMM+SG
0.239069	0.260529	1.36908	1.52136	0.742217	0.80716
0.287385	0.293133	0.97825	1.29868	0.651693	1.29857
0.271532	0.281269	1.3118	0.877904	0.433741	0.969527
	0.286612	0.802151	0.833313	0.304698	1.0998
		0.882842	0.691721	0.37697	0.457908
				0.427396	0.627674
				0.77649	1.41951
					1.04769
					1.1414

FigureS8C	Insulin receptor / β-actin average Intensity (fold change)			
	Ctrl	TNF-α	SG	TNF-α +SG
	1	0.51	1.1	0.62
	0.97	0.32	0.92	0.45
	1.03	0.42	1.01	0.37

FigureS8D

FigureS8F	MMP13 / β-actin average Intensity (fold change)						
	Ctrl	TNF-α	SG	P-1R inhibi	IR inhibitor	LP-1R inhi	+IR inhibit
	1.01	2.11	1.21	1.23	1.11	2.01	1.51
	0.98	2.32	1.03	1.22	0.99	2.18	1.42
	1	1.99	0.92	0.82	0.79	2.39	1.35

GLP1R / β-actin average Intensity (fold change)			
Ctrl	TNF-α	SG	TNF-α +SG
1.03	0.41	1.63	1.21
1	0.35	1.81	1.12
0.98	0.22	1.42	0.83

or

FigureS8G	Aggrecan/ β-actin average Intensity (fold change)					
	Ctrl	TNF-α	SG	P-1R inhibi	IR inhibitor	GLP-1R inhi
	1.01	0.54	2.13	1.12	1.14	0.74
	1	0.52	2.33	1.23	1.05	0.52
	0.99	0.41	2.62	0.81	0.95	0.65

G+IR inhibitor
0.98
0.87
0.83

Figure 6.A

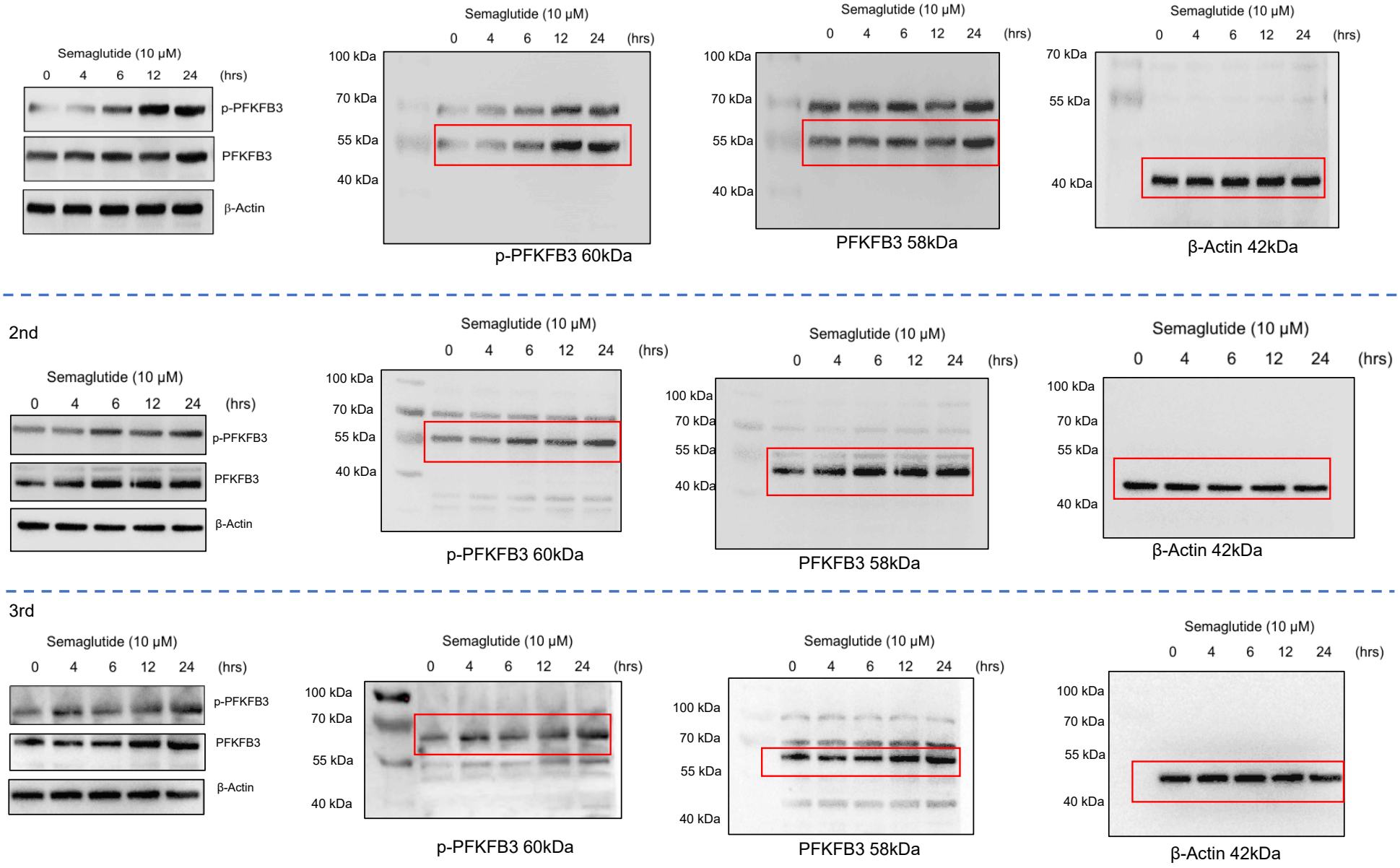
Semaglutide (10 μM)
0 4 6 12 24 (hrs)
p-PFKFB3
PFKFB3
β-Actin
100 kDa
70 kDa
55 kDa
40 kDa
p-PFKFB3 60kDa
PFKFB3 58kDa
β-Actin 42kDa
2nd
3rd

Figure 6.C

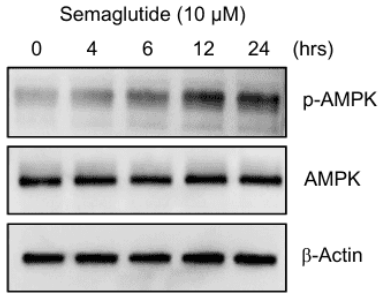

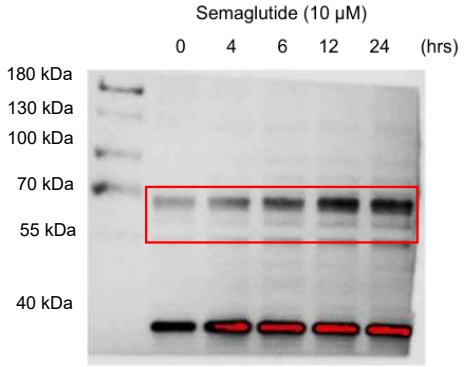

p-AMPK 62kDa

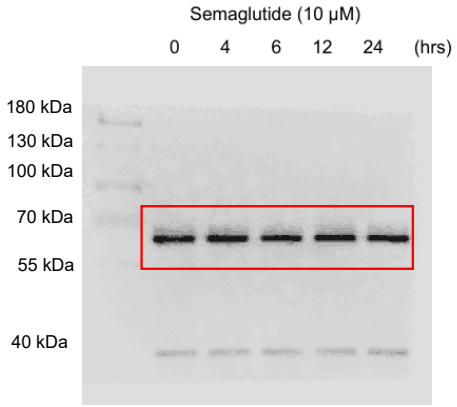

AMPK 64kDa

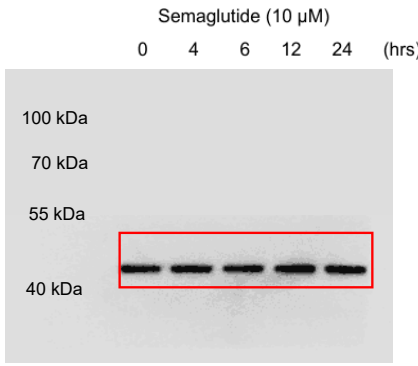

β-Actin 42kDa

2nd

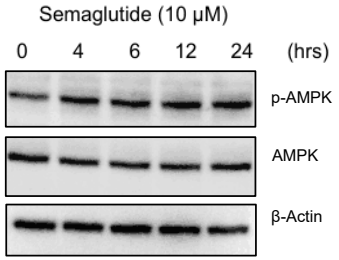

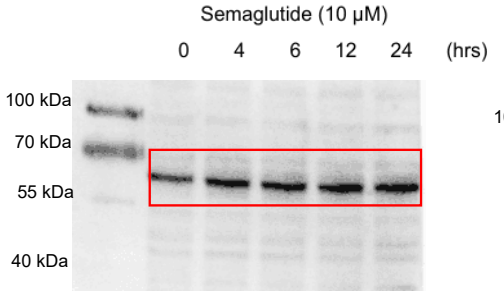

p-AMPK 62kDa

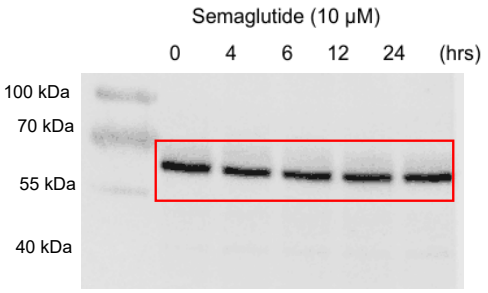

AMPK 64kDa

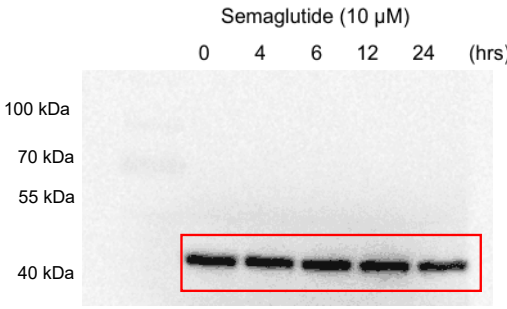

β-Actin 42kDa

3rd

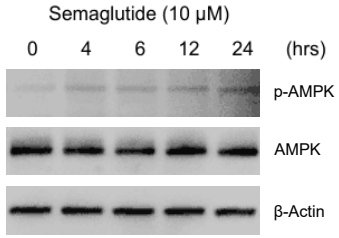

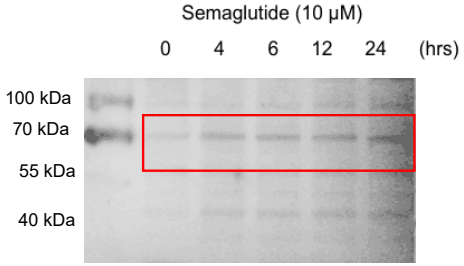

p-AMPK 62kDa

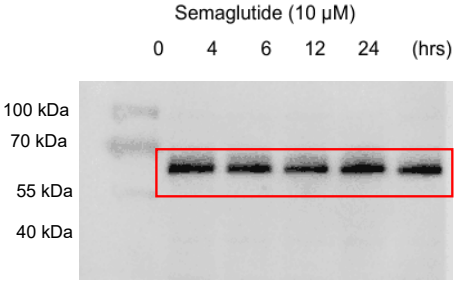

AMPK 64kDa

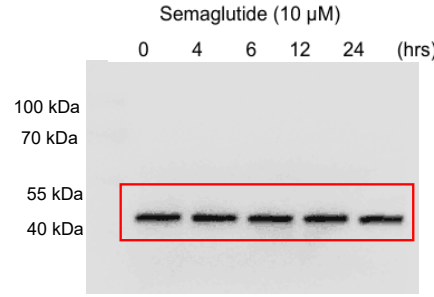

β-Actin 42kDa

Figure 6.E

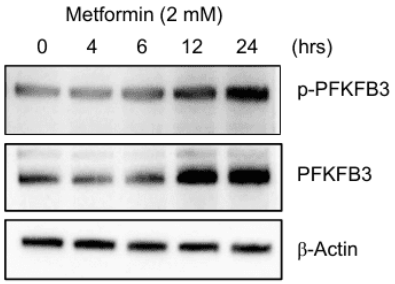

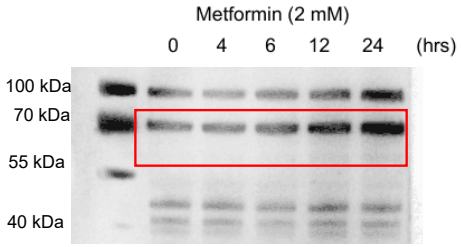

p-PFKFB3 60kDa

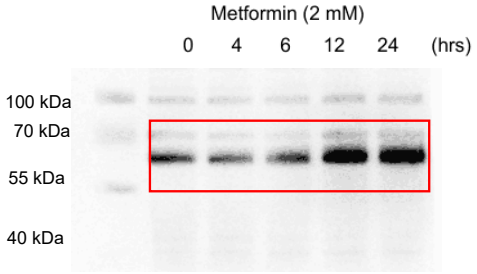

PFKFB3 58kDa

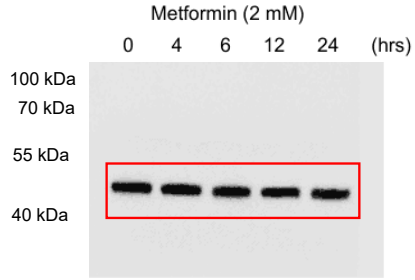

β-Actin 42kDa

2nd

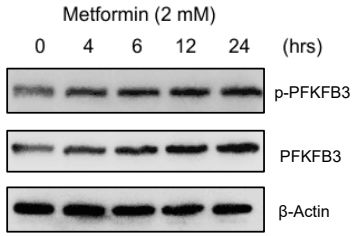

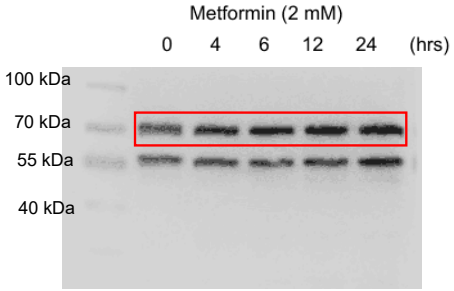

p-PFKFB3 60kDa

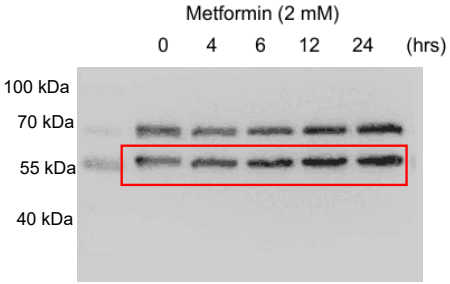

PFKFB3 58kDa

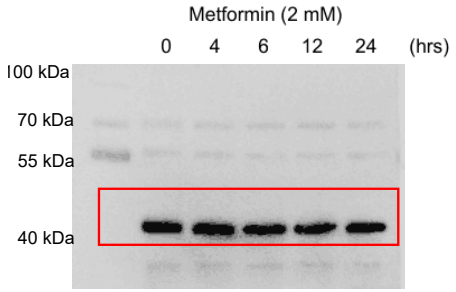

β-Actin 42kDa

3rd

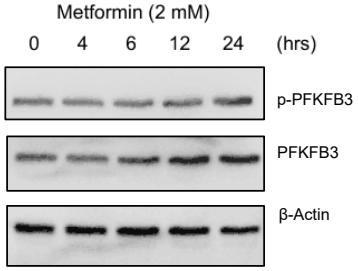

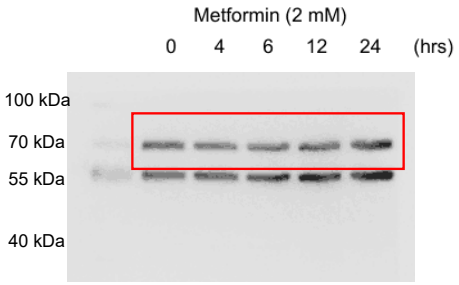

p-PFKFB3 60kDa

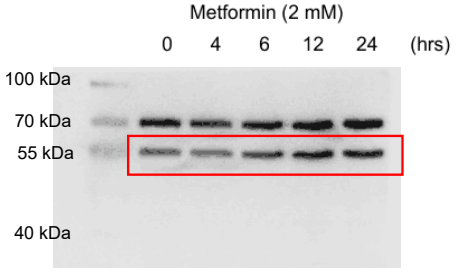

PFKFB3 58kDa

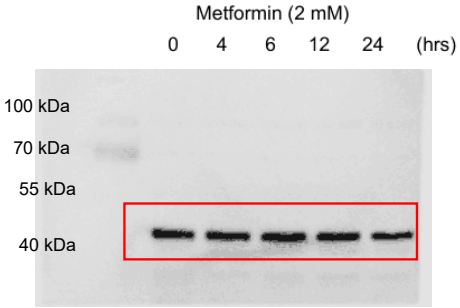

β-Actin 42kDa

Figure 6.F

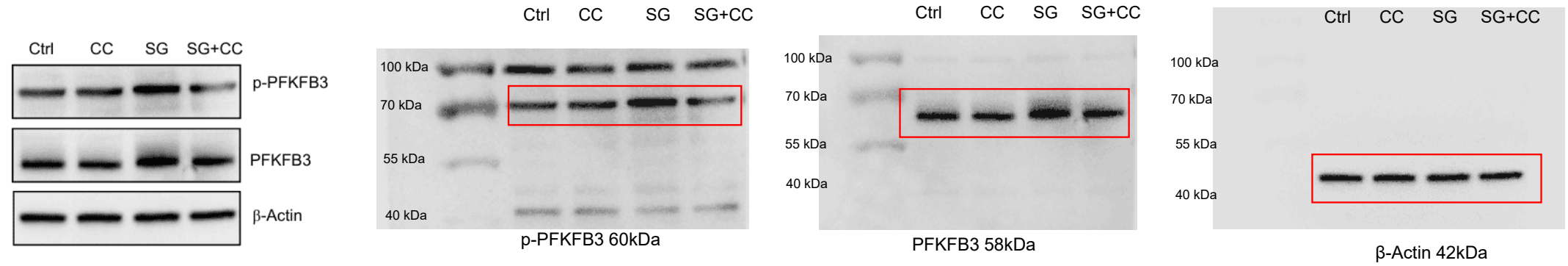

2nd

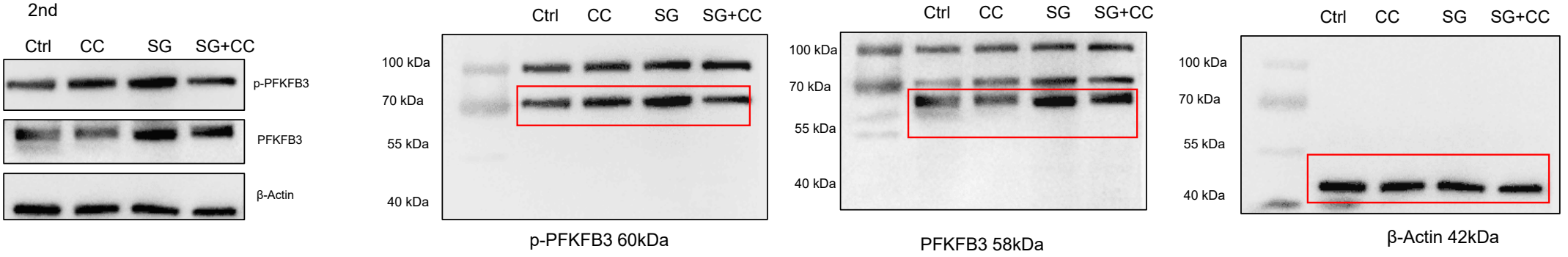

3rd

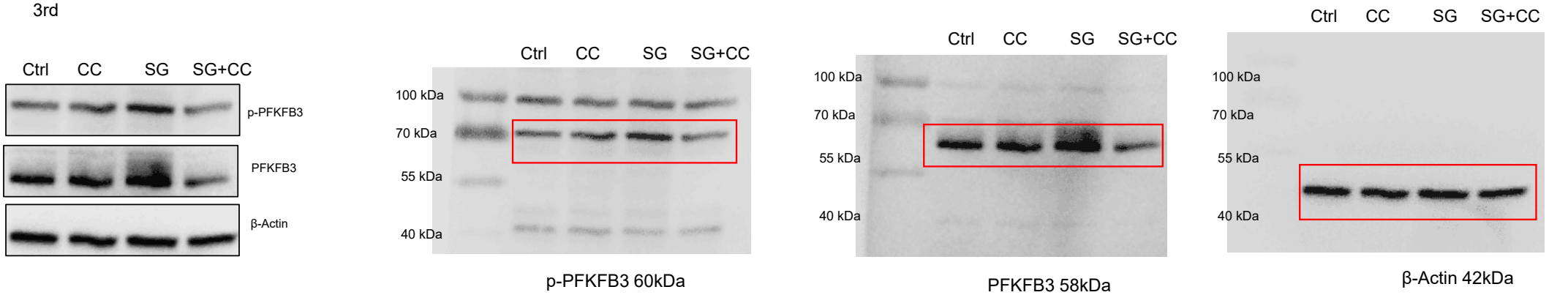

Figure 6.H

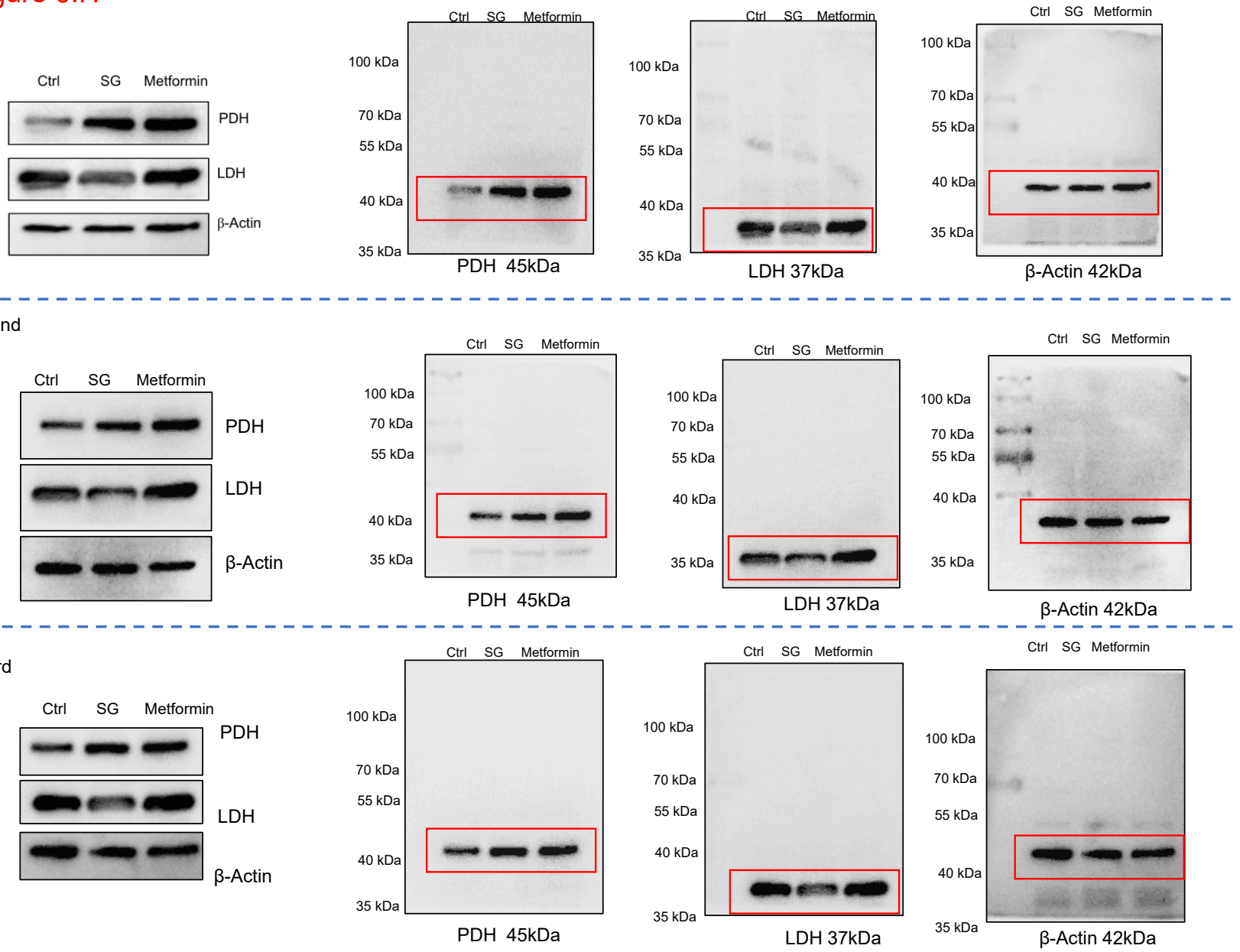
Ctrl SG Metformin
PDH
LDH
β-Actin
100 kDa
70 kDa
55 kDa
40 kDa
35 kDa
PDH 45kDa
LDH 37kDa
β-Actin 42kDa
2nd
3rd

Figure 6.M

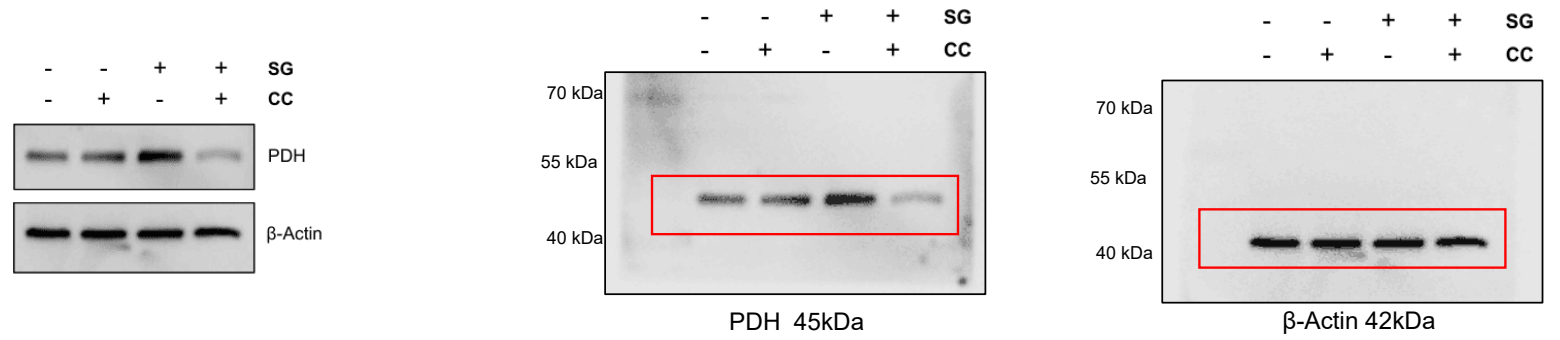

2nd

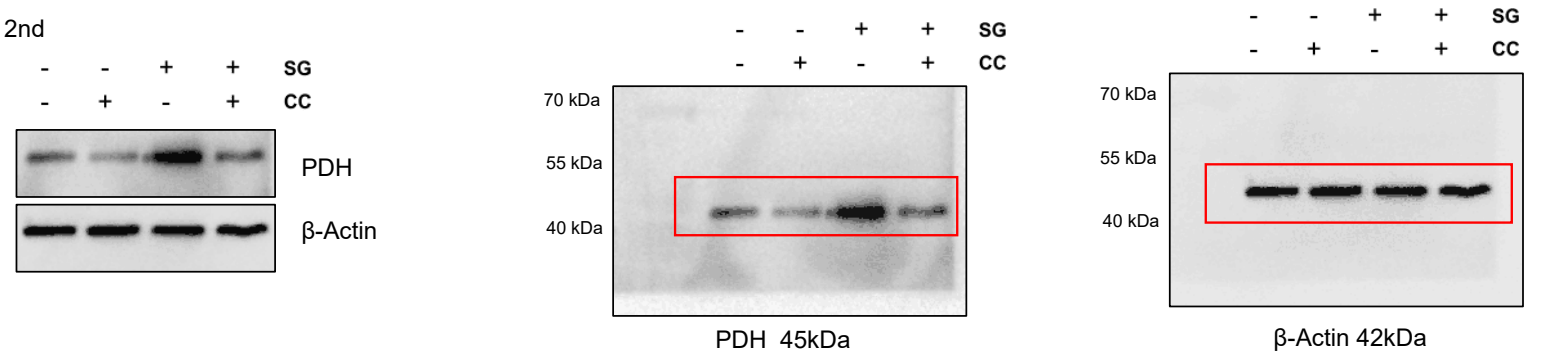

3rd

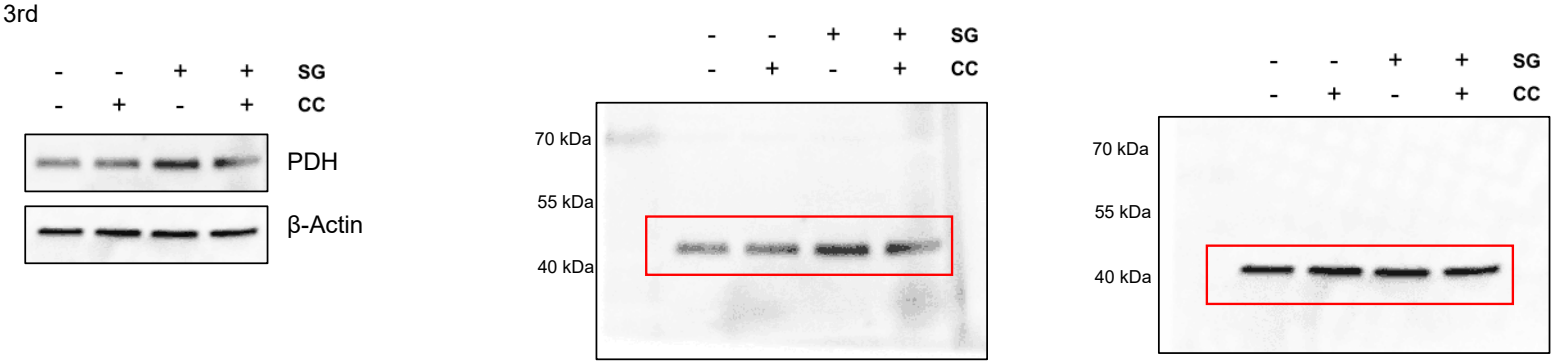

Figure 6.Q

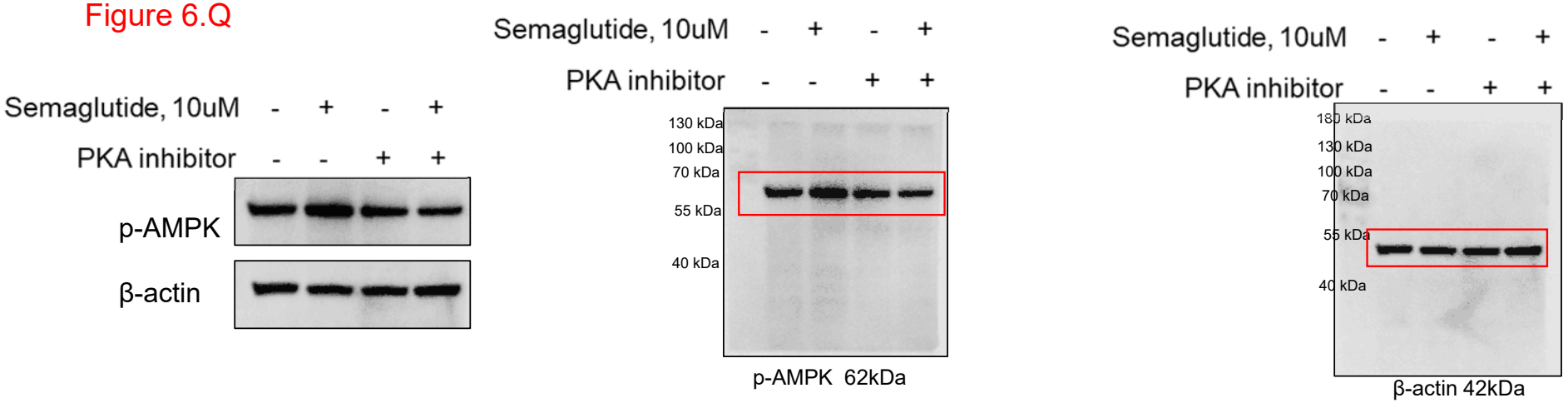

2nd

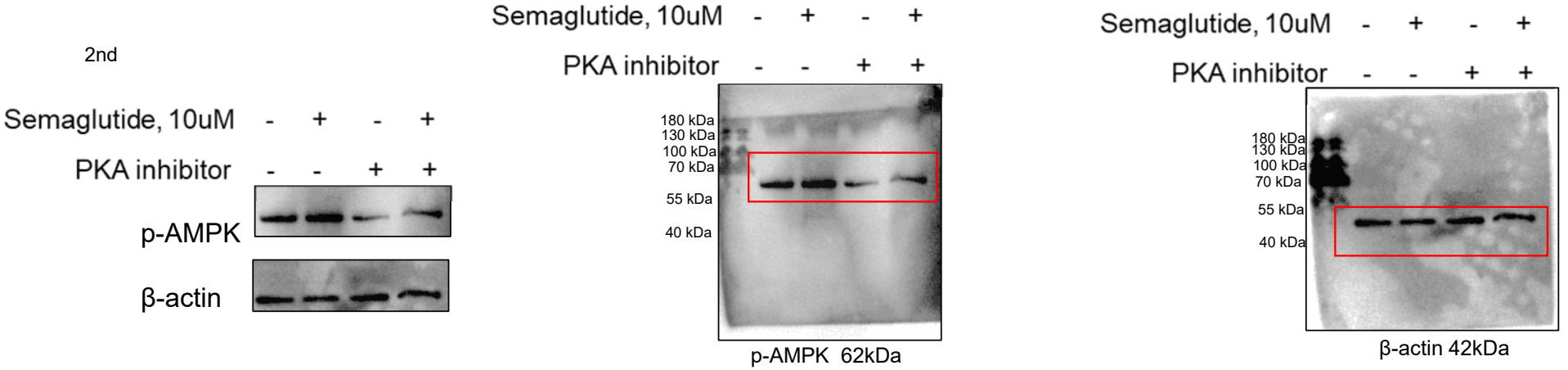

3rd

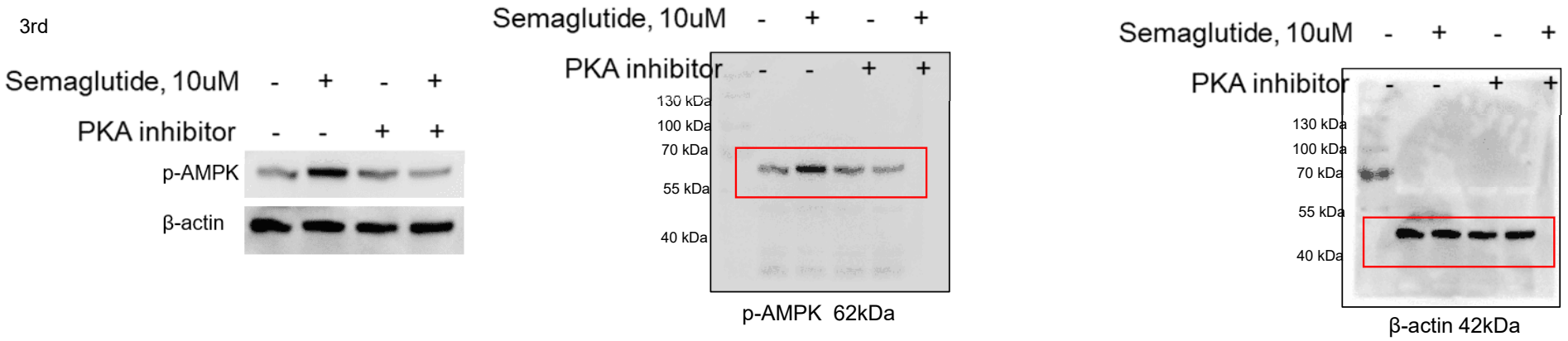

Figure S5.E

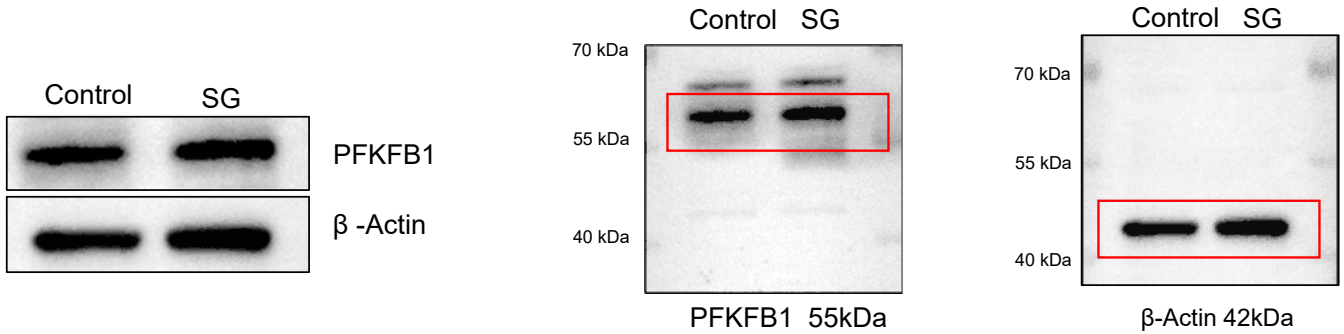

2nd

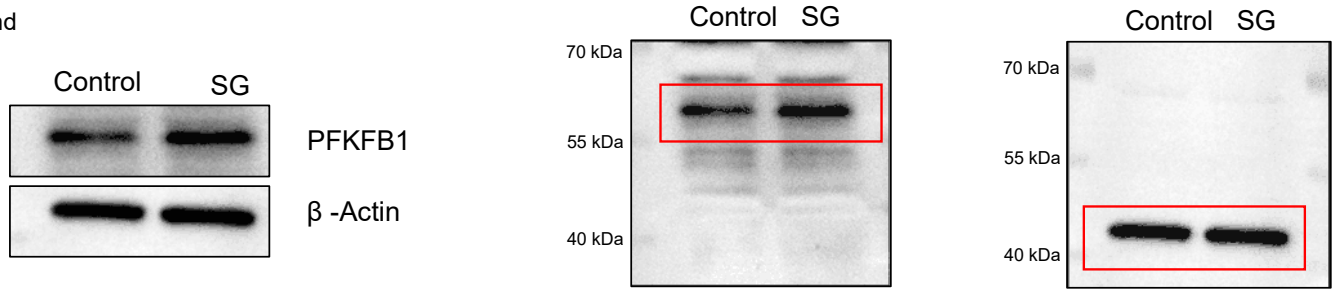

3rd

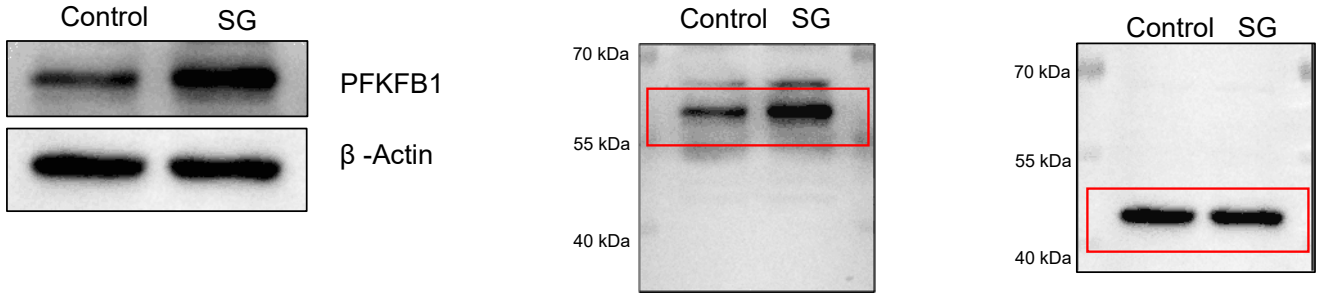

Figure S5.F

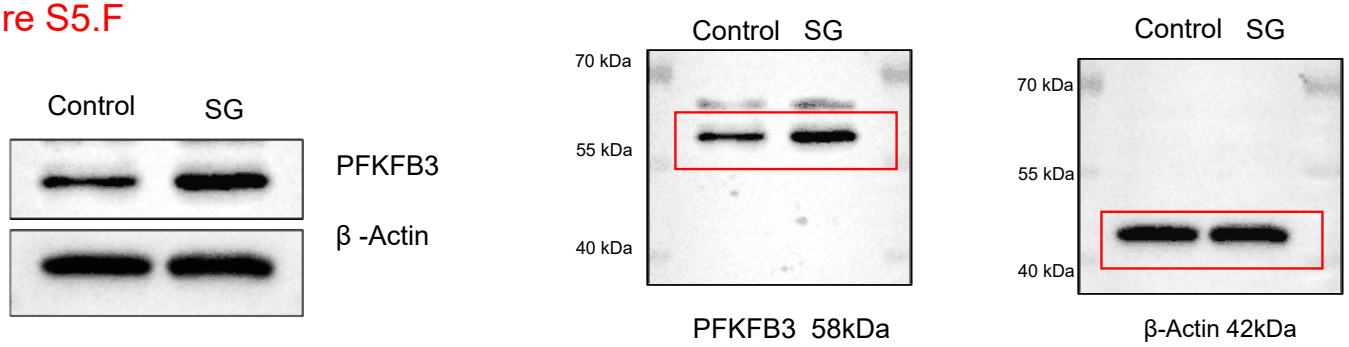

2nd

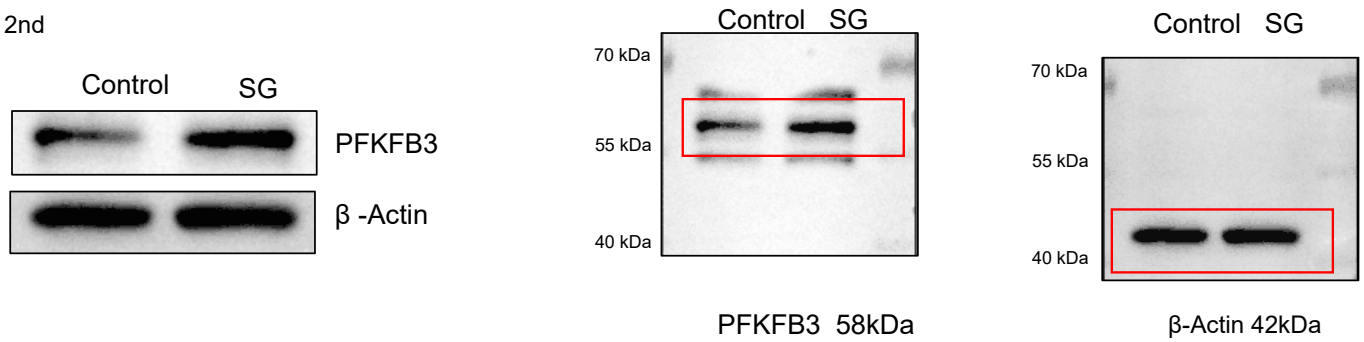

3rd

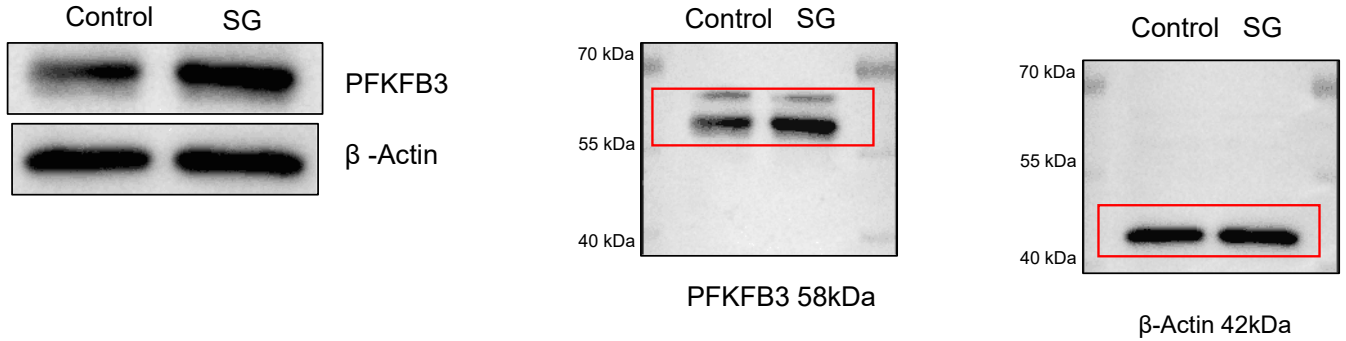

Figure S5.H

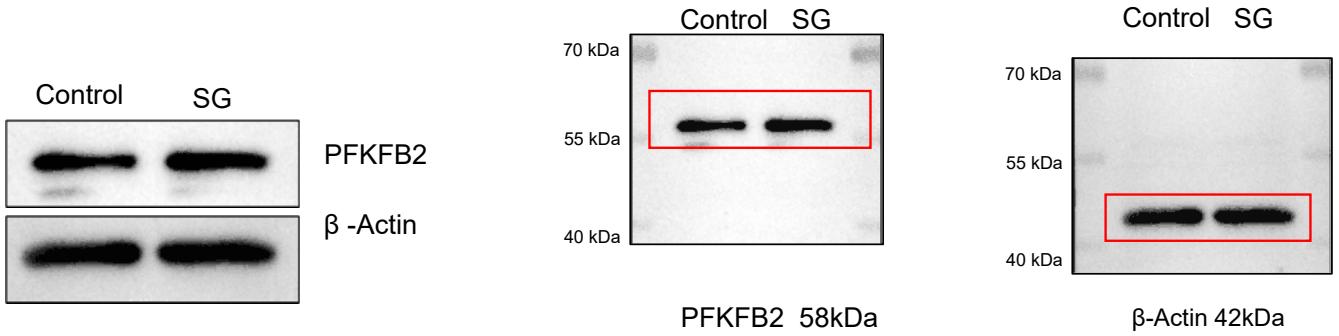

2nd

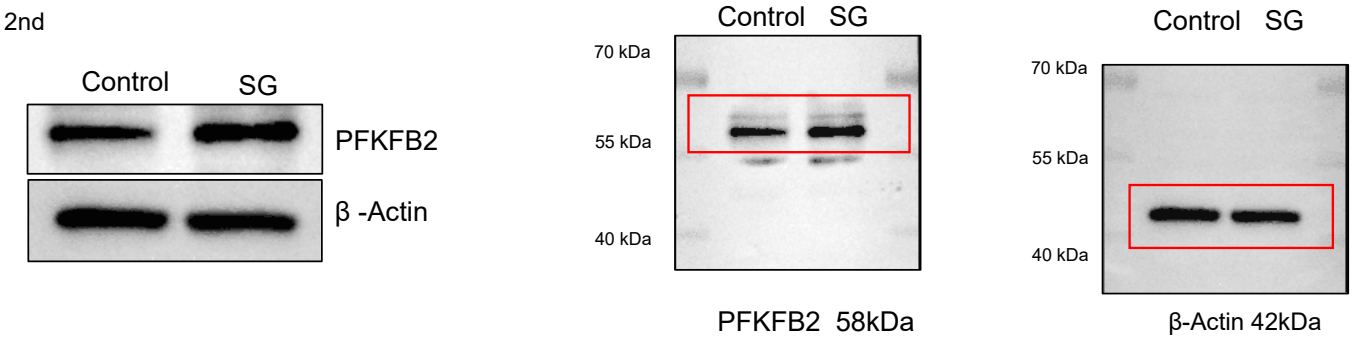

3rd

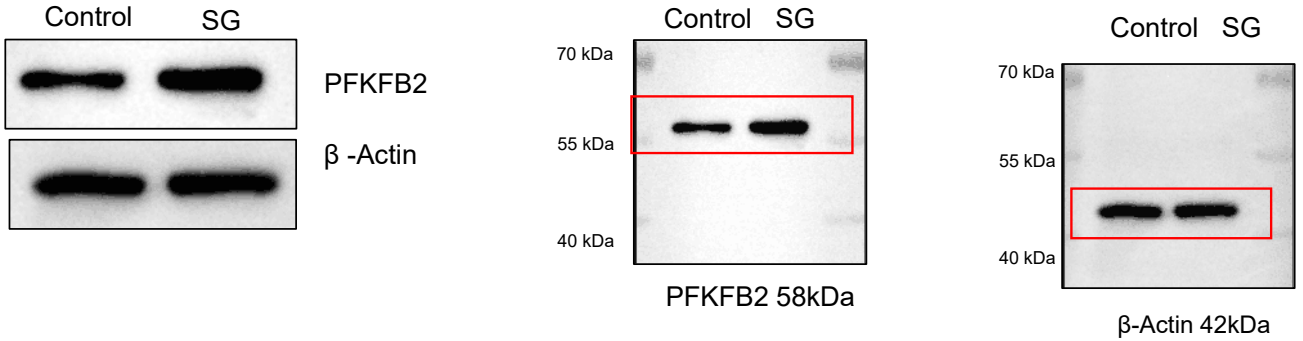

Figure S5.I

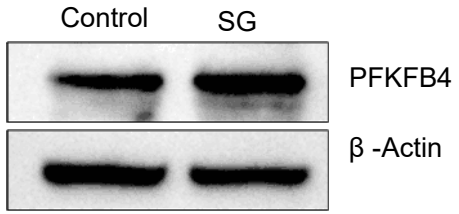

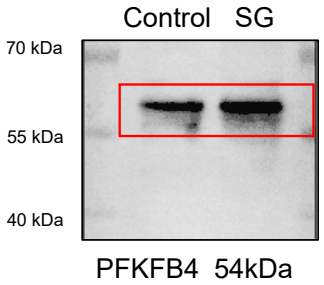

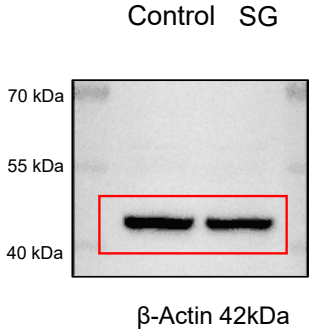

2nd

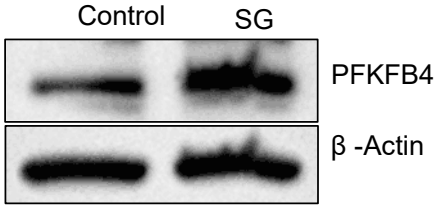

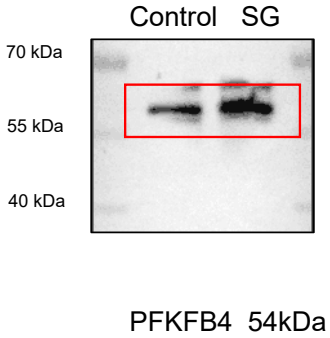

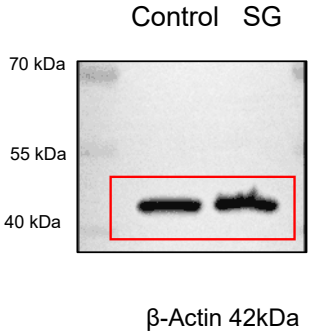

3rd

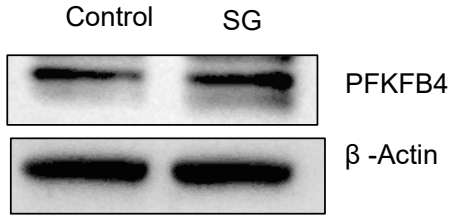

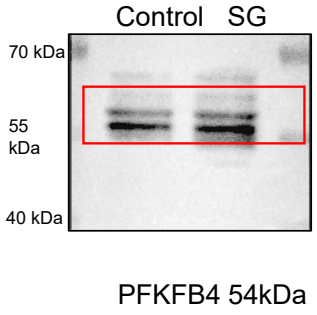

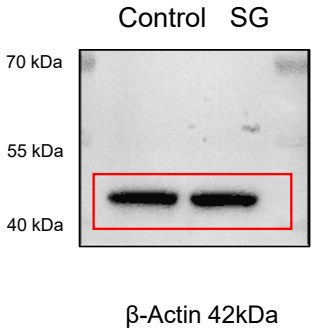

Figure S8.A

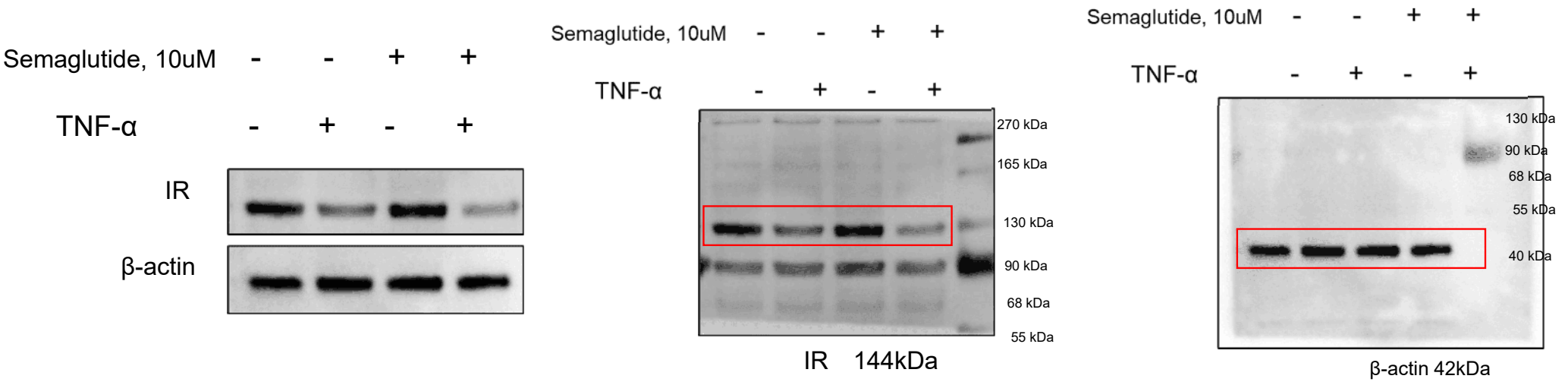

2nd

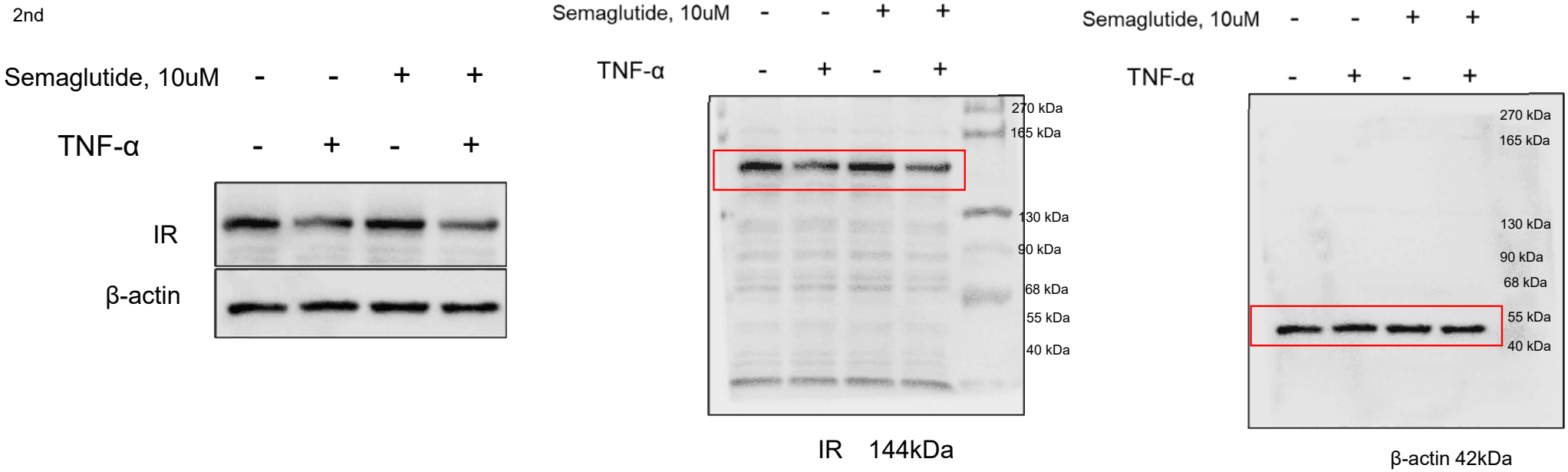

Figure S8.A

3rd

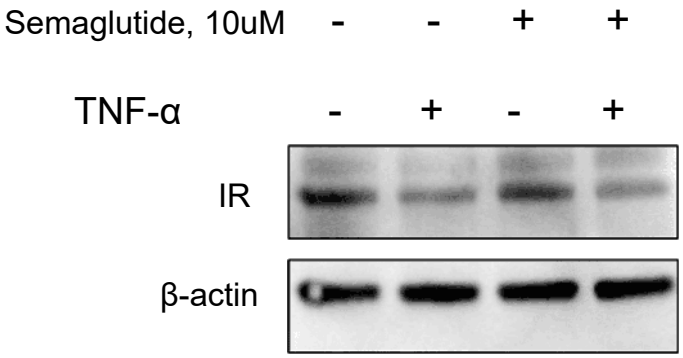

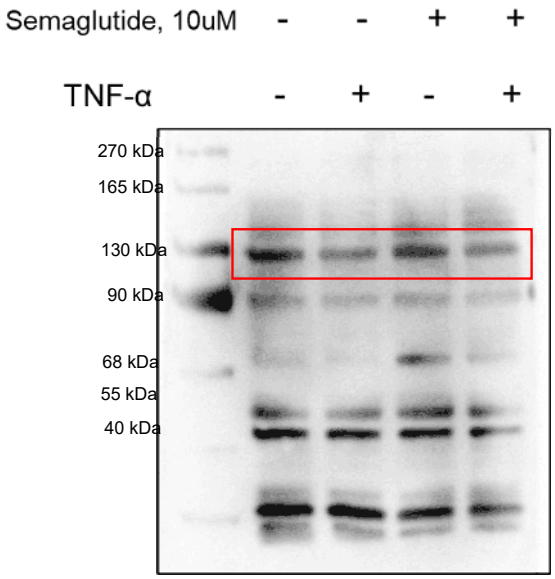

IR 144kDa

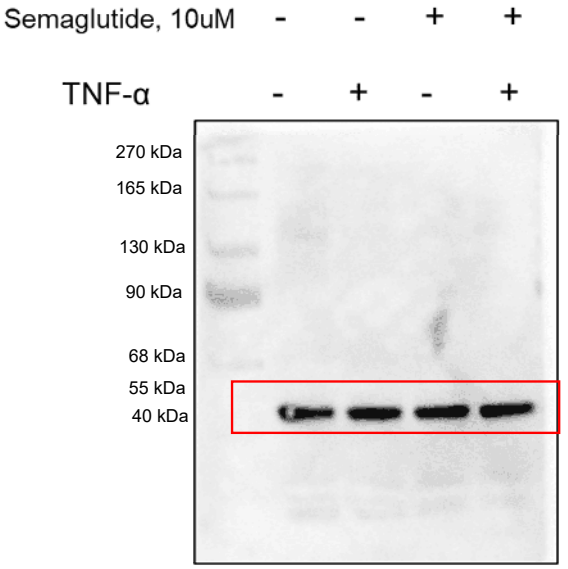

β-actin 42kDa

Figure S8.B

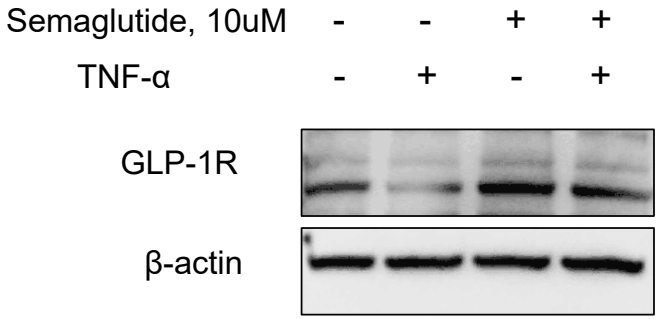

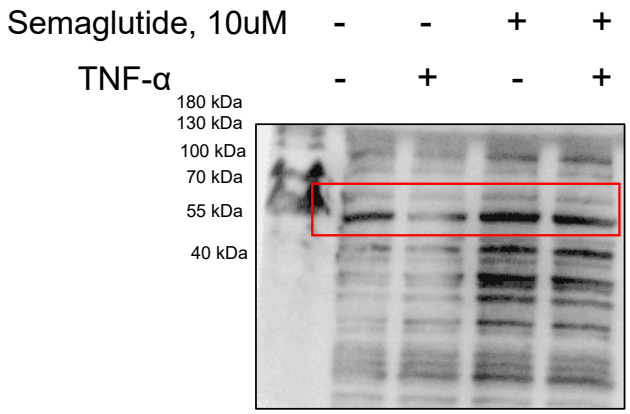

GLP-1R 55kDa

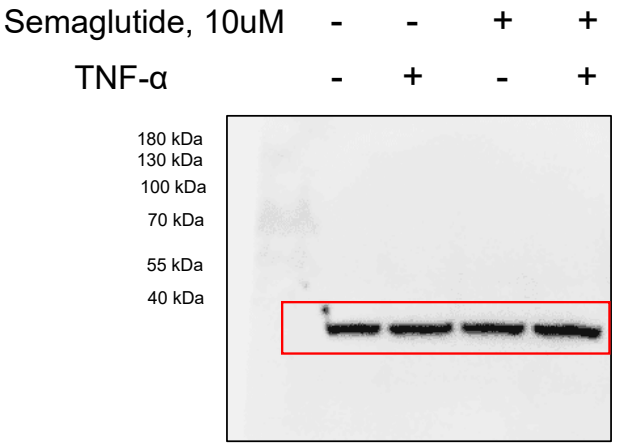

β-actin 42kDa

2nd

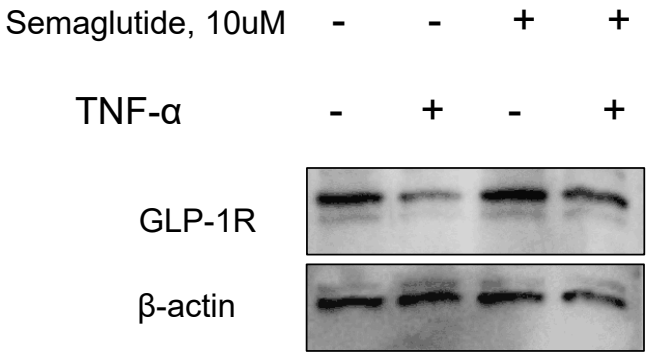

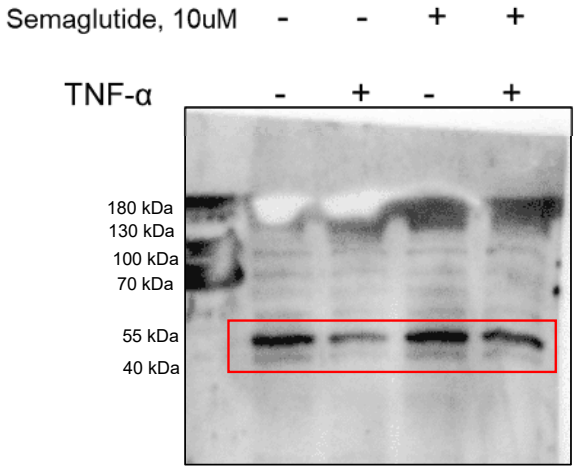

GLP-1R 55kDa

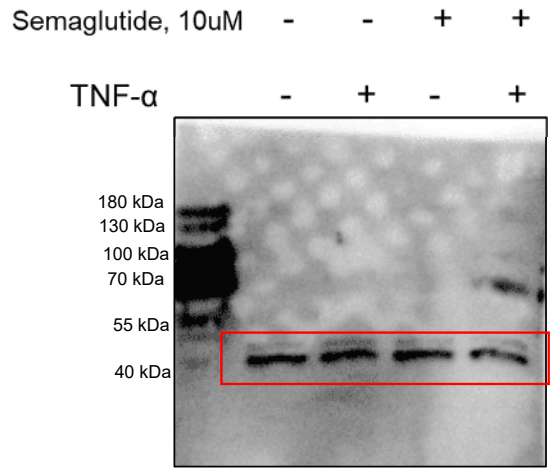

β-actin 42kDa

Figure S8.B

3rd

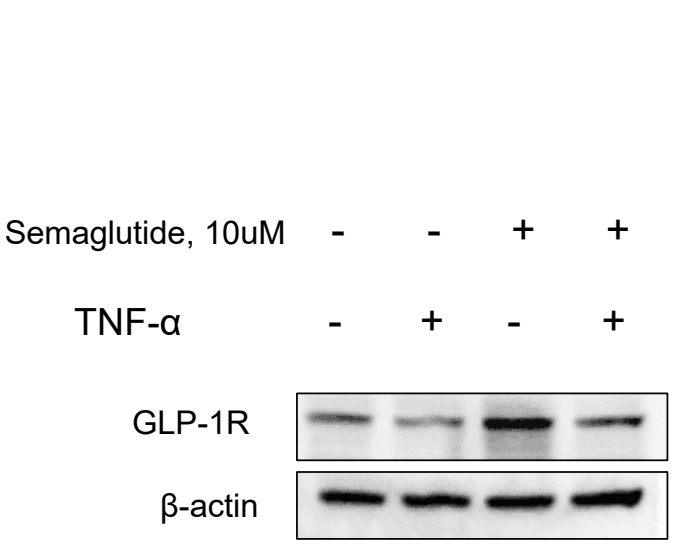

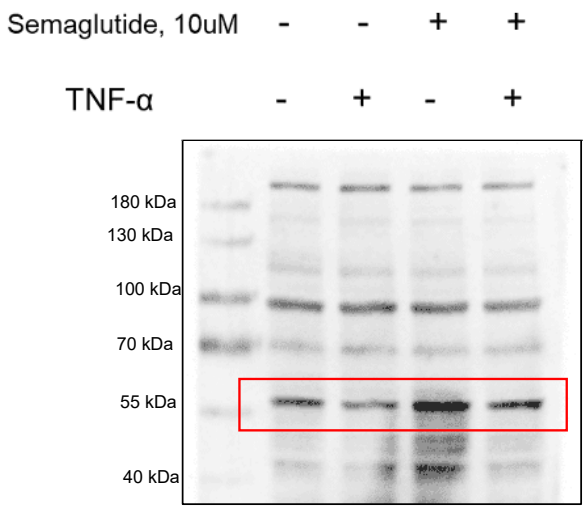

GLP-1R 55kDa

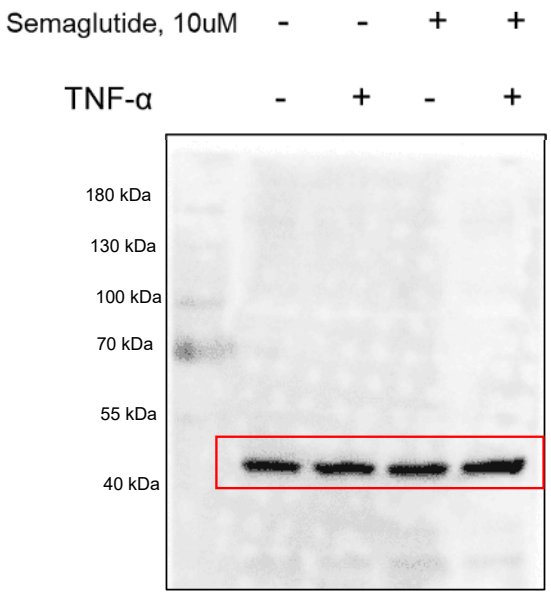

β-actin 42kDa

Figure S8.E

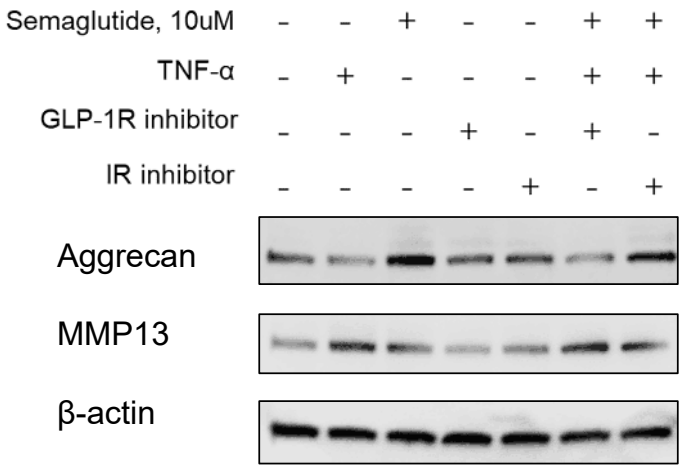

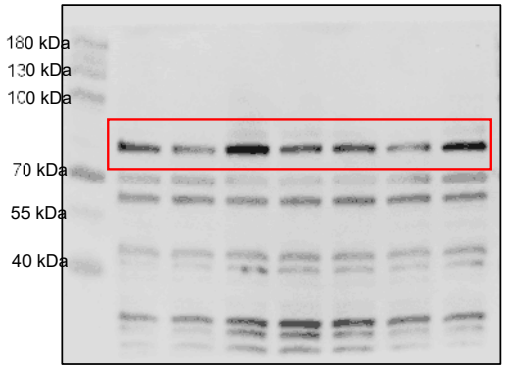

Aggrecan 100kDa

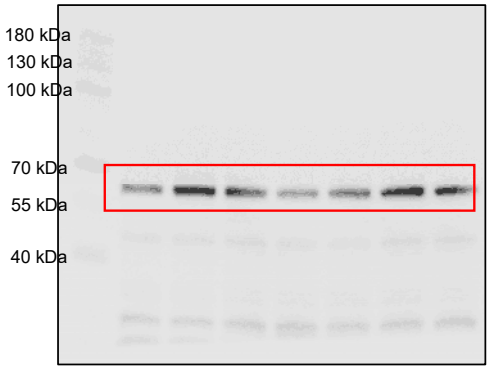

MMP13 70kDa

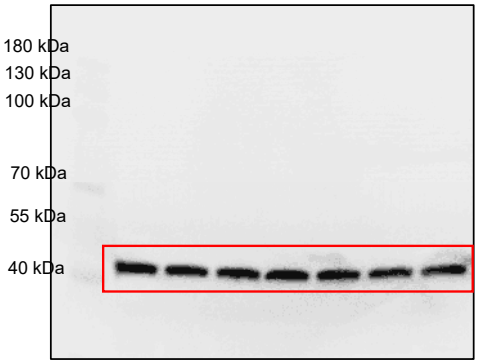

β-actin 42kDa

2nd

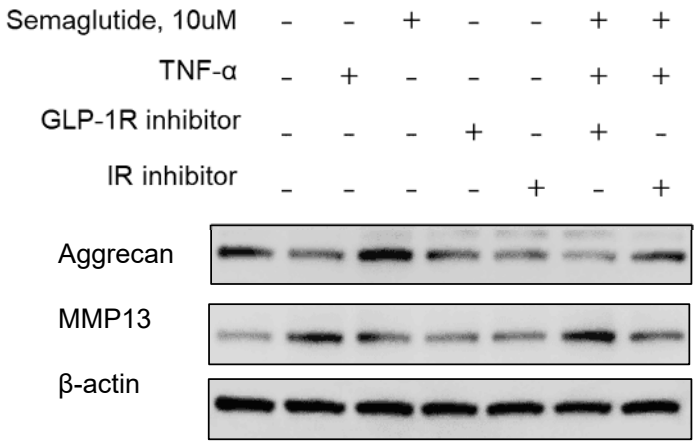

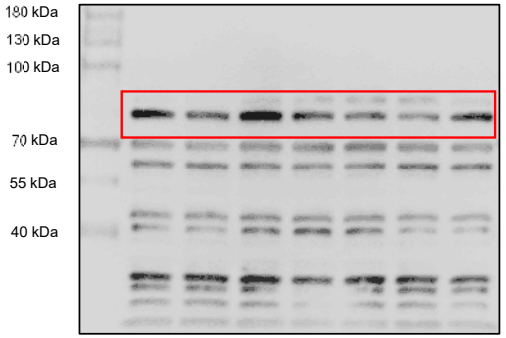

Aggrecan 100kDa

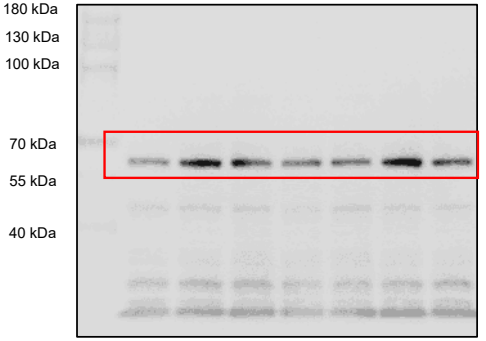

MMP13 70kDa

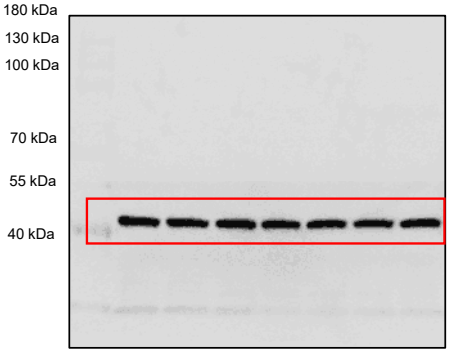

β-actin 42kDa

Figure S8.C

3rd

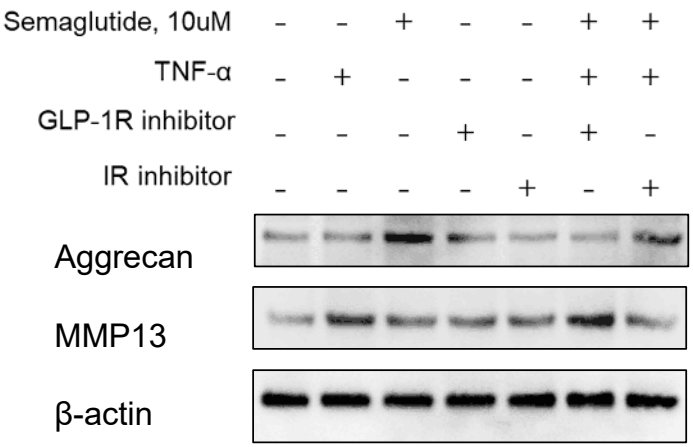

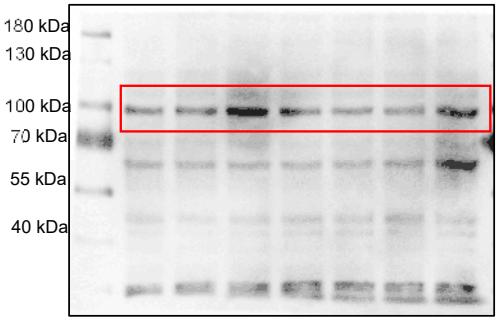

Aggrecan 100kDa

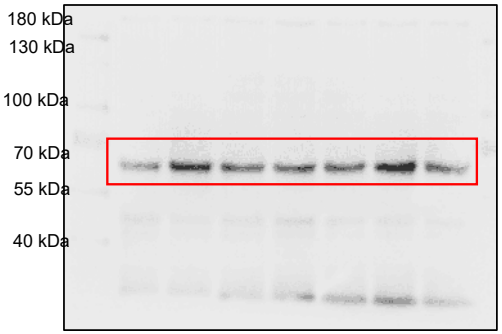

MMP13 70kDa

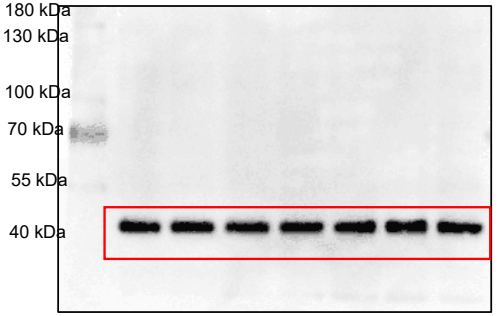

β-actin 42kDa